Three dimensional flow of couple stress fluid over nonlinear stretching surface

By

Arsalan Aziz

Department of Mathematics
Quaid-i-Azam University
Islamabad, Pakistan
2016

Three dimensional flow of couple stress fluid over nonlinear stretching surface

By

Arsalan Aziz

Supervised By

Prof. Dr. Tasawar Hayat

Department of Mathematics
Quaid-i-Azam University
Islamabad, Pakistan
2016

Three dimensional flow of couple stress fluid over nonlinear stretching surface

By

Arsalan Aziz

A DISSERTATION SUBMITTED IN THE PARTIAL FULFILLMENT OF THE REQUIREMENT FOR THE DEGREE OF

MASTER OF PHILOSOPHY

IN

MATHEMATICS

Supervised By

Prof. Dr. Tasawar Hayat

Department of Mathematics
Quaid-i-Azam University
Islamabad, Pakistan
2016

DEDICATED TO

MY BELOVED PARENTS

AND

MY SUPERVISOR

Acknowledgement

All praises and glories be to Allah, the Creator, Who created every thing from spinning electrons to spiraling galaxies with astonishing beauty and symmetry. Also, his uncountable blessings on Panjtan Pak, who taught us to unveil the truth behind the natural phenomena which gives us motivation for research.

I would also like to express my heartiest gratitude to my worthy supervisor **Prof. Dr. Tasawar Hayat (National Distinguished Professor)** for his constant guidance, support, valuable discussions and inspiring attitude throughout my research work. Here I specially like to mention that he has been very kind to me, without his motivationand encouragement I would never be able to complete this dissertation. It was a great privilege and honor for me to work under his kind supervision. I thank him for housing me as a research student and providing me with all his invaluable ideas and time.

At this great occasion I can never forget my teachers for what they have taught me, especially the thought provoking lectures and inspiring personality of **Dr. Muhammad Ayub**, **Dr. Muhammad Shabir,Dr. SohailNadeem, Dr. Masood Khan, Dr. Malik Yousaf**, **Dr. Khalid Saifullah**, **Dr. Muhammad Aslam**, **Dr. TufailNaseem**and **Mr. Irshad Khan**.

I want to convey my deepest thanks and compliments to my father **Malik Tariq Aziz**, in spite of his illness, he continuously support and encourage me to complete my M.Phil degree. Without him I cannot be able to complete this dissertation. And specially to my mother **ShaukatJabeen**whose support has been as important for me as my father's. Their unconditional love is priceless for me. I would also like to

Preface

The boundary layer flow over a continuous stretching surface has various engineering and industrial applications. Such flow commonly involves in the paper production, wire drawing, hot rolling, glass fiber production, extrusion of plastic sheets, cooling ofmetallic plate in a cooling bath and many others. Many researchers have discussed different problems through the linear stretching of the surface but there are various situations in the industrial and technological processes where the stretching of the surface is not necessary linear. Particularly the flow induced by a nonlinear stretching surface has played important role in the polymer extrusion process. With this viewpoint Vajravelu [1] provided a study to examine the flow and heat transfer characteristics of viscous fluid induced by a nonlinearly stretching surface. Cortell [2] performed a numerical study to investigate the flow of viscous fluid over a nonlinearly stretching surface. He studied the two cases of heat transfer namely the constant surface temperature and the prescribed surface temperature. Cortell [3] also explored the flow of viscous fluid over a nonlinearly stretching surface in the presence of viscous dissipation and radiation effects. Hayat et al. [4] addressed the magnetohydrodynamic (MHD) flow over a nonlinearly stretching surface by using the modified Adomian decomposition and Padé approximation techniques. Flow and heat transfer properties of nanofluid over a nonlinearly stretching surface is reported by Rana and Bhargava [5]. Mukhopadhyay [6] discussed the boundary layer flow over a permeable nonlinearly stretching surface subject to partial slip condition. Mabood et al. [7] studied the MHD flow of water-based nanofluid over a nonlinear stretching surface in the presenceof viscous dissipation. Recently Mustafa et al. [8] investigated the flow of nanofluid over a nonlinearly stretching surface subject to the convective surface boundary condition.

Insertion of ultrafine nanoparticles (<100 nm) in the base liquid is termed as nanofluid. The nanoparticles utilized in nanofluids are basically made of metals (Cu, Al, Ag), oxides (Al_2O_3), carbides (SiC), nitrides (AlN, SiN) or nonmetals (graphite, carbon nanotubes) and the base liquids like water, oil or ethylene glycol. Addition of nanoparticles in the base liquids greatly enhances the thermal properties of the base liquids. Due to such interesting properties, nanofluids are useful in various industrial and technological processes such as the cooling of electronic

devices, transformer cooling, vehicle cooling, heat exchanger, nuclear reactor, biomedicine and many others. Especially the magneto nanofluids are useful in MHD power generators, removal of blockage in the arteries, hyperthermia, cancer tumor treatment, wound treatment, magnetic resonance imaging etc. The term nanofluid was first introduced by Choi and Eastman [9] and they illustrated that the thermal properties of base liquids are enhanced when we add up the nanoparticles into it. Boungiorno [10] constructed a mathematical model to explore the thermal properties of base fluids. Here the effects of Brownian motion and thermophoresisare utilized to enhance the thermal properties of base liquids. Khan and Pop [11] employed the Boungiorno model [10] to analyze the boundary layer flow of nanofluid over a stretching surface. Afterwards various attempts have been made in this direction. Few of these can be quoted through the investigations [12-22] and several refs. therein.

Most of the studies in the literature explain viscous materials by the classical Navier-Stokes equations. There are several complex rheological materials such as paints, shampoos, slurries, toothpastes, polymer solutions, ketchup, paper pulp, blood, greases, drilling muds, lubricating oils and many others that cannot be characterized through the classical Navier-Stokes expressions. Such materials are known as the non-Newtonian fluids. However there is no single relation that can predict the properties of all non-Newtonian fluids. Hence various models of non-Newtonian fluids are developed in the literature. The couple stress fluid model [23-28] is one of such materials. This model has important features due to the presence of couple stresses, body couples and non-symmetric stress tensor. Some interesting examples of the couple stress fluid are blood, suspension fluids, lubricants and electro rheological fluids.

The present dissertation consists of three chapters. Chapter one contains some basic concepts, definitions and equations. Chapter two addresses the two-dimensional flow of viscous nanofluid over a nonlinearly stretching surface with convective surface boundary condition. Thermophoresis and Brownian motion effects are considered. Boundary condition with the zero nanoparticles mass flux at the surface is incorporated. Homotopy analysis technique is adopted to solve the governing nonlinear differential system. Graphs are plotted to see the effects of various physical parameters on the temperature and concentration distributions. This chapter provides the detailed review of article by Mustafa et al. [8]. Chapter three is the generalization of chapter two into three directions. Firstly to consider the three-dimensional flow of couple stress nanofluid. Effects of Brownian motion and thermophoresis are taken into account. We imposed the thermal

convective [29,30] and zero nanoparticles mass flux conditions at the surface [31,32]. Secondly to analyze the influence of non-uniform magnetic field under low magnetic Reynolds number assumption. Thirdly to compute the convergent series solutions through the homotopy analysis method (HAM) [33-40]. Effects of various pertinent flow parameters on the velocities, temperature and concentration distributions are sketched and discussed. Numerical values of skin-friction coefficients and local Nusselt number are computed and analyzed.
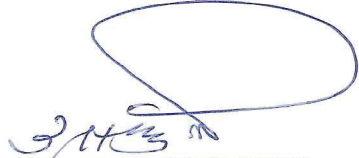
Three dimensional flow of couple stress fluid over nonlinear stretching surface

By

Arsalan Aziz

CERTIFICATE

A DISSERTATION SUBMITTED IN THE PARTIAL FULFILLMENT OF THE REQUIREMENTS FOR THE DEGREE OF THE MASTER OF PHILOSOPHY

We accept this dissertation as conforming to the required standard

1. _____
   Prof. Dr. Tasawar Hayat
   (Supervisor)

2. _____
   Dr. Tanvir Akbar Kiani
   (External Examiner)

3. _____
   Prof. Dr. Tasawar Hayat
   (Chairman)

Department of Mathematics
Quaid-I-Azam University
Islamabad, Pakistan
2016

Contents

Chapter 1

Some fundamental equations and laws

The purpose of this chapter is to address some laws, definitions and equations which are more essential to understand the analysis explained in the chapters two and three.

1.1 Fluid

A substance which continuosly deforms under the implementation of applied shear stress of any magnitude is called fluid. Liquids and gases are examples of fluid.

1.1.1 Liquid

It is type of fluid that has a definite volume but no definite shape. Blood, water and milk are examples of liquids.

1.1.2 Gas

It is type of fluid that has no definite volume and shape is known as gas. For example oxygen, hydrogen and nitrogen etc.

1.2 Fluid mechanics

Fluid mechanics is the class of physical sciences which deals with the fluid's characteristics at rest or in motion. It can be classified into two main branches which are defined as follows:

1.2.1 Fluid statics

It describes the fluid properties or features in state of rest.

1.2.2 Fluid dynamics

Fluid dynamics deals with the characteristics of fluids in state of motion.

1.3 Stress

Stress is an applied force that acts on the surface area of unit dimension within a deformable body. Mathematically it can be expressed as

$$\text{Stress } (\sigma) = \frac{\text{Force}}{\text{Area}} = \frac{\mathbf{F}}{A}, \tag{1.1}$$

The unit and dimension of stress are Nm^{-2} and $\left[ML^{-1}T^{-2}\right]$ respectively. Stress is mainly classified into two types.

1.3.1 Shear/tangential stress

Stress is known as shear/tangential stress when an applied force acts parallel to the surface area of unit dimension within deformable body.

1.3.2 Normal/tension stress

Stress is known as normal/tension stress when an applied force acts normal to the surface area of unit dimension within deformable body.

1.4   Strain

Strain is utilized to measure the deformation of an object, when a force is acting on it.

1.5   Viscosity

Viscosity is an inherent characteristic of fluid which measures the fluid resistance against any gradual deformation under the action of various forces. There are two ways to denote the viscosity.

1.5.1   Dynamic viscosity

It is the fluid characteristic which measures the resistance of fluid against any gradual deformation when a force is acted on it. Mathematically, one can write it as

$$\text{dynamic viscosity } (\mu) = \frac{\text{Shear stress}}{\text{gradient of velocity}}, \tag{1.2}$$

SI unit and dimension of dynamic viscosity are $Kgm^{-1}s^{-1}$ and dimension $\left[ML^{-1}T^{-1}\right]$ respectively.

1.5.2   Kinematic viscosity (ν)

It is stated as ratio of dynamic viscosity (μ) to the density of fluid (ρ). Mathematically it can be expressed as

$$\nu = \frac{\mu}{\rho}, \tag{1.3}$$

Kinematic viscosity has the unit $m^2 s^{-1}$ and dimension $\left[L^2 T^{-1}\right]$.

1.6   Newton's viscosity law

It is stated that the shear force which deforms the element of fluid is linearly and directly proportional to the shear rate (i.e rate of deformation). In mathematical form we can express it as follows

$$\tau_{yx} \propto \frac{du}{dy}, \tag{1.4}$$

6

or

$$\tau_{yx} = \mu \left(\frac{du}{dy} \right), \tag{1.5}$$

In above relation τ_{yx} denotes the shear stress and μ represents proportionality constant.

1.6.1 Newtonian fluids

Those fluids which satisfy the Newton's viscosity law are characterized as Newtonian fluids. In these types of fluids a direct and linear relation always exist between the shear force (τ_{yx}) and deformation rate $\left(\frac{du}{dy} \right)$. Examples of Newtonian fluids are water, mercury and aqueous glycerine solution etc.

1.6.2 Non-Newtonian fluids

The fluids for which Newton's viscosity law do not hold are the non-Newtonian fluids. In these types of fluids shear force has a direct and nonlinear relationship to the rate of deformation. In mathematical form we can express it as follows

$$\boldsymbol{\tau}_{yx} \propto \left(\frac{du}{dy} \right)^n, \ n \neq 1, \tag{1.6}$$

or

$$\boldsymbol{\tau}_{yx} = k \left(\frac{du}{dy} \right)^n, \tag{1.7}$$

Here k denotes the consistency index which is used to estimate the consistency of fluid and n depicts the flow behavior's index which elucidates that the fluid differs from a Newtonian fluid. When $n = 1$ and $k = \mu$ then Eq. (1.7) transforms to the Newton's viscosity law. From Eq. (1.7) we have

$$\boldsymbol{\tau}_{yx} = \eta^\star \left(\frac{du}{dy} \right), \tag{1.8}$$

with the following expression of apparent viscosity $\eta^\star$ is

$$\eta^\star = k \left(\frac{du}{dy} \right)^{n-1}, \tag{1.9}$$

In above expression $\eta^\star$ represents the apparent viscosity. Blood, ketchup and paints show the non-Newtonian fluid behavior. The fluid model which is considered in this dissertation is couple stress fluid model. The force stress tensor τ and the couple stress tensor M appears in couple stress fluids theory which are defined in the following forms

$$\boldsymbol{\tau} = \left(-p + \lambda \operatorname{div} \tilde{\mathbf{V}}\right) I + \mu \left(\left(\operatorname{grad}\tilde{\mathbf{V}}\right) + \left(\operatorname{grad}\tilde{\mathbf{V}}\right)^{\breve{\mathbf{T}}}\right) + \frac{1}{2} I \times (\operatorname{div} M + \rho C), \qquad (1.10)$$

and

$$M = mI + 2n^* \operatorname{grad}(\operatorname{curl}\tilde{\mathbf{V}}) + 2\eta'(\operatorname{grad}(\operatorname{curl}\tilde{\mathbf{V}}))^{\breve{\mathbf{T}}}, \qquad (1.11)$$

where the quantity λ represents the material constant, ρC denotes the body couple tensor, m is the $(1/3)$rd trace of M and η' depicts the constant associated with couple stresses. Material constant λ has dimension as that of viscosity where as the dimensions of n^* and η' are those of momentum. These material constants are considered by the following inequalities

$$\mu \geq 0, \;\; 3\lambda + 2\mu \geq 0, \;\; n^* \geq 0, \;\; \eta' \leq n^*, \qquad (1.12)$$

Using the Cartesian coordinates, we have

$$\operatorname{grad}\tilde{\mathbf{V}} = \begin{bmatrix} \frac{\partial u}{\partial x} & \frac{\partial u}{\partial y} & \frac{\partial u}{\partial z} \\ \frac{\partial v}{\partial x} & \frac{\partial v}{\partial y} & \frac{\partial v}{\partial z} \\ \frac{\partial w}{\partial x} & \frac{\partial w}{\partial y} & \frac{\partial w}{\partial z} \end{bmatrix}, \quad \left(\operatorname{grad}\tilde{\mathbf{V}}\right)^{\breve{\mathbf{T}}} = \begin{bmatrix} \frac{\partial u}{\partial x} & \frac{\partial v}{\partial x} & \frac{\partial w}{\partial x} \\ \frac{\partial u}{\partial y} & \frac{\partial v}{\partial y} & \frac{\partial w}{\partial y} \\ \frac{\partial u}{\partial z} & \frac{\partial v}{\partial z} & \frac{\partial w}{\partial z} \end{bmatrix}, \qquad (1.13)$$

By using the above expressions $(1.10) - (1.13)$, the momentum equation for couple stress fluid takes the following form

$$\rho \frac{d\tilde{\mathbf{V}}}{dt} = \nabla p + \mu \nabla^2 \tilde{\mathbf{V}} - n^* \nabla^4 \tilde{\mathbf{V}}, \qquad (1.14)$$

By employing the operator ∇ on the velocity field, the quantities $\nabla^2 \tilde{\mathbf{V}}$ and $\nabla^4 \tilde{\mathbf{V}}$ can be easily found which are

$$\nabla^2 \tilde{\mathbf{V}} = \begin{bmatrix} \frac{\partial^2 u}{\partial x^2} + \frac{\partial^2 u}{\partial y^2} + \frac{\partial^2 u}{\partial z^2} \\ \frac{\partial^2 v}{\partial x^2} + \frac{\partial^2 v}{\partial y^2} + \frac{\partial^2 v}{\partial z^2} \\ \frac{\partial^2 w}{\partial x^2} + \frac{\partial^2 w}{\partial y^2} + \frac{\partial^2 w}{\partial z^2} \end{bmatrix}, \quad \nabla^4 \tilde{\mathbf{V}} = \begin{bmatrix} \frac{\partial^4 u}{\partial x^4} + \frac{\partial^4 u}{\partial y^4} + \frac{\partial^4 u}{\partial z^4} \\ \frac{\partial^4 v}{\partial x^4} + \frac{\partial^4 v}{\partial y^4} + \frac{\partial^4 v}{\partial z^4} \\ \frac{\partial^4 w}{\partial x^4} + \frac{\partial^4 w}{\partial y^4} + \frac{\partial^4 w}{\partial z^4} \end{bmatrix}, \qquad (1.15)$$

By using Eqs. (1.14) and (1.15), we write

$$\frac{\partial u}{\partial t} + u\frac{\partial u}{\partial x} + v\frac{\partial u}{\partial y} + w\frac{\partial u}{\partial z} = \nu\left(\frac{\partial^2 u}{\partial x^2} + \frac{\partial^2 u}{\partial y^2} + \frac{\partial^2 u}{\partial z^2}\right)$$
$$-\nu'\left(\frac{\partial^4 u}{\partial x^4} + \frac{\partial^4 u}{\partial y^4} + \frac{\partial^4 u}{\partial z^4}\right), \qquad (1.16)$$

$$\frac{\partial v}{\partial t} + u\frac{\partial v}{\partial x} + v\frac{\partial v}{\partial y} + w\frac{\partial v}{\partial z} = \nu\left(\frac{\partial^2 v}{\partial x^2} + \frac{\partial^2 v}{\partial y^2} + \frac{\partial^2 v}{\partial z^2}\right)$$
$$-\nu'\left(\frac{\partial^4 v}{\partial x^4} + \frac{\partial^4 v}{\partial y^4} + \frac{\partial^4 v}{\partial z^4}\right), \qquad (1.17)$$

in which $\nu' = n^*/\rho$ is the couple stress viscosity. The governing boundary layer expressions for three dimensional flow of couple stress fluid are

$$\frac{\partial u}{\partial t} + u\frac{\partial u}{\partial x} + v\frac{\partial u}{\partial y} + w\frac{\partial u}{\partial z} = \nu\left(\frac{\partial^2 u}{\partial z^2}\right) - \nu'\left(\frac{\partial^4 u}{\partial z^4}\right), \qquad (1.18)$$

$$\frac{\partial v}{\partial t} + u\frac{\partial v}{\partial x} + v\frac{\partial v}{\partial y} + w\frac{\partial v}{\partial z} = \nu\left(\frac{\partial^2 v}{\partial z^2}\right) - \nu'\left(\frac{\partial^4 v}{\partial z^4}\right). \qquad (1.19)$$

1.7 Modes of heat transfer

Heat transfer is a mechanism which deals with the transfer of heat within the system. Transport of heat is the transfer of thermal energy from high to low temperature regions when two physical system or two objects are in contact. Three basic modes are utilized to develop heat transfer mechanism which are define as follows:

1.7.1 Conduction

Conduction is the mode of heat transfer in which heat is shifted from one place to another place due to the collisions of particles which are in contact but particles do not change their positions. Conduction is always occured in solid materials. In very rare cases conduction may be possible in liquids.

1.7.2   Convection

Convection is the mode of heat transfer in which heat is transferred from hot places to cold places by the transfer of particles or molecules. Convection plays major role in both liquid and gases.

Forced convection

Forced convection is a process of heat transfer in which some external source is utilized to produce motion in fluid. Examples of forced convection are pump, stretching, pressure and many others.

Natural convection

This mechanism is always occured due to the differences of temperature without any external source. It is also known as free convection. Free convection is always occured due to gravity effects.

Mixed convection

Mixed convection is that type of convection in which transfer of heat takes place due to both natural and forced convections.

1.7.3   Radiation

Radiation is that mechanism in which transfer of heat occurs directly by electromagnetic radiations.

1.8 Non-dimensional numbers

1.8.1 Prandtl number

It describes the ratio of momentum diffusivity (ν) to the thermal diffusivity (α). In mathematical form it can be written as

$$\text{Pr} = \frac{\text{momentum diffusivity } (\nu)}{\text{thermal diffusivity } (\alpha)} = \frac{\mu c_p}{k}, \tag{1.20}$$

where μ stands for the dynamic viscosity, c_p represents the specific heat and k designates the thermal conductivity. In heat transfer mechanism, Prandtl number controls the momentum and thermal boundary layers thicknesses.

1.8.2 Lewis number

Lewis number is defined as the nondimensional quantity which explains the thermal diffusivity to Brownian diffusivity ratio. Mathematically

$$Le = \frac{\text{thermal diffusivity}}{\text{Brownian diffusivity}} = \frac{\alpha}{D_B} \tag{1.21}$$

Note that in above expression α signifies the thermal diffusivity and D_B represents the Brownian diffusivity.

1.8.3 Magnetic number

It is described as the ratio of electromagnetic to viscous forces. Mathematically it can be expressed as

$$M^2 = \frac{\sigma B_0^2 L}{\rho U_w}, \tag{1.22}$$

In which σ denotes the electrical conductivity, B_0 signifies the uniform magnetic field, L shows the characteristic length, ρ represents the fluid density and U_w depicts the velocity.

1.8.4 Reynolds number

Inertial to viscous forces ratio is termed as Reynolds number. Mathematically one can write it as

$$\text{Re} = \frac{\text{inertial force}}{\text{viscous force}} = \frac{\rho V L}{\mu} = \frac{V L}{\nu}, \qquad (1.23)$$

Here ρ denotes the fluid density, V represents the mean velocity of fluid, L stands for characteristic length and μ signifies the dynamic viscosity. Reynolds number is utilized to observe different flow behaviors like laminar or turbulent flows. Laminar flow is arised due to the low Reynolds number, where the viscous forces are dominant. At high Reynolds number turbulent flow arise, where the inertial forces are dominant.

1.8.5 Coefficient of skin friction

It is the drag force between the fluid and solid's surface when fluid is passing through it which leads to slow down the motion of fluid. Mathematically it is stated as

$$C_f = \frac{\tau_w}{\frac{1}{2}\rho U_w^2}, \qquad (1.24)$$

where

$$\tau_w = \mu \left(\frac{\partial u}{\partial y}\right)_{y=0}, \qquad (1.25)$$

In above relation τ_w represents the shear stress at the surface, U_w stands for velocity and ρ denotes the fluid density.

1.8.6 Nusselt number

Convective to conductive heat transfer coefficients ratio is known as Nusselt number. In mathematical form one can write

$$Nu = \frac{x q_w}{k(T_w - T_\infty)}, \qquad (1.26)$$

where

$$q_w = -k \left(\frac{\partial T}{\partial y}\right)_{y=0}, \qquad (1.27)$$

where q_w denotes the wall heat flux, T_w represents the wall temperature, T_∞ stands for ambient fluid temperature and k represents the thermal conductivity.

1.9 Fundamental laws

1.9.1 Mass conservation law

It is stated that the total mass in any closed system will remain constant. Mathematically

$$\frac{D\rho}{Dt} + \rho\boldsymbol{\nabla}.\mathbf{V} = 0, \tag{1.28}$$

or

$$\frac{\partial\rho}{\partial t} + (\mathbf{V}.\boldsymbol{\nabla})\,\rho + \rho\boldsymbol{\nabla}.\mathbf{V} = 0, \tag{1.29}$$

or

$$\frac{\partial\rho}{\partial t} + \boldsymbol{\nabla}.\,(\rho\mathbf{V}) = 0. \tag{1.30}$$

The above expression represents the continuity equation. Here ρ stands for fluid density and $\mathbf{V}$ depicts the velocity profile. Due to steady state flow Eq. (1.30) takes the following form

$$\boldsymbol{\nabla}.\,(\rho\mathbf{V}) = 0, \tag{1.31}$$

and if the fluid is incompressible then above equation takes the following form

$$\boldsymbol{\nabla}.\mathbf{V} = 0. \tag{1.32}$$

1.9.2 Momentum conservation law

This law states that the total momentum of a closed system is conserved. General form of this law is given below

$$\rho\frac{D\mathbf{V}}{Dt} = \boldsymbol{\nabla}.\boldsymbol{\tau} + \rho\mathbf{b}, \tag{1.33}$$

Here inertial, surface and body forces are indicated by the terms $\rho\frac{D\mathbf{V}}{Dt}$, $\nabla.\boldsymbol{\tau}$ and $\rho\mathbf{b}$ respectively. Cauchy stress tensor is represented by $\boldsymbol{\tau} = -p\mathbf{I} + \mathbf{S}$, pressure is designated by p, $\mathbf{I}$ shows the

identity tensor, $\frac{D}{Dt}$ shows the material time derivative, $\mathbf{S}$ stands for extra stress tensor and $\mathbf{b}$ denotes the body force.

1.9.3 Energy conservation law

The energy equation for nanofluid can be written as

$$\rho_f c_f \frac{DT}{Dt} = \boldsymbol{\tau}.\mathbf{L} + k\boldsymbol{\nabla}^2 T + \rho_p c_p \left(D_B \boldsymbol{\nabla} C.\boldsymbol{\nabla} T + \frac{D_T}{T_\infty} \boldsymbol{\nabla} T.\boldsymbol{\nabla} T \right), \tag{1.34}$$

Where ρ_f stands for base fluid density, c_f represents the specific heat of base fluid, T stands for temperature, $\boldsymbol{\tau}$ represents the stress tensor, $\mathbf{L}$ stands for rate of strain tensor, k denotes the thermal conductivity, ρ_p depicts the density of nanoparticles, D_B denotes Brownian diffusivity and D_T stands for thermophoretic diffusion coefficient.

1.9.4 Concentration conservation law

The concentration equation for nanofluid can be written as

$$\frac{DC}{Dt} = D_B \boldsymbol{\nabla}^2 C + \frac{D_T}{T_\infty} \boldsymbol{\nabla}^2 T \tag{1.35}$$

where C stands for nanoparticles concentration, D_B represents the Brownian diffusion coefficient, D_T stands for thermophoretic coefficient and T depicts the temperature.

1.10 Homotopic analysis technique

This technique is developed by Liao [33] to find the series solutions of nonlinear problems. This technique gives us convergent solutions for nonlinear problems. In order to understand the basic concept of homotopy analysis technique (HAM), we assume a differential equation

$$\mathcal{N}[u(x)] = 0, \tag{1.36}$$

In above equation $\mathcal{N}$ represents the non-linear operator and $u(x)$ depicts the unknown function in which x is the independent variable. Zeroth-order deformation equation is written in the

following form

$$(1 - Þ^*) \mathcal{L} [\breve{u}(x; Þ^*) - u_0(x)] = Þ^* \hbar \mathcal{N} [\breve{u}(x; Þ^*)], \tag{1.37}$$

where $u_0(x)$ depicts the initial approximation, $\mathcal{L}$ denotes the auxiliary linear operator, $Þ^*$ $\in [0, 1]$ designates an embedding parameter, $\hbar$ represents the nonzero auxiliary parameter and $\breve{u}(x; Þ^*)$ stands for unknown function of x and $Þ^*$. Setting $Þ^* = 0$ and $Þ^* = 1$, one has

$$\breve{u}(x; 0) = u_0(x) \quad \text{and} \quad \breve{u}(x; 1) = u(x). \tag{1.38}$$

The solution $\breve{u}(x; Þ^*)$ shows the variation from initial approximation $u_0(x)$ to the final desired solution $u(x)$ when $Þ^*$ goes from 0 to 1. Taylor series expansion gives us the following relations

$$\breve{u}(x; Þ^*) = u_0(x) + \sum_{\hat{m}=1}^{\infty} u_{\hat{m}}(x) Þ^{*\hat{m}}, \ u_{\hat{m}}(x) = \frac{1}{\hat{m}!} \left. \frac{\partial^{\hat{m}} \breve{u}(x, Þ^*)}{\partial Þ^{*\hat{m}}} \right|_{Þ^*=0}. \tag{1.39}$$

For $Þ^* = 1$ we get

$$u(x) = u_0(x) + \sum_{\hat{m}=1}^{\infty} u_{\hat{m}}(x). \tag{1.40}$$

By differentiating $\hat{m}$ times the zeroth order deformation i.e., Eq. (1.37) with respect to $Þ^*$ then divided by $\hat{m}!$ and by setting $Þ^* = 0$ we have the following $\hat{m}$th order equation

$$\mathcal{L}[u_{\hat{m}}(x) - \chi_{\hat{m}} u_{\hat{m}-1}(x)] = \hbar \tilde{\mathcal{R}}_{\hat{m}}(x), \tag{1.41}$$

$$\tilde{\mathcal{R}}_{\hat{m}}(x) = \frac{1}{(\hat{m}-1)!} \left. \frac{\partial^{\hat{m}} \mathcal{N}[\breve{u}(x; Þ^*)]}{\partial Þ^{*\hat{m}}} \right|_{Þ^*=0}, \tag{1.42}$$

where

$$\chi_{\hat{m}} = \begin{cases} 0, & \hat{m} \leq 1, \\ 1, & \hat{m} > 1. \end{cases} \tag{1.43}$$

15

Chapter 2

Flow of nanofluid over a nonlinearly stretching surface with convective effect

2.1   Introduction

This chapter addresses the two-dimensional flow of an incompressible viscous fluid subject to the convective surface boundary condition. The flow is generated due to an impermeable sheet which is stretched nonlinearly. Heat and mass transfer is studied through the Brownian motion and thermophoresis effects. Newly constructed boundary condition having zero mass flux of nanoparticles at the boundary is incorporated. Mathematical formulation is made under boundary layer and small magnetic Reynolds number assumptions. Suitable transformations are employed to convert the nonlinear partial differential system into the nonlinear ordinary differential system. Homotopic solutions of resulting nonlinear system are constructed and verified. Graphs are sketched to explore the effects of distinct emerging flow parameters on the temperature and concentration profiles. Nusselt number is also computed and discussed. The contents of present chapter provides review of research work examined by Mustafa et al. [8].

2.2   Problem development

We assume a steady two dimensional incompressible flow of Newtonian fluid past over a surface which is stretched nonlinearly. Here we consider the Cartesian coordinate system in such a manner that the $x-$axis is taken in that direction along which the sheet is stretched and $y-$axis is orthogonal to the sheet. Stretching of the sheet is assumed with velocity $U_w(x) = ax^n$ along the $x-$direction with a, $n > 0$ as the constants. Effects of Brownian motion and thermophoresis in the present flow problem are also taken into account. The surface temperature is regulated by a convective heating mechanism which is peculiarized by the heat transfer coefficient h_f and temperature of hot fluid T_f under the sheet. The governing boundary layer expressions for present flow analysis are
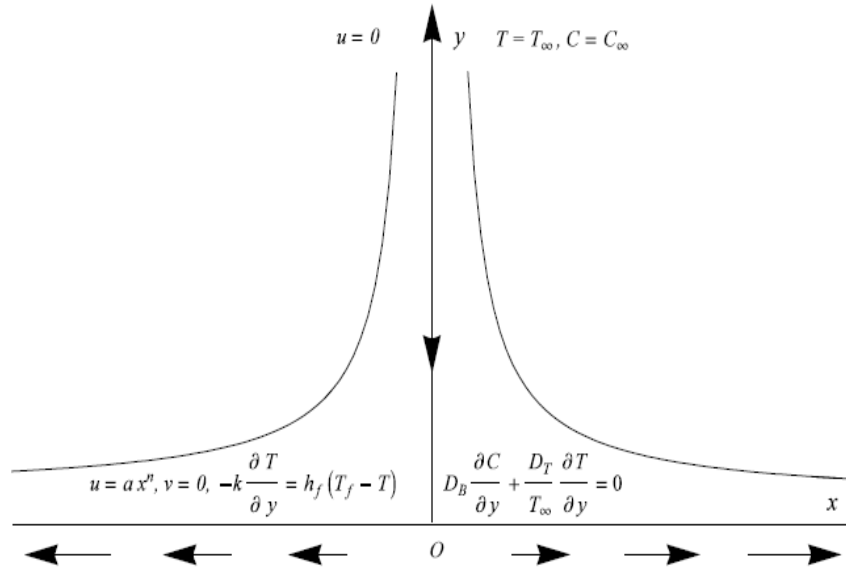
Fig. 2.1 : Physical sketch of the problem.

$$\frac{\partial u}{\partial x} + \frac{\partial v}{\partial y} = 0, \tag{2.1}$$

$$u\frac{\partial u}{\partial x} + v\frac{\partial u}{\partial y} = \nu\frac{\partial^2 u}{\partial y^2}, \tag{2.2}$$

$$u\frac{\partial T}{\partial x} + v\frac{\partial T}{\partial y} = \alpha\frac{\partial^2 T}{\partial y^2} + \frac{(\rho c)_p}{(\rho c)_f}\left(D_B\left(\frac{\partial T}{\partial y}\frac{\partial C}{\partial y}\right) + \frac{D_T}{T_\infty}\left(\frac{\partial T}{\partial y}\right)^2\right), \tag{2.3}$$

17

$$u\frac{\partial C}{\partial x} + v\frac{\partial C}{\partial y} = D_B\left(\frac{\partial^2 C}{\partial y^2}\right) + \frac{D_T}{T_\infty}\left(\frac{\partial^2 T}{\partial y^2}\right). \tag{2.4}$$

The subjected boundary conditions for the considered flow problem are

$$u = U_w(x) = ax^n, \ v = 0, \ -k\frac{\partial T}{\partial y} = h_f\left(T_f - T\right), \ D_B\frac{\partial C}{\partial y} + \frac{D_T}{T_\infty}\frac{\partial T}{\partial y} = 0 \text{ at } y = 0, \tag{2.5}$$

$$u \to 0, \quad T \to T_\infty, \quad C \to C_\infty \quad \text{as } y \to \infty. \tag{2.6}$$

Here u and v represent the flow velocities in the horizontal and vertical directions respectively, $\nu\left(=\mu/\rho_f\right)$ stands for kinematic viscosity, μ denotes the dynamic viscosity, ρ_f stands for density of base fluid, T stands for temperature, $\alpha\left(=k/(\rho c)_f\right)$ denotes the thermal diffusivity, k stands for thermal conductivity of fluid, $(\rho c)_f$ stands for heat capacity of fluid, $(\rho c)_p$ stands for effective heat capacity of nanoparticles, D_B denotes the Brownian diffusivity, C represents concentration, D_T stands for thermophoretic diffusion coefficient, $h_f = hx^{\frac{n-1}{2}}$ stands for non-uniform heat transfer coefficient. T_∞ denotes the ambient fluid temperature and C_∞ represents the ambient fluid concentration. Using the following transformations

$$\left.\begin{array}{l} u = ax^n f'(\eta), \ v = -\left(\frac{a\nu(n+1)}{2}\right)^{1/2}(x)^{\frac{n-1}{2}}\{f + \frac{n-1}{n+1}\eta f'\}, \\ \theta(\eta) = \frac{T-T_\infty}{T_f-T_\infty}, \ \phi(\eta) = \frac{C-C_\infty}{C_\infty}, \ \eta = \left(\frac{a(n+1)}{2\nu}\right)^{1/2}(x)^{\frac{n-1}{2}}y. \end{array}\right\} \tag{2.7}$$

Eq. (2.1) is now identically satisfied and Eqs. (2.2) − (2.6) take the following forms

$$f''' + ff'' - \frac{2n}{n+1}f'^2 = 0, \tag{2.8}$$

$$\theta'' + \Pr\left(f\theta' + Nb\theta'\phi' + Nt\theta'^2\right) = 0, \tag{2.9}$$

$$\phi'' + Le\,\Pr f\phi' + \frac{Nt}{Nb}\theta'' = 0, \tag{2.10}$$

$$f(0) = 0, \ f'(0) = 1, \ \theta'(0) = -\gamma\left(1 - \theta\left(0\right)\right), \ Nb\phi'(0) + Nt\theta'(0) = 0, \tag{2.11}$$

$$f'(\infty) \to 0, \ \theta(\infty) \to 0, \ \phi(\infty) \to 0. \tag{2.12}$$

In above expressions Pr stands for Prandtl number, Nb depicts the Brownian motion parameter, Nt represents the thermophoresis parameter, γ stands for Biot number and Le denotes the Lewis

number. These parameters can be specified by the following definitions

$$\left.\begin{array}{c} \Pr = \frac{\nu}{\alpha}, \ Nb = \frac{(\rho c)_p D_B C_\infty}{(\rho c)_f \nu}, \\ Nt = \frac{(\rho c)_p D_T (T_f - T_\infty)}{(\rho c)_f \nu T_\infty}, \ \gamma = \frac{h_f}{k} \sqrt{\frac{\nu}{a}}, \ Le = \frac{\alpha}{D_B}. \end{array}\right\} \tag{2.13}$$

The nondimensional forms of coefficient of skin-friction and Nusselt number are given below

$$C_{fx} \operatorname{Re}_x^{1/2} = \left(\frac{n+1}{2}\right)^{1/2} f''(0),$$

$$Nu_x \operatorname{Re}_x^{-1/2} = -\left(\frac{n+1}{2}\right)^{1/2} \theta'(0). \tag{2.14}$$

where $\operatorname{Re}_x = U_w x / \nu$ represent the local Reynold number. From the above it can be analyzed that the nondimensional mass flux represented by a Sherwood number Sh_x is zero.

2.3 Series solutions

The approximate series solutions through the homotopy analysis technique (HAM) requires the appropriate initial approximations and auxiliary linear operators for the governing problems which are given below

$$f_0(\eta) = 1 - \exp(-\eta), \quad \theta_0(\eta) = \frac{\gamma}{1+\gamma} \exp(-\eta), \quad \phi_0(\eta) = -\frac{\gamma}{1+\gamma} \frac{Nt}{Nb} \exp(-\eta), \tag{2.15}$$

$$\mathcal{L}_f = \frac{d^3 f}{d\eta^3} - \frac{df}{d\eta}, \quad \mathcal{L}_\theta = \frac{d^2 \theta}{d\eta^2} - \theta, \quad \mathcal{L}_\phi = \frac{d^2 \phi}{d\eta^2} - \phi. \tag{2.16}$$

The above linear operators have the following properties

$$\left.\begin{array}{c} \mathcal{L}_f \left[B_1 + B_2 \exp(\eta) + B_3 \exp(-\eta)\right] = 0, \\ \mathcal{L}_\theta \left[B_4 \exp(\eta) + B_5 \exp(-\eta)\right] = 0, \\ \mathcal{L}_\phi \left[B_6 \exp(\eta) + B_7 \exp(-\eta)\right] = 0, \end{array}\right\} \tag{2.17}$$

in which B_j $(j = 1 - 7)$ stands for arbitrary constants.

2.3.1 Zeroth-order deformation equations

$$(1 - \text{P}^*)\mathcal{L}_f\left[\breve{f}(\eta, \text{P}^*) - f_0(\eta)\right] = \text{P}^*\hbar_f\mathcal{N}_f[\breve{f}(\eta, \text{P}^*)], \tag{2.18}$$

$$(1 - \text{P}^*)\mathcal{L}_\theta\left[\breve{\theta}(\eta, \text{P}^*) - \theta_0(\eta)\right] = \text{P}^*\hbar_\theta\mathcal{N}_\theta[\breve{f}(\eta, \text{P}^*), \breve{\theta}(\eta, \text{P}^*), \breve{\phi}(\eta, \text{P}^*)], \tag{2.19}$$

$$(1 - \text{P}^*)\mathcal{L}_\phi[\breve{\phi}(\eta, \text{P}^*) - \phi_0(\eta)] = \text{P}^*\hbar_\phi\mathcal{N}_\phi[\breve{f}(\eta, \text{P}^*), \breve{\theta}(\eta, \text{P}^*), \breve{\phi}(\eta, \text{P}^*)], \tag{2.20}$$

$$\left.\begin{array}{l}\breve{f}(0, \text{P}^*) = 0, \ \breve{f}'(0, \text{P}^*) = 1, \ \breve{f}'(\infty, \text{P}^*) = 0, \ \breve{\theta}'(0, \text{P}^*) = -\gamma\left(1 - \breve{\theta}(0, \text{P}^*)\right), \\ \breve{\theta}(\infty, \text{P}^*) = 0, \ Nb\breve{\phi}'(0, \text{P}^*) + Nt\breve{\theta}'(0, \text{P}^*) = 0, \ \breve{\phi}(\infty, \text{P}^*) = 0, \end{array}\right\} \tag{2.21}$$

$$\mathcal{N}_f\left[\breve{f}(\eta; \text{P}^*)\right] = \frac{\partial^3\breve{f}}{\partial\eta^3} + \breve{f}\frac{\partial^2\breve{f}}{\partial\eta^2} - \frac{2n}{n+1}\left(\frac{\partial\breve{f}}{\partial\eta}\right)^2, \tag{2.22}$$

$$\mathcal{N}_\theta\left[\breve{f}(\eta; \text{P}^*), \breve{\theta}(\eta, \text{P}^*), \breve{\phi}(\eta, \text{P}^*)\right] = \frac{\partial^2\breve{\theta}}{\partial\eta^2} + \text{Pr}\,\breve{f}\frac{\partial\breve{\theta}}{\partial\eta} + \text{Pr}\,Nb\frac{\partial\breve{\theta}}{\partial\eta}\frac{\partial\breve{\phi}}{\partial\eta} + \text{Pr}\,Nt\left(\frac{\partial\breve{\theta}}{\partial\eta}\right)^2, \tag{2.23}$$

$$\mathcal{N}_\phi\left[\breve{f}(\eta; \text{P}^*), \breve{\theta}(\eta, \text{P}^*), \breve{\phi}(\eta, \text{P}^*)\right] = \frac{\partial^2\breve{\phi}}{\partial\eta^2} + Le\,\text{Pr}\,\breve{f}\frac{\partial\breve{\phi}}{\partial\eta} + \frac{Nt}{Nb}\frac{\partial^2\breve{\theta}}{\partial\eta^2}. \tag{2.24}$$

Here $\text{P}^* \in [0, 1]$ denotes the embedding parameter, $\hbar_f$, $\hbar_\theta$ and $\hbar_\phi$ stands for nonzero auxiliary parameters and $\mathcal{N}_f$, $\mathcal{N}_\theta$ and $\mathcal{N}_\phi$ represent the nonlinear operators.

2.3.2 $\hat{m}$th-order deformation problems

$$\mathcal{L}_f\left[f_{\hat{m}}(\eta) - \chi_{\hat{m}}f_{\hat{m}-1}(\eta)\right] = \hbar_f\tilde{\mathcal{R}}_{\hat{m}}^f(\eta), \tag{2.25}$$

$$\mathcal{L}_\theta\left[\theta_{\hat{m}}(\eta) - \chi_{\hat{m}}\theta_{\hat{m}-1}(\eta)\right] = \hbar_\theta\tilde{\mathcal{R}}_{\hat{m}}^\theta(\eta), \tag{2.26}$$

$$\mathcal{L}_\phi\left[\phi_{\hat{m}}(\eta) - \chi_{\hat{m}}\phi_{\hat{m}-1}(\eta)\right] = \hbar_\phi\tilde{\mathcal{R}}_{\hat{m}}^\phi(\eta), \tag{2.27}$$

$$\left.\begin{array}{l}f_{\hat{m}}(0) = f'_{\hat{m}}(0) = f'_{\hat{m}}(\infty) = 0, \ \theta'_{\hat{m}}(0) + \gamma\theta_{\hat{m}}(0) = 0, \\ Nb\phi'_{\hat{m}}(0) + Nt\theta'_{\hat{m}}(0) = 0, \ \theta_{\hat{m}}(\infty) = \phi_{\hat{m}}(\infty) = 0, \end{array}\right\} \tag{2.28}$$

$$\tilde{\mathcal{R}}_{\hat{m}}^f(\eta) = f'''_{\hat{m}-1} + \sum_{k=0}^{\hat{m}-1}(f_{\hat{m}-1-k}f''_k) - \left(\frac{2n}{n+1}\right)\sum_{k=0}^{\hat{m}-1}(f'_{\hat{m}-1-k}f'_k), \tag{2.29}$$

$$\tilde{\mathcal{R}}_{\hat{m}}^\theta(\eta) = \theta''_{\hat{m}-1} + \text{Pr}\sum_{k=0}^{\hat{m}-1}(f_{\hat{m}-1-k}\theta'_k) + \text{Pr}\,Nb\sum_{k=0}^{\hat{m}-1}(\theta'_{\hat{m}-1-k}\phi'_k) + \text{Pr}\,Nt\sum_{k=0}^{\hat{m}-1}(\theta'_{\hat{m}-1-k}\theta'_k), \tag{2.30}$$

20

$$\tilde{\mathcal{R}}^{\phi}_{\hat{m}}(\eta) = \phi''_{\hat{m}-1}(\eta) + Le \Pr \sum_{k=0}^{\hat{m}-1} (f_{\hat{m}-1-k}\phi'_k) + \frac{Nt}{Nb}\theta''_{\hat{m}-1}, \tag{2.31}$$

$$\chi_{\hat{m}} = \begin{cases} 0, & \hat{m} \leq 1, \\ 1, & \hat{m} > 1, \end{cases} \tag{2.32}$$

Putting $Þ^* = 0$ and $Þ^* = 1$ we have

$$\breve{f}(\eta; 0) = f_0(\eta), \ \breve{f}(\eta; 1) = f(\eta), \tag{2.33}$$

$$\breve{\theta}(\eta, 0) = \theta_0(\eta), \ \breve{\theta}(\eta, 1) = \theta(\eta), \tag{2.34}$$

$$\breve{\phi}(\eta, 0) = \phi_0(\eta), \ \breve{\phi}(\eta, 1) = \phi(\eta). \tag{2.35}$$

When $Þ^*$ varies from 0 to 1 then $\breve{f}(\eta;Þ^*)$, $\breve{\theta}(\eta,Þ^*)$ and $\breve{\phi}(\eta, Þ^*)$ display variation from the initial approximations $f_0(\eta)$, $\theta_0(\eta)$ and $\phi_0(\eta)$ to the desired final solutions $f(\eta)$, $\theta(\eta)$ and $\phi(\eta)$ respectively. By using Taylor's series expansion we get the following expressions

$$\breve{f}(\eta; Þ^*) = f_0(\eta) + \sum_{\hat{m}=1}^{\infty} f_{\hat{m}}(\eta)Þ^{*\hat{m}}, \ f_{\hat{m}}(\eta) = \frac{1}{\hat{m}!}\frac{\partial^{\hat{m}}\breve{f}(\eta, Þ^*)}{\partial Þ^{*\hat{m}}}\bigg|_{Þ^*=0}, \tag{2.36}$$

$$\breve{\theta}(\eta, Þ^*) = \theta_0(\eta) + \sum_{\hat{m}=1}^{\infty} \theta_{\hat{m}}(\eta)Þ^{*\hat{m}}, \ \theta_{\hat{m}}(\eta) = \frac{1}{\hat{m}!}\frac{\partial^{\hat{m}}\breve{\theta}(\eta, Þ^*)}{\partial Þ^{*\hat{m}}}\bigg|_{Þ^*=0}, \tag{2.37}$$

$$\breve{\phi}(\eta, Þ^*) = \phi_0(\eta) + \sum_{\hat{m}=1}^{\infty} \phi_{\hat{m}}(\eta)Þ^{*\hat{m}}, \ \phi_{\hat{m}}(\eta) = \frac{1}{\hat{m}!}\frac{\partial^{\hat{m}}\breve{\phi}(\eta, Þ^*)}{\partial Þ^{*\hat{m}}}\bigg|_{Þ^*=0}, \tag{2.38}$$

The convergence of Eqs. $(2.36) - (2.38)$ highly depends upon the $\hbar_f$, $\hbar_\theta$ and $\hbar_\phi$. Considering that the values of non-zero auxiliary parameters $\hbar_f$, $\hbar_\theta$ and $\hbar_\phi$ are selected in such a way that Eqs. $(2.36) - (2.38)$ converge at $Þ^* = 1$, then

$$f(\eta) = f_0(\eta) + \sum_{\hat{m}=1}^{\infty} f_{\hat{m}}(\eta), \tag{2.39}$$

$$\theta(\eta) = \theta_0(\eta) + \sum_{\hat{m}=1}^{\infty} \theta_{\hat{m}}(\eta), \tag{2.40}$$

$$\phi(\eta) = \phi_0(\eta) + \sum_{\hat{m}=1}^{\infty} \phi_{\hat{m}}(\eta). \tag{2.41}$$

The general solutions $(f_{\hat{m}}, \theta_{\hat{m}}, \phi_{\hat{m}})$ of the Eqs. $(2.25) - (2.27)$ in terms of special solutions $(f_{\hat{m}}^*,$ $\theta_{\hat{m}}^*, \phi_{\hat{m}}^*)$ are presented by the following expressions

$$f_{\hat{m}}(\eta) = f_{\hat{m}}^*(\eta) + B_1 + B_2 \exp(\eta) + B_3 \exp(-\eta), \tag{2.42}$$

$$\theta_{\hat{m}}(\eta) = \theta_{\hat{m}}^*(\eta) + B_4 \exp(\eta) + B_5 \exp(-\eta), \tag{2.43}$$

$$\phi_{\hat{m}}(\eta) = \phi_{\hat{m}}^*(\eta) + B_6 \exp(\eta) + B_7 \exp(-\eta). \tag{2.44}$$

in which the constants B_j $(j = 1 - 7)$ through the boundary conditions (2.28) are given by

$$B_2 = B_4 = B_6 = 0, \ \ B_3 = \left. \frac{\partial f_{\hat{m}}^*(\eta)}{\partial \eta} \right|_{\eta=0}, \ \ B_1 = -B_3 - f_{\hat{m}}^*(0), \tag{2.45}$$

$$B_5 = \frac{1}{1+\gamma} \left(\left. \frac{\partial \theta_{\hat{m}}^*(\eta)}{\partial \eta} \right|_{\eta=0} - \gamma \theta_{\hat{m}}^*(0) \right), \tag{2.46}$$

$$B_7 = \left. \frac{\partial \phi_{\hat{m}}^*(\eta)}{\partial \eta} \right|_{\eta=0} + \frac{Nt}{Nb} \left(-B_5 + \left. \frac{\partial \theta_{\hat{m}}^*(\eta)}{\partial \eta} \right|_{\eta=0} \right). \tag{2.47}$$

2.3.3   Convergence analysis

Here the series solutions $(2.39) - (2.41)$ involve the auxiliary parameters $\hbar_f$, $\hbar_\theta$ and $\hbar_\phi$. No doubt the auxiliary parameters $\hbar_f$, $\hbar_\theta$ and $\hbar_\phi$ in series solutions accelerate the convergence. The $\hbar-$curves at 15th order of approximations are sketched to see the appropriate range of $\hbar_f$, $\hbar_\theta$ and $\hbar_\phi$. It is apparent from Figs. $(2.2) - (2.4)$ that the admissible ranges of $\hbar_f$, $\hbar_\theta$ and $\hbar_\phi$ are $-1.70 \leq \hbar_f \leq -0.15$, $-1.90 \leq \hbar_\theta \leq -0.28$ and $-2.20 \leq \hbar_\phi \leq -0.20$. Moreover the series

22

solutions are convergent in the entire zone of η when $\hbar_f = -1.0 = \hbar_\theta = \hbar_\phi$.

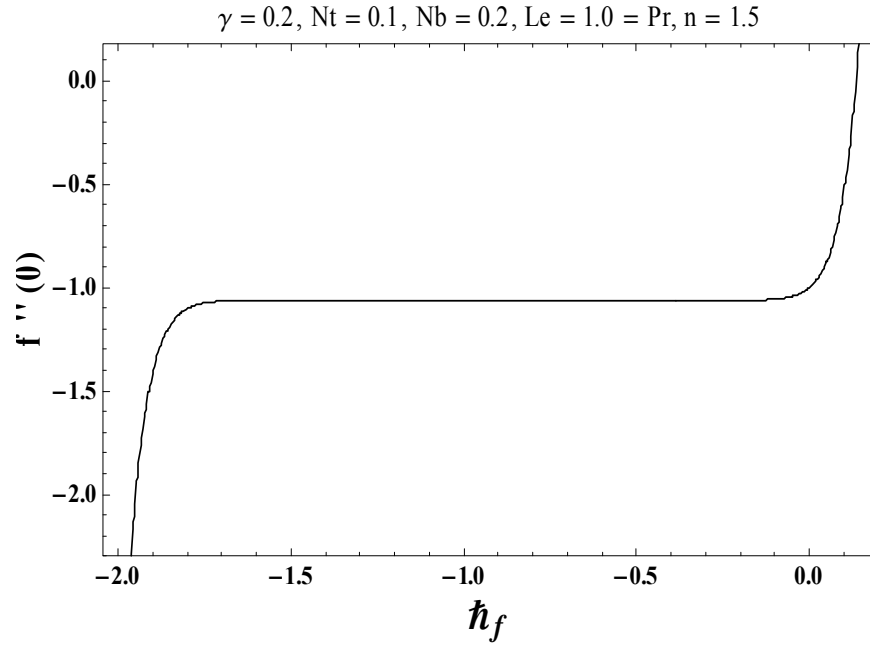$$\gamma = 0.2,\; Nt = 0.1,\; Nb = 0.2,\; Le = 1.0 = Pr,\; n = 1.5$$

Fig. 2.2 : $\hbar-$curve for the function $f(\eta)$.

$$n = 1.5,\; \gamma = 0.2,\; Nt = 0.1,\; Nb = 0.2,\; Le = 1.0 = Pr$$
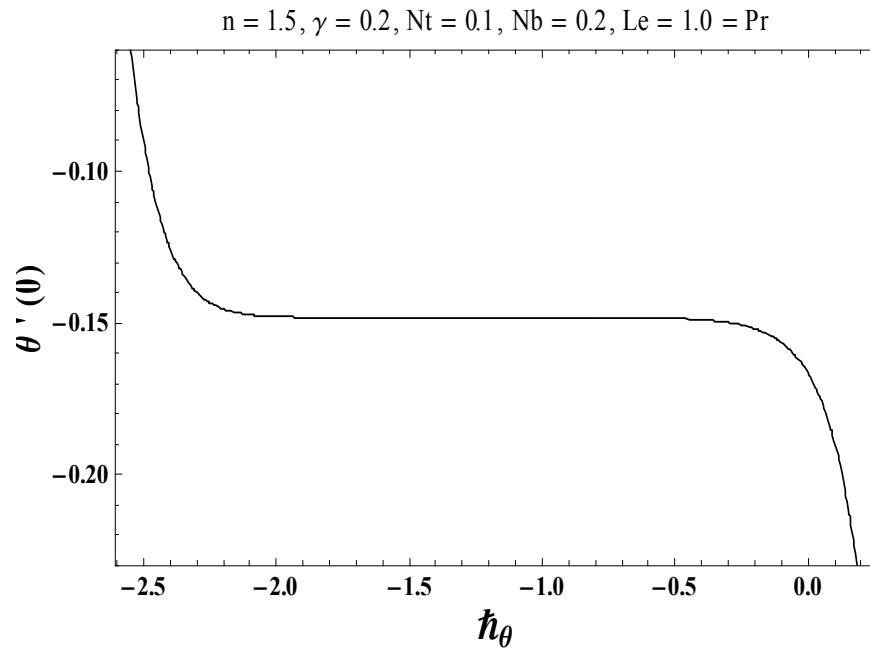
Fig. 2.3 : $\hbar-$curve for the function $\theta(\eta)$.
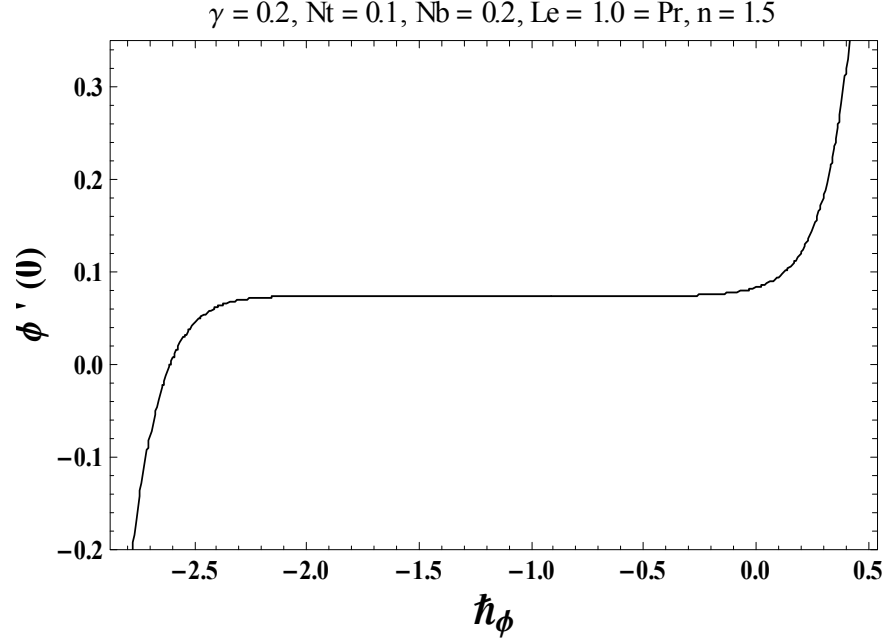
Fig. 2.4 : $\hbar-$curve for the function $\phi(\eta)$.

Table 2.1: Convergence of homotopic solutions when $n = 1.5$, $\gamma = 0.2$, $Nb = 0.2$, $Nt = 0.1$, $Le = 1.0$ and $\mathrm{Pr} = 1.0$.

Order of Approximation	$-f''(0)$	$-\theta'(0)$	$\phi'(0)$
1	1.06667	0.15741	0.07870
5	1.06162	0.14918	0.07459
11	1.06160	0.14829	0.07414
16	1.06160	0.14824	0.07412
25	1.06160	0.14824	0.07412
35	1.06160	0.14824	0.07412
50	1.06160	0.14824	0.07412

2.4 Results and discussion

Figs. $(2.5) - (2.12)$ are sketched to investigate the behaviors of some physical parameters on the nondimensional temperature $\theta(\eta)$ and concentration $\phi(\eta)$. The results are achieved at two distinct values of n just to compare the corresponding profiles in cases of linear and nonlinear stretching surfaces. Fig. 2.5 elucidates the influence of Prandtl number (Pr) on the temper-

ature profile $\theta(\eta)$. From fig. 2.5 it is observed that when we enhance the value of Prandtl number Pr reduction is occured in the temperature distribution and its related thickness of thermal layer. Physically larger and smaller Prandtl fluids correspond to weaker and stronger thermal diffusivities respectively. An enhancement in Prandtl number causes a weaker thermal diffusivity. Such weaker thermal diffusivity causes a lower temperature distribution $\theta(\eta)$ and less thickness of the thermal layer. Fig. 2.6 is plotted to see the impact of Biot number γ on the temperature distribution $\theta(\eta)$. An increment in γ causes a stronger convection which depicts higher temperature distribution and thicker thickness of the thermal layer. Fig. 2.7 is drawn to see the influence of thermophoresis parameter Nt on the temperature distribution $\theta(\eta)$. Larger values of thermophoresis parameter Nt causes a stronger temperature distribution. An enhancement in Nt leads to a stronger thermophoretic force which is responsible for a deeper transfer of nanoparticles in the ambient fluid which corresponds to a stronger temperature distribution and more thickness of thermal layer. From Fig. 2.8 we have seen that the concentration field $\phi(\eta)$ and thickness of concentration boundary layer are depreciated with an increment in Lewis number Le. Lewis number is based on Brownian diffusivity. The higher Lewis number corresponds to lower Brownian diffusivity. This lower Brownian diffusivity yields weaker concentration field $\phi(\eta)$. Fig. 2.9 depicts the behavior of Prandtl number (Pr) on the concentration distribution $\phi(\eta)$. Due to higher Prandtl number Pr decreasing behavior is noted in the concentration field $\phi(\eta)$. From Fig. 2.10, it is clearly analyzed that the concentration field $\phi(\eta)$ enhances for the higher values of Biot number γ. Fig. 2.11 displays the behavior of Brownian motion parameter Nb on concentration field $\phi(\eta)$. From this Fig. it is clearly analyzed that both concentration $\phi(\eta)$ and associated thickness of boundary layer are reduced with an increment in Nb. Fig. 2.12 shows concentration field $\phi(\eta)$ corresponding to various values of thermophoresis parameter Nt. Here we examined that by increasing thermophoresis parameter Nt, an enhancement is occured in the concentration field $\phi(\eta)$ and its related thickness of boundary layer. Table 2.1 is developed to analyze the numerical values of $-f''(0)$, $-\theta'(0)$ and $\phi'(0)$ at distinct order of homotopic deformations when $n = 1.5$, $\gamma = 0.2$, $Nb = 0.2$, $Nt = 0.1$, $Le = 1.0$, $Pr = 1.0$. It is clearly shown that the solution of velocity converges from 11th order of deformations while solutions of temperature and concentration converge from 16th order of homotopic approximations. Hence 16th order of deformation is essential for convergent solu-

tions of velocity, temperature and concentration profiles. Table 2.2 is computed to investigate the numerical values of Nusselt number $Nu_x \operatorname{Re}_x^{-1/2}$ for several values of physical parameters. From this table we noticed that the values of Nusselt number are decreased with an increment in Lewis number Le. However the Nusselt number is a constant function of Brownian motion parameter Nb.
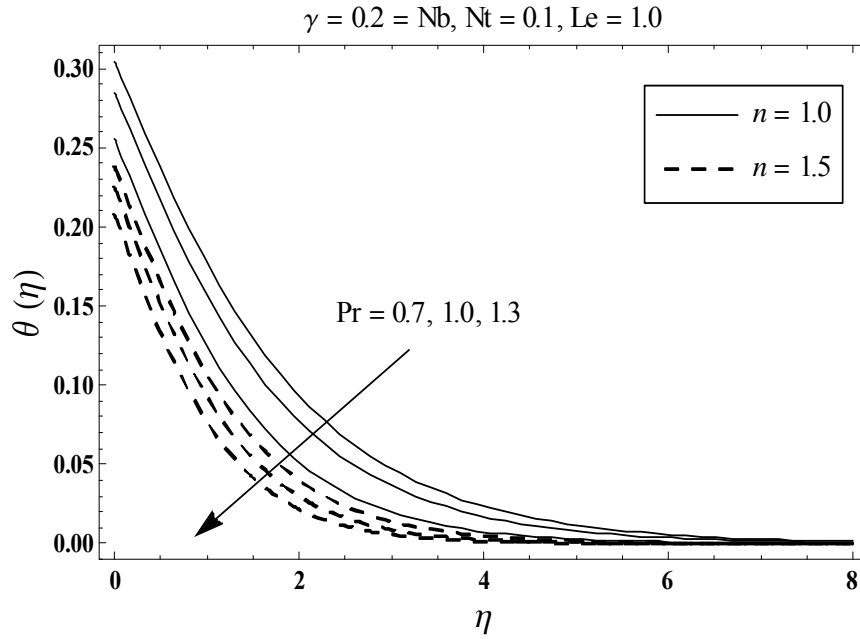
Fig. 2.5 : Behavior of Pr on $\theta(\eta)$.
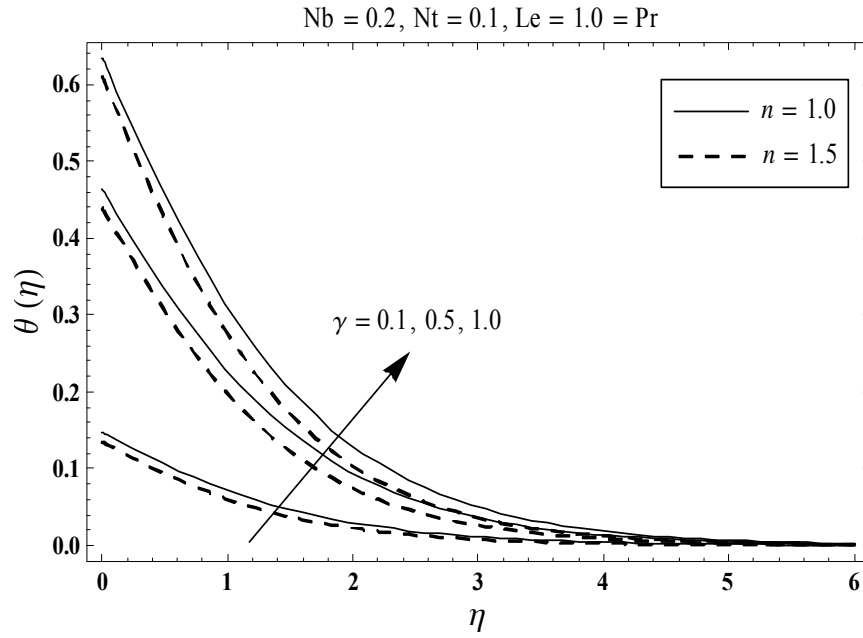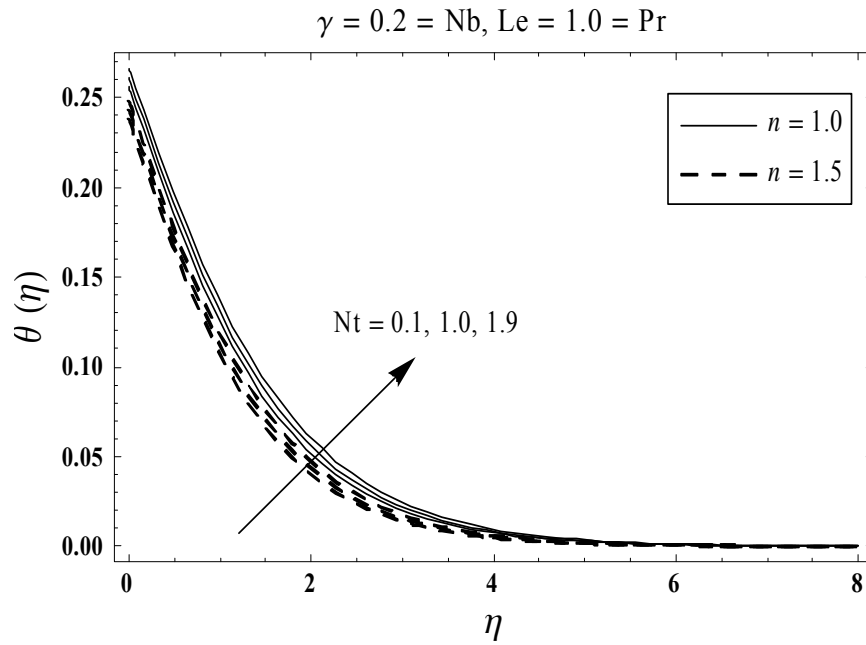
Nb = 0.2, Nt = 0.1, Le = 1.0 = Pr

Fig. 2.6 : Behavior of γ on $\theta(\eta)$.

$\gamma = 0.2$ = Nb, Le = 1.0 = Pr

Fig. 2.7 : Behavior of Nt on $\theta(\eta)$.

$\gamma = 0.2 = $ Nb, Nt $= 0.1$, Pr $=1.0$

Le $= 1.0, 1.25, 1.5$

$n = 1.0$
$n = 1.5$

Fig. 2.8 : Behavior of Le on $\phi(\eta)$.

$\gamma = 0.2 = $ Nb, Nt $= 0.1$, Le $= 1.0$

Pr $= 0.7, 1.0, 1.3$

$n = 1.0$
$n = 1.5$

Fig. 2.9 : Behavior of Pr on $\phi(\eta)$.

28

Nb = 0.2, Nt = 0.1, Le = 1.0 = Pr

$\gamma = 0.1, 0.5, 1.0$

$n = 1.0$

$n = 1.5$

Fig. 2.10 : Behavior of γ on $\phi(\eta)$.

$\gamma = 0.2$, Nt = 0.1, Le = 1.0 = Pr

Nb = 0.2, 0.5, 0.8

$n = 1.0$

$n = 1.5$
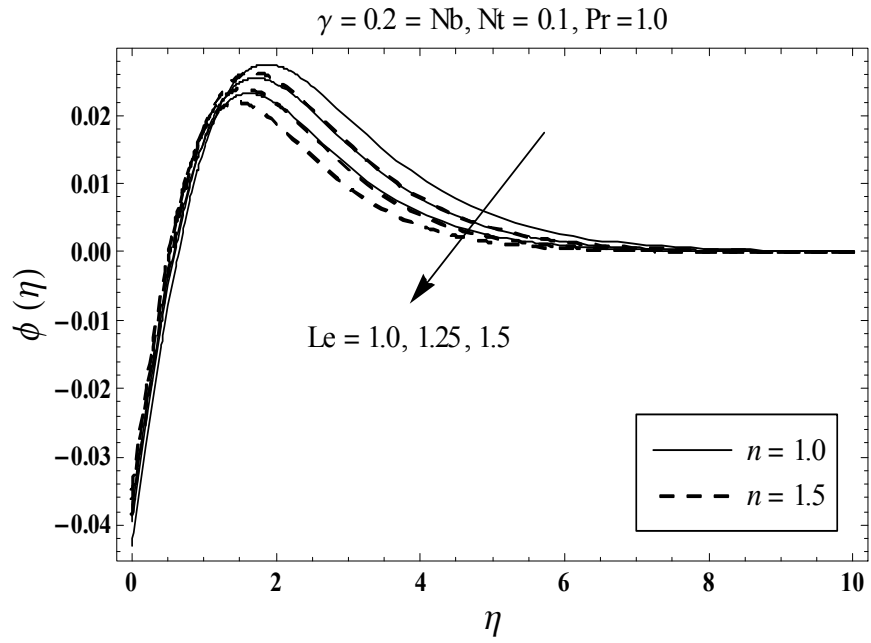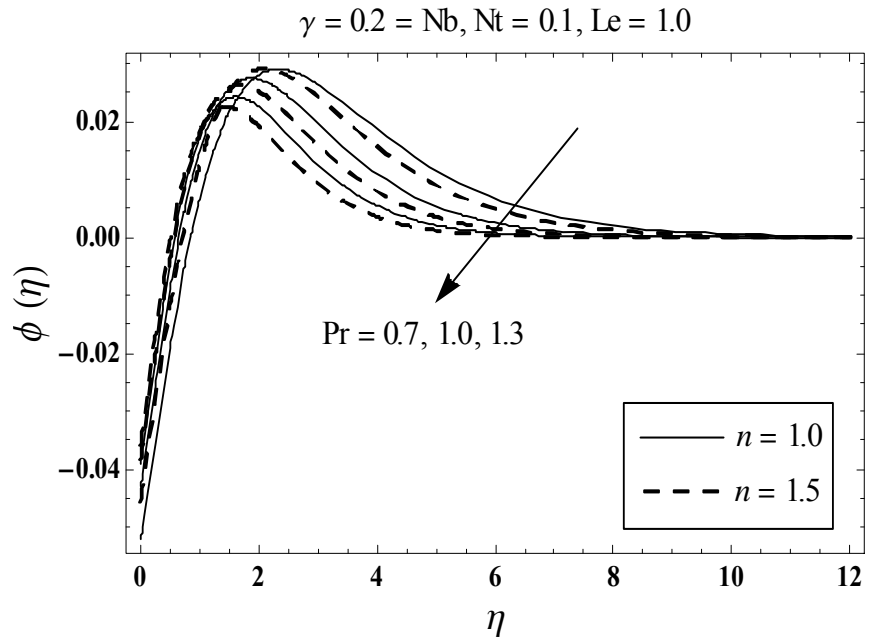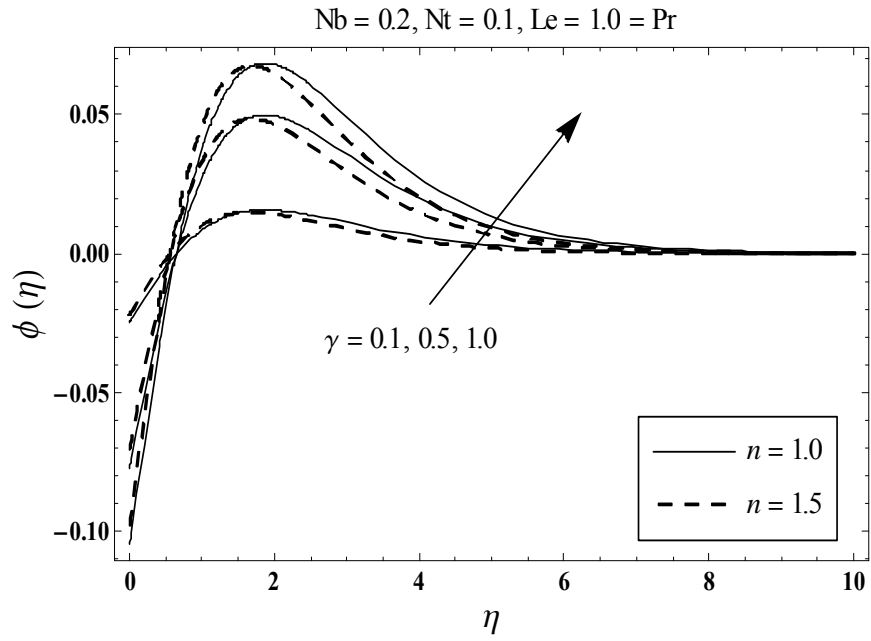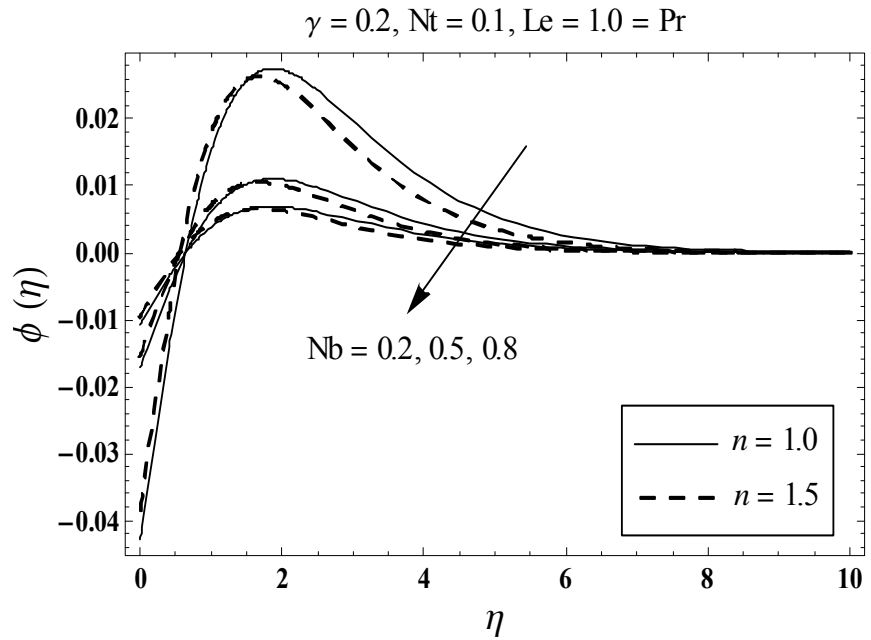
Fig. 2.11 : Behavior of Nb on $\phi(\eta)$.

29
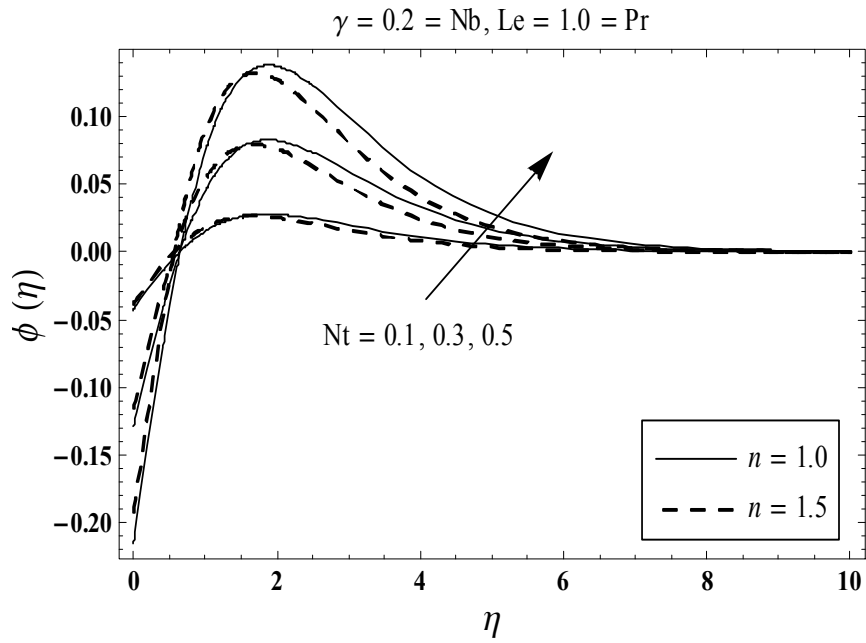
Fig. 2.12 : Behavior of Nt on $\phi(\eta)$.

Table 2.2: Numerical values of Nusselt number $Nu_x \operatorname{Re}_x^{-1/2}$ for several values of γ, Nt, Nb, Le and $\Pr$.

γ	Nt	Nb	Le	$\Pr$	$Nu_x \, \mathrm{Re}_x^{-1/2}$	
					$n = 1.0$	$n = 1.5$
0.1	0.1	0.2	1.0	1.0	0.0853	0.0953
0.7					0.3166	0.3515
1.2					0.3896	0.4319
0.2	0.0	0.2	1.0	1.0	0.1488	0.1659
	0.5				0.1482	0.1652
	1.0				0.1476	0.1644
0.2	0.1	0.5	1.0	1.0	0.1487	0.1658
		1.0			0.1487	0.1658
		1.5			0.1487	0.1658
0.2	0.1	0.2	0.5	1.0	0.1488	0.1658
			1.0		0.1487	0.1657
			1.5		0.1486	0.1656
0.2	0.1	0.2	1.0	0.7	0.1388	0.1545
				1.0	0.1487	0.1658
				1.3	0.1551	0.1729

2.5 Main findings

Two-dimensional flow of viscous nanofluid over a nonlinearly stretching sheet subject to the convective surface boundary condition is addressed. The key points of the present chapter are given below:

- An enhancement in the Biot number γ shows stronger temperature and concentration profiles.

- Influence of Prandtl number $\Pr$ on the temperature and concentration fields are qualitatively similar.

- Temperature profile $\theta(\eta)$ enhances by increasing thermophoresis parameter Nt.

- concentration profile $\phi(\eta)$ is decreased by an increment in Nb while it is enhanced for higher values of Nt.

- Nusselt number reduces by increasing Nt but it remains constant in case of Nb.

Chapter 3

MHD three dimensional flow of couple stress nanofluid over a nonlinearly stretching surface with convective effect

3.1 Introduction

This chapter explores the magnetohydrodynamic (MHD) steady three-dimensional flow of couple stress nanofluid in the presence of convective surface boundary condition. The sheet is stretched nonlinearly in two lateral directions in order to generate the flow. Temperature and concentration distributions are studied in the presence of Brownian motion and thermophoresis effects. Couple stress fluid is considered electrically conducting through non-uniform applied magnetic field. Mathematical formulation is developed via boundary layer approach. Nonlinear ordinary differential systems are constructed by employing suitable transformations. The resulting system has been solved for the convergent homotopic series solutions of velocities, temperature and concentration. Effects of various pertinent parameters on the temperature and concentration distributions are sketched and discussed. Numerical computations are performed to analyze the values of skin friction coefficients and local Nusselt number.

3.2 Problem development

We assume the steady three-dimensional flow of an incompressible couple stress nanofluid due to a bidirectional nonlinear stretching sheet. The fluid is assumed an electrically conducting through non-uniform magnetic field applied in the $z-$direction. Here the electric field and Hall effects are not considered. Due to the low magnetic Reynolds number, induced magnetic field effects are neglected. Brownian motion and thermophoresis effects are also taken into the consideration. We adopt the Cartesian coordinate system in such a manner that $x-$ and $y-$axis are taken along the stretched surface and $z-$axis is perpendicular to the surface (see Fig. 3.1). The sheet at $z = 0$ is stretched in the $x-$ and $y-$directions with velocities $U_w(x, y) = a(x + y)^n$ and $V_w(x, y) = b(x + y)^n$ respectively with a, b, $n > 0$ as the constants. The surface temperature is managed through a convective heating mechanism which is characterized by a coefficient of heat transfer h_f and temperature of the hot fluid T_f under the sheet. Boundary layer expressions governing the flow of couple stress nanofluid are given by
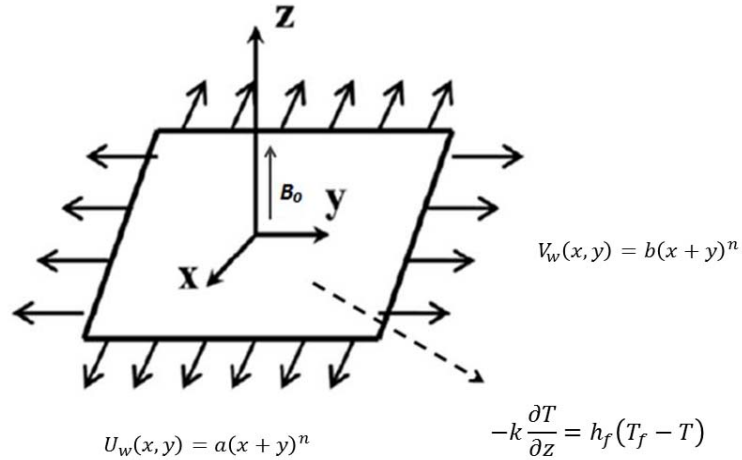

Fig. 3.1 : Physical sketch of the problem.

$$\frac{\partial u}{\partial x} + \frac{\partial v}{\partial y} + \frac{\partial w}{\partial z} = 0, \tag{3.1}$$

34

$$u\frac{\partial u}{\partial x} + v\frac{\partial u}{\partial y} + w\frac{\partial u}{\partial z} = \nu\frac{\partial^2 u}{\partial z^2} - \nu'\frac{\partial^4 u}{\partial z^4} - \frac{\sigma B^2(x,y)}{\rho_f}u, \tag{3.2}$$

$$u\frac{\partial v}{\partial x} + v\frac{\partial v}{\partial y} + w\frac{\partial v}{\partial z} = \nu\frac{\partial^2 v}{\partial z^2} - \nu'\frac{\partial^4 v}{\partial z^4} - \frac{\sigma B^2(x,y)}{\rho_f}v, \tag{3.3}$$

$$u\frac{\partial T}{\partial x} + v\frac{\partial T}{\partial y} + w\frac{\partial T}{\partial z} = \alpha\frac{\partial^2 T}{\partial z^2} + \frac{(\rho c)_p}{(\rho c)_f}\left(D_B\left(\frac{\partial T}{\partial z}\frac{\partial C}{\partial z}\right) + \frac{D_T}{T_\infty}\left(\frac{\partial T}{\partial z}\right)^2\right), \tag{3.4}$$

$$u\frac{\partial C}{\partial x} + v\frac{\partial C}{\partial y} + w\frac{\partial C}{\partial z} = D_B\left(\frac{\partial^2 C}{\partial z^2}\right) + \frac{D_T}{T_\infty}\left(\frac{\partial^2 T}{\partial z^2}\right). \tag{3.5}$$

The subjected boundary conditions are

$$u = U_w,\ v = V_w,\ w = 0,\ -k\frac{\partial T}{\partial z} = h_f\left(T_f - T\right),\ D_B\frac{\partial C}{\partial z} + \frac{D_T}{T_\infty}\frac{\partial T}{\partial z} = 0 \text{ at } z = 0, \tag{3.6}$$

$$u \to 0,\quad v \to 0,\quad T \to T_\infty,\quad C \to C_\infty \quad \text{as } z \to \infty, \tag{3.7}$$

Note that u, v and w are the fluid velocities in the $x-$, $y-$ and $z-$directions respectively, $\nu\left(=\mu/\rho_f\right)$ denotes the kinematic viscosity, μ stands for dynamic viscosity, ρ_f represents the density of base liquid, $\nu'(=n^*/\rho_f)$ stands for couple stress viscosity, n^* denotes the couple stress viscosity parameter, σ stands for electrical conductivity, $B(x,y) = B_0(x+y)^{\frac{n-1}{2}}$ denotes the non-uniform magnetic field, T stands for temperature, $\alpha = k/(\rho c)_f$ represents the thermal diffusivity, k stands for thermal conductivity of fluid, $(\rho c)_f$ stands for heat capacity of fluid, $(\rho c)_p$ stands for effective heat capacity of nanoparticles, D_B represents Brownian diffusivity, C stands for concentration and D_T represents thermophoretic diffusion coefficient, $h_f = h(x+y)^{\frac{n-1}{2}}$ stands for non-uniform heat transfer coefficient. T_∞ denotes the ambient fluid temperature and C_∞ represents the ambient fluid concentration. We now introduce the following transformations

$$\left.\begin{array}{l}u = a(x+y)^n f'(\eta),\ v = a(x+y)^n g'(\eta),\\[2mm] w = -\left(\frac{a\nu(n+1)}{2}\right)^{1/2}(x+y)^{\frac{n-1}{2}}\{(f+g) + \frac{n-1}{n+1}\eta(f'+g')\},\\[2mm] \theta(\eta) = \frac{T-T_\infty}{T_f-T_\infty},\ \phi(\eta) = \frac{C-C_\infty}{C_\infty},\ \eta = \left(\frac{a(n+1)}{2\nu}\right)^{1/2}(x+y)^{\frac{n-1}{2}}z.\end{array}\right\} \tag{3.8}$$

Eq. (3.1) is now automatically satisfied and Eqs. (3.2) − (3.7) have the following forms

$$f''' + (f+g)f'' - \frac{2n}{n+1}(f'+g')f' - Kf^{(\nu)} - M^2 f' = 0, \tag{3.9}$$

$$g''' + (f+g)g'' - \frac{2n}{n+1}(f'+g')g' - Kg^{(\nu)} - M^2 g' = 0, \tag{3.10}$$

$$\theta'' + \Pr\left((f+g)\theta' + Nb\theta'\phi' + Nt\theta'^2\right) = 0, \tag{3.11}$$

$$\phi'' + Le\Pr(f+g)\phi' + \frac{Nt}{Nb}\theta'' = 0, \tag{3.12}$$

$$f(0) = g(0) = 0, \ f'(0) = 1, \ g'(0) = c, \ \theta'(0) = -\gamma\left(1-\theta\left(0\right)\right), \ Nb\phi'(0) + Nt\theta'(0) = 0, \tag{3.13}$$

$$f'(\infty) \to 0, \ g'(\infty) \to 0, \ \theta(\infty) \to 0, \ \phi(\infty) \to 0. \tag{3.14}$$

In above expressions K denotes couple stress parameter, M represents the magnetic number, c stands for ratio parameter, $\Pr$ stands for Prandtl number, Nb depicts Brownian motion parameter, Nt stands for thermophoresis parameter, γ stands for Biot number and Le stands for Lewis number. These parameters are defined by

$$\left. \begin{array}{l} K = \frac{(n+1)\nu'a}{2\nu^2}(x+y)^{n-1}, \ M^2 = \frac{2\sigma B_0^2}{a\rho_f(n+1)}, \ c = \frac{b}{a}, \ \Pr = \frac{\nu}{\alpha}, \\ Nb = \frac{(\rho c)_p D_B C_\infty}{(\rho c)_f \nu}, Nt = \frac{(\rho c)_p D_T\left(T_f - T_\infty\right)}{(\rho c)_f \nu T_\infty}, \ \gamma = \frac{h_f}{k}\sqrt{\frac{\nu}{a}}, \ Le = \frac{\alpha}{D_B}. \end{array} \right\} \tag{3.15}$$

Dimensionless forms of skin friction coefficients and Nusselt number can be written as follows

$$\left. \begin{array}{l} C_{fx}\mathrm{Re}_x^{1/2} = (\frac{n+1}{2})^{1/2}(f''(0) - Kf^{iv}(0)), \\ C_{fy}\mathrm{Re}_y^{1/2} = c^{-3/2}(\frac{n+1}{2})^{1/2}(g''(0) - Kg^{iv}(0)), \\ Nu_x\mathrm{Re}_x^{-1/2} = -(\frac{n+1}{2})^{1/2}\theta'(0). \end{array} \right\} \tag{3.16}$$

where $\mathrm{Re}_x = U_w(x+y)/\nu$ and $\mathrm{Re}_y = V_w(x+y)/\nu$ depict the local Reynolds numbers. It is also noted that the dimensionless mass flux showed by a Sherwood number Sh_x is now identically zero

3.3 Series solutions

Our purpose now is to compute the series solutions via homotopy analysis technique (HAM). In homotopic solutions, the suitable initial approximations (f_0, g_0, θ_0, ϕ_0) and the corresponding

auxiliary linear operators $(\mathcal{L}_f, \mathcal{L}_g, \mathcal{L}_\theta,\ \mathcal{L}_\phi)$ for the above problem are

$$f_0(\eta) = 1-\exp(-\eta),\ \ g_0(\eta) = c(1-\exp(-\eta)),\ \ \theta_0(\eta) = \frac{\gamma}{1+\gamma}\exp(-\eta),\ \ \phi_0(\eta) = -\frac{\gamma}{1+\gamma}\frac{Nt}{Nb}\exp(-\eta),$$
$$(3.17)$$

$$\mathcal{L}_f = \frac{d^3 f}{d\eta^3} - \frac{df}{d\eta},\ \ \mathcal{L}_g = \frac{d^3 g}{d\eta^3} - \frac{dg}{d\eta},\ \ \mathcal{L}_\theta = \frac{d^2\theta}{d\eta^2} - \theta,\ \ \mathcal{L}_\phi = \frac{d^2\phi}{d\eta^2} - \phi. \qquad (3.18)$$

The above operators have the properties given below

$$\left.\begin{array}{l} \mathcal{L}_f\left[B_1 + B_2\exp(\eta) + B_3\exp(-\eta)\right] = 0,\quad \mathcal{L}_g\left[B_4 + B_5\exp(\eta) + B_6\exp(-\eta)\right] = 0, \\[2mm] \mathcal{L}_\theta\left[B_7\exp(\eta) + B_8\exp(-\eta)\right] = 0,\quad \mathcal{L}_\phi\left[B_9\exp(\eta) + B_{10}\exp(-\eta)\right] = 0, \end{array}\right\} \quad (3.19)$$

in which B_j $(j = 1 - 10)$ denote the arbitrary constants.

3.3.1 Zeroth-order deformation equations

$$(1 - P^*)\mathcal{L}_f\left[\breve{f}(\eta, P^*) - f_0(\eta)\right] = P^*\hbar_f \mathcal{N}_f[\breve{f}(\eta, P^*), \breve{g}(\eta, P^*)], \qquad (3.20)$$

$$(1 - P^*)\mathcal{L}_g\left[\breve{g}(\eta, P^*) - g_0(\eta)\right] = P^*\hbar_g \mathcal{N}_g[\breve{f}(\eta, P^*), \breve{g}(\eta, P^*)], \qquad (3.21)$$

$$(1 - P^*)\mathcal{L}_\theta\left[\breve{\theta}(\eta, P^*) - \theta_0(\eta)\right] = P^*\hbar_\theta \mathcal{N}_\theta[\breve{f}(\eta, P^*), \breve{g}(\eta, P^*), \breve{\theta}(\eta, P^*), \breve{\phi}(\eta, P^*)], \qquad (3.22)$$

$$(1 - P^*)\mathcal{L}_\phi\left[\breve{\phi}(\eta, P^*) - \phi_0(\eta)\right] = P^*\hbar_\phi \mathcal{N}_\phi[\breve{f}(\eta, P^*), \breve{g}(\eta, P^*), \breve{\theta}(\eta, P^*), \breve{\phi}(\eta, P^*)], \qquad (3.23)$$

$$\left.\begin{array}{l} \breve{f}(0, P^*) = 0,\ \ \breve{f}'(0, P^*) = 1,\ \ \breve{f}'(\infty, P^*) = 0,\ \ \breve{g}(0, P^*) = 0, \\[2mm] \breve{g}'(0, P^*) = c,\ \ \breve{g}'(\infty, P^*) = 0,\ \ \breve{\theta}'(0, P^*) = -\gamma\left(1 - \breve{\theta}(0, P^*)\right), \\[2mm] \breve{\theta}(\infty, P^*) = 0,\ \ Nb\breve{\phi}'(0, P^*) + Nt\breve{\theta}'(0, P^*) = 0,\ \ \breve{\phi}(\infty, P^*) = 0, \end{array}\right\} \quad (3.24)$$

$$\mathcal{N}_f\left[\breve{f}(\eta; P^*), \breve{g}(\eta; P^*)\right] = \frac{\partial^3\breve{f}}{\partial\eta^3} + \left(\breve{f} + \breve{g}\right)\frac{\partial^2\breve{f}}{\partial\eta^2} - \frac{2n}{n+1}\left(\frac{\partial\breve{f}}{\partial\eta} + \frac{\partial\breve{g}}{\partial\eta}\right)\frac{\partial\breve{f}}{\partial\eta} - K\frac{\partial^{(5)}\breve{f}}{\partial\eta^{(5)}} - M^2\frac{\partial\breve{f}}{\partial\eta},$$
$$(3.25)$$

$$\mathcal{N}_g\left[\breve{g}(\eta; P^*), \breve{f}(\eta; P^*)\right] = \frac{\partial^3\breve{g}}{\partial\eta^3} + \left(\breve{f} + \breve{g}\right)\frac{\partial^2\breve{g}}{\partial\eta^2} - \frac{2n}{n+1}\left(\frac{\partial\breve{f}}{\partial\eta} + \frac{\partial\breve{g}}{\partial\eta}\right)\frac{\partial\breve{g}}{\partial\eta} - K\frac{\partial^{(5)}\breve{g}}{\partial\eta^{(5)}} - M^2\frac{\partial\breve{g}}{\partial\eta},\ \ (3.26)$$

$$\mathcal{N}_\theta \left[\breve{f}(\eta; \text{Þ}^*), \breve{g}(\eta; \text{Þ}^*), \breve{\theta}(\eta, \text{Þ}^*), \breve{\phi}(\eta, \text{Þ}^*) \right] = \frac{\partial^2 \breve{\theta}}{\partial \eta^2} + \Pr \left(\breve{f} + \breve{g} \right) \frac{\partial \breve{\theta}}{\partial \eta}$$

$$+ \Pr Nb \frac{\partial \breve{\theta}}{\partial \eta} \frac{\partial \breve{\phi}}{\partial \eta} + \Pr Nt \left(\frac{\partial \breve{\theta}}{\partial \eta} \right)^2, \quad (3.27)$$

$$\mathcal{N}_\phi \left[\breve{f}(\eta; \text{Þ}^*), \breve{g}(\eta; \text{Þ}^*), \breve{\theta}(\eta, \text{Þ}^*), \breve{\phi}(\eta, \text{Þ}^*) \right] = \frac{\partial^2 \breve{\phi}}{\partial \eta^2} + Le \Pr \left(\breve{f} + \breve{g} \right) \frac{\partial \breve{\phi}}{\partial \eta} + \frac{Nt}{Nb} \frac{\partial^2 \breve{\theta}}{\partial \eta^2}. \quad (3.28)$$

Here $\text{Þ}^* \in [0, 1]$ denotes the embedding parameter, the non-zero auxiliary parameters are depicted by $\hbar_f$, $\hbar_g$, $\hbar_\theta$ and $\hbar_\phi$ and $\mathcal{N}_f$, $\mathcal{N}_g$, $\mathcal{N}_\theta$ and $\mathcal{N}_\phi$ represent the non-linear operators.

3.3.2 $\hat{m}$th-order deformation equations

$$\mathcal{L}_f \left[f_{\hat{m}}(\eta) - \chi_{\hat{m}} f_{\hat{m}-1}(\eta) \right] = \hbar_f \tilde{\mathcal{R}}_{\hat{m}}^f(\eta), \quad (3.29)$$

$$\mathcal{L}_g \left[g_{\hat{m}}(\eta) - \chi_{\hat{m}} g_{\hat{m}-1}(\eta) \right] = \hbar_g \tilde{\mathcal{R}}_{\hat{m}}^g(\eta), \quad (3.30)$$

$$\mathcal{L}_\theta \left[\theta_{\hat{m}}(\eta) - \chi_{\hat{m}} \theta_{\hat{m}-1}(\eta) \right] = \hbar_\theta \tilde{\mathcal{R}}_{\hat{m}}^\theta(\eta), \quad (3.31)$$

$$\mathcal{L}_\phi \left[\phi_{\hat{m}}(\eta) - \chi_{\hat{m}} \phi_{\hat{m}-1}(\eta) \right] = \hbar_\phi \tilde{\mathcal{R}}_{\hat{m}}^\phi(\eta), \quad (3.32)$$

$$f_{\hat{m}}(0) = f'_{\hat{m}}(0) = f'_{\hat{m}}(\infty) = 0, \ g_{\hat{m}}(0) = g'_{\hat{m}}(0) = g'_{\hat{m}}(\infty) = 0,$$

$$\theta'_{\hat{m}}(0) + \gamma \theta_{\hat{m}}(0) = 0, \ Nb\phi'_{\hat{m}}(0) + Nt\theta'_{\hat{m}}(0) = 0, \ \theta_{\hat{m}}(\infty) = \phi_{\hat{m}}(\infty) = 0, \quad (3.33)$$

$$\tilde{\mathcal{R}}_{\hat{m}}^f(\eta) = f'''_{\hat{m}-1} - \left(\frac{2n}{n+1} \right) \sum_{k=0}^{\hat{m}-1} (f'_{\hat{m}-1-k} f'_k + g'_{\hat{m}-1-k} f'_k)$$

$$+ \sum_{k=0}^{\hat{m}-1} (f_{\hat{m}-1-k} f''_k + g_{\hat{m}-1-k} f''_k) - K f_{\hat{m}-1}^{(\nu)} - M^2 f'_{\hat{m}-1}, \quad (3.34)$$

$$\tilde{\mathcal{R}}_{\hat{m}}^g(\eta) = g'''_{\hat{m}-1} - \left(\frac{2n}{n+1} \right) \sum_{k=0}^{\hat{m}-1} (f'_{\hat{m}-1-k} g'_k + g'_{\hat{m}-1-k} g'_k)$$

$$+ \sum_{k=0}^{\hat{m}-1} (f_{\hat{m}-1-k} g''_k + g_{\hat{m}-1-k} g''_k) - K g_{\hat{m}-1}^{(\nu)} - M^2 g'_{\hat{m}-1}, \quad (3.35)$$

38

$$\tilde{\mathcal{R}}_{\hat{m}}^{\theta}(\eta) = \theta_{\hat{m}-1}'' + \Pr \sum_{k=0}^{\hat{m}-1} (f_{\hat{m}-1-k}\theta_k' + g_{\hat{m}-1-k}\theta_k')$$

$$+ \Pr Nb \sum_{k=0}^{\hat{m}-1} (\theta_{\hat{m}-1-k}'\phi_k') + \Pr Nt \sum_{k=0}^{\hat{m}-1} (\theta_{\hat{m}-1-k}'\theta_k'), \tag{3.36}$$

$$\tilde{\mathcal{R}}_{\hat{m}}^{\phi}(\eta) = \phi_{\hat{m}-1}''(\eta) + Le \Pr \sum_{k=0}^{\hat{m}-1} (f_{\hat{m}-1-k}\phi_k' + g_{\hat{m}-1-k}\phi_k') + \frac{Nt}{Nb}\theta_{\hat{m}-1}'', \tag{3.37}$$

$$\chi_{\hat{m}} = \begin{cases} 0, & \hat{m} \le 1, \\ 1, & \hat{m} > 1, \end{cases} \tag{3.38}$$

Putting $Þ^* = 0$ and $Þ^* = 1$ we have

$$\breve{f}(\eta; 0) = f_0(\eta), \ \breve{f}(\eta; 1) = f(\eta), \tag{3.39}$$

$$\breve{g}(\eta; 0) = g_0(\eta), \ \breve{g}(\eta; 1) = g(\eta), \tag{3.40}$$

$$\breve{\theta}(\eta, 0) = \theta_0(\eta), \ \breve{\theta}(\eta, 1) = \theta(\eta), \tag{3.41}$$

$$\breve{\phi}(\eta, 0) = \phi_0(\eta), \ \breve{\phi}(\eta, 1) = \phi(\eta). \tag{3.42}$$

When $Þ^*$ varies from 0 to 1 then $\breve{f}(\eta;Þ^*)$, $\breve{g}(\eta;Þ^*)$, $\breve{\theta}(\eta,Þ^*)$ and $\breve{\phi}(\eta,Þ^*)$ vary from the initial approximations $f_0(\eta)$, $g_0(\eta)$, $\theta_0(\eta)$ and $\phi_0(\eta)$ to the desired final solutions $f(\eta)$, $g(\eta)$, $\theta(\eta)$ and $\phi(\eta)$ respectively. The following expressions are obtained via Taylor's series expansion

$$\breve{f}(\eta; Þ^*) = f_0(\eta) + \sum_{\hat{m}=1}^{\infty} f_{\hat{m}}(\eta)Þ^{*\hat{m}}, \ f_{\hat{m}}(\eta) = \frac{1}{\hat{m}!}\frac{\partial^{\hat{m}}\breve{f}(\eta, Þ^*)}{\partial Þ^{*\hat{m}}}\bigg|_{Þ^*=0}, \tag{3.43}$$

$$\breve{g}(\eta; Þ^*) = g_0(\eta) + \sum_{\hat{m}=1}^{\infty} g_{\hat{m}}(\eta)Þ^{*\hat{m}}, \ g_{\hat{m}}(\eta) = \frac{1}{\hat{m}!}\frac{\partial^{\hat{m}}\breve{g}(\eta, Þ^*)}{\partial Þ^{*\hat{m}}}\bigg|_{Þ^*=0}, \tag{3.44}$$

$$\breve{\theta}(\eta, Þ^*) = \theta_0(\eta) + \sum_{\hat{m}=1}^{\infty} \theta_{\hat{m}}(\eta)Þ^{*\hat{m}}, \ \theta_{\hat{m}}(\eta) = \frac{1}{\hat{m}!}\frac{\partial^{\hat{m}}\breve{\theta}(\eta, Þ^*)}{\partial Þ^{*\hat{m}}}\bigg|_{Þ^*=0}, \tag{3.45}$$

$$\breve{\phi}(\eta, Þ^*) = \phi_0(\eta) + \sum_{\hat{m}=1}^{\infty} \phi_{\hat{m}}(\eta)Þ^{*\hat{m}}, \ \phi_{\hat{m}}(\eta) = \frac{1}{\hat{m}!}\frac{\partial^{\hat{m}}\breve{\phi}(\eta, Þ^*)}{\partial Þ^{*\hat{m}}}\bigg|_{Þ^*=0}. \tag{3.46}$$

The convergence of Eqs. $(3.43) - (3.46)$ strongly depends upon the $\hbar_f$, $\hbar_g$, $\hbar_\theta$ and $\hbar_\phi$. Considering that $\hbar_f$, $\hbar_g$, $\hbar_\theta$ and $\hbar_\phi$ are selected in such a way that Eqs. $(3.43) - (3.46)$ converge at $\text{Þ}^* = 1$, Then

$$f(\eta) = f_0(\eta) + \sum_{\hat{m}=1}^{\infty} f_{\hat{m}}(\eta), \tag{3.47}$$

$$g(\eta) = g_0(\eta) + \sum_{\hat{m}=1}^{\infty} g_{\hat{m}}(\eta), \tag{3.48}$$

$$\theta(\eta) = \theta_0(\eta) + \sum_{\hat{m}=1}^{\infty} \theta_{\hat{m}}(\eta), \tag{3.49}$$

$$\phi(\eta) = \phi_0(\eta) + \sum_{\hat{m}=1}^{\infty} \phi_{\hat{m}}(\eta). \tag{3.50}$$

The general solutions $(f_{\hat{m}}, g_{\hat{m}}, \theta_{\hat{m}}, \phi_{\hat{m}})$ of the Eqs. $(3.29) - (3.32)$ in terms of special solutions $(f_{\hat{m}}^*, g_{\hat{m}}^*, \theta_{\hat{m}}^*, \phi_{\hat{m}}^*)$ are presented by the following expressions

$$f_{\hat{m}}(\eta) = f_{\hat{m}}^*(\eta) + B_1 + B_2 \exp(\eta) + B_3 \exp(-\eta), \tag{3.51}$$

$$g_{\hat{m}}(\eta) = g_{\hat{m}}^*(\eta) + B_4 + B_5 \exp(\eta) + B_6 \exp(-\eta), \tag{3.52}$$

$$\theta_{\hat{m}}(\eta) = \theta_{\hat{m}}^*(\eta) + B_7 \exp(\eta) + B_8 \exp(-\eta), \tag{3.53}$$

$$\phi_{\hat{m}}(\eta) = \phi_{\hat{m}}^*(\eta) + B_9 \exp(\eta) + B_{10} \exp(-\eta). \tag{3.54}$$

in which B_j $(j = 1 - 10)$ by means of the boundary conditions (3.33) have the following values

$$B_2 = B_5 = B_7 = B_9 = 0, \ B_3 = \left. \frac{\partial f_{\hat{m}}^*(\eta)}{\partial \eta} \right|_{\eta=0}, \ B_1 = -B_3 - f_{\hat{m}}^*(0), \tag{3.55}$$

$$B_6 = \left. \frac{\partial g_{\hat{m}}^*(\eta)}{\partial \eta} \right|_{\eta=0}, \ B_4 = -B_6 - g_{\hat{m}}^*(0), \ B_8 = \frac{1}{1+\gamma} \left(\left. \frac{\partial \theta_{\hat{m}}^*(\eta)}{\partial \eta} \right|_{\eta=0} - \gamma \theta_{\hat{m}}^*(0) \right), \tag{3.56}$$

$$B_{10} = \left. \frac{\partial \phi_{\hat{m}}^*(\eta)}{\partial \eta} \right|_{\eta=0} + \frac{Nt}{Nb} \left(-B_8 + \left. \frac{\partial \theta_{\hat{m}}^*(\eta)}{\partial \eta} \right|_{\eta=0} \right). \tag{3.57}$$

40

3.3.3   Convergence analysis

No doubt the auxiliary parameters $\hbar_f$, $\hbar_g$, $\hbar_\theta$ and $\hbar_\phi$ in the series solutions $(3.47) - (3.50)$ have key role regarding convergence. In order to develop the convergent approximate series solutions, the suitable values of these parameters play a key role. To select the appropriate values of $\hbar_f$, $\hbar_g$, $\hbar_\theta$ and $\hbar_\phi$, $\hbar-$curves are sketched at 15th order of deformations. Figs. $(3.2) - (3.5)$ clearly denote that the region of convergence lies within the ranges $-1.35 \leq \hbar_f \leq -0.35$, $-1.40 \leq \hbar_g \leq -0.25$, $-1.40 \leq \hbar_\theta \leq -0.25$ and $-1.50 \leq \hbar_\phi \leq -0.25$. Moreover the series solutions are convergent in the entire zone of η when $\hbar_f = \hbar_g = -1.0 = \hbar_\theta = \hbar_\phi$. Table 3.1 presents that the 11th deformations is enough for the convergent series solutions of velocities, temperature and concentration profiles.
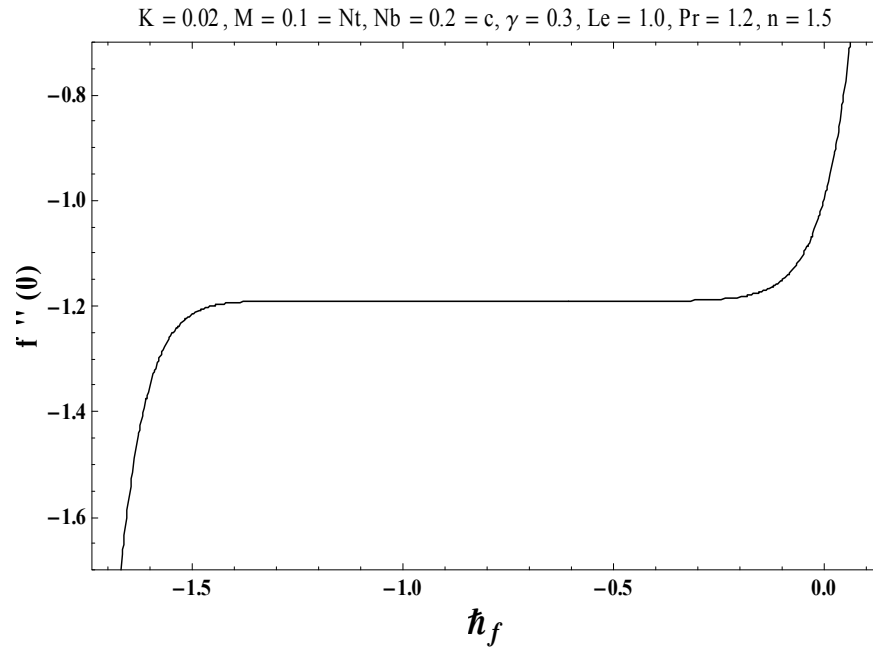
Fig. 3.2 : $\hbar-$curve for the function $f(\eta)$.
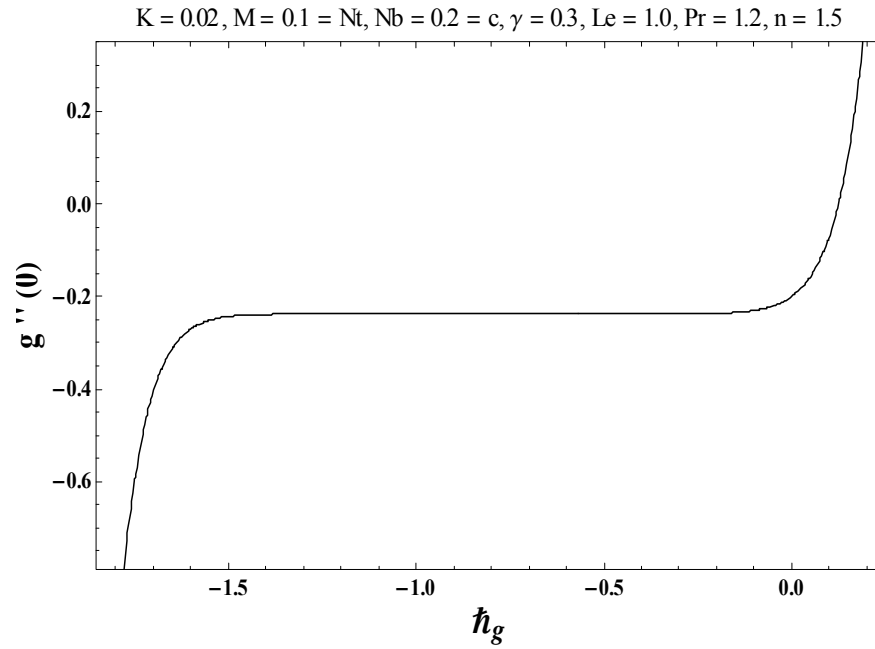
Fig. 3.3 : $\hbar$−curve for the function $g(\eta)$.
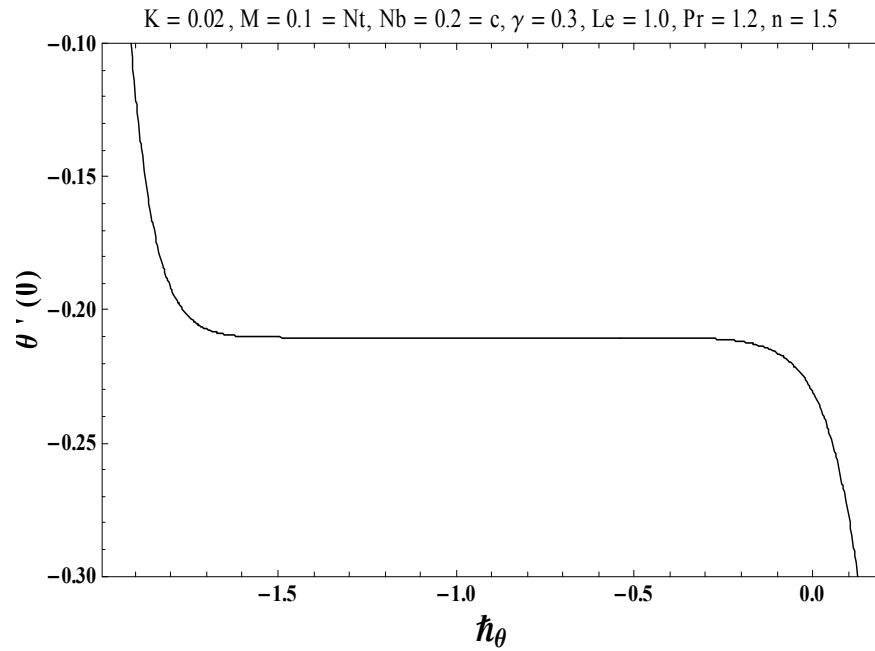
Fig. 3.4 : $\hbar$−curve for the function $\theta(\eta)$.
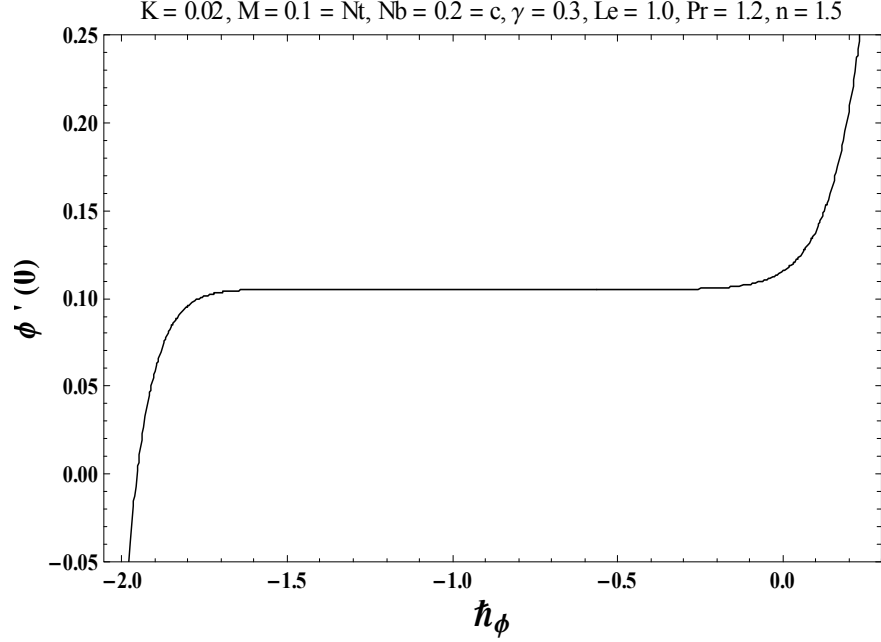
K = 0.02, M = 0.1 = Nt, Nb = 0.2 = c, γ = 0.3, Le = 1.0, Pr = 1.2, n = 1.5

Fig. 3.5 : $\hbar-$curve for the function $\phi(\eta)$.

Table 3.1: Convergence of homotopic solutions when $n = 1.5$, $K = 0.02,$, $M = 0.1 = Nt$, $c = 0.2 = Nb$, $\gamma = 0.3$, $Le = 1.0$ and $\mathrm{Pr} = 1.2$.

Order of Approximation	$-f''(0)$	$-g''(0)$	$-\theta'(0)$	$\phi'(0)$
1	1.19500	0.23900	0.21692	0.10846
5	1.19041	0.23808	0.21043	0.10521
11	1.19035	0.23807	0.21033	0.10516
15	1.19035	0.23807	0.21033	0.10516
25	1.19035	0.23807	0.21033	0.10516
35	1.19035	0.23807	0.21033	0.10516
50	1.19035	0.23807	0.21033	0.10516

3.4 Results and discussion

In this section the impact of various emerging flow parameters like couple stress parameter K, magnetic number M, ratio parameter c, Biot number γ, Brownian motion parameter Nb, thermophoresis parameter Nt, Lewis number Le and Prandtl number Pr on the velocity components $f'(\eta)$ and $g'(\eta)$, temperature $\theta(\eta)$ and concentration $\phi(\eta)$ are sketched in the Figs.

43

$(3.6) - (3.25)$. The results are achieved for two distinct values of n just to compare the corresponding profiles in cases of linear and nonlinear stretching surfaces. The influence of couple stress parameter K on the component of velocity $f'(\eta)$ has been shown in Fig. 3.5. It has been observed that component of velocity reduces by increasing couple stress parameter K. The couple stress parameter involves couple stress viscosity n which makes the fluid more viscous and hence the velocity is retarted. Fig. 3.6 depicts the impact of magnetic number M on the velocity component $f'(\eta)$. An enhancement in magnetic number causes reduction in velocity field and its associated boundary layer thickness. Physically Lorentz force enhances by increasing magnetic number M which shows retarding effect. Hence Lorentz force opposes the fluid motion and the velocity of the fluid decreases. Fig. 3.7 illustrates that how ratio parameter effects the component of velocity $f'(\eta)$. Here the velocity and its associated momentum boundary layer thickness show decreasing behavior by increasing ratio parameter c. The reason behind this phenomena is that with an increment in the ratio parameter, the $x-$component of velocity decreases which yields reduction in the velocity and its associated boundary layer thickness. Influence of couple stress parameter K on the component of velocity $g'(\eta)$ is sketched in Fig. 3.8. In this Fig. we observe that the velocity $g'(\eta)$ and its associated boundary layer thickness decreases by enhancing couple stress parameter K. Fig. 3.9 shows that how velocity component get effected by magnetic number M. This Fig presents that velocity $g'(\eta)$ and its related boundary layer thickness decreases by enhancing magnetic number M. The influence of ratio parameter c on the component of velocity $g'(\eta)$ has been sketched in Fig. 3.10, which represents that the velocity $g'(\eta)$ and its associated boundary layer thickness are enhancing functions of ratio parameter c. Variation of couple stress parameter K on temperature field $\theta(\eta)$ is displayed in Fig. 3.11. Larger values of couple stress parameter K gives rise the temperature field and their related thickness of thermal boundary layer. Fig. 3.12 is interpreted to examine the effect of magnetic number M on temperature field $\theta(\eta)$. Here $M \neq 0$ yields hydromagnetic flow situation and $M = 0$ represents hydrodynamic flow case. We examined that the temperature distribution and thickness of the thermal boundary layer are higher for hydromagnetic flow as compared to the hydrodynamic flow situation. An increment in the values of magnetic number M corresponds stronger temperature distribution and more thickness of the thermal boundary layer. Impact of ratio parameter c on the temperature field $\theta(\eta)$ is drawn in Fig. 3.13. From

this Fig. it is observed that greater values of ratio parameter c creates a demotion in the temperature field $\theta(\eta)$ alongwith its related thermal boundary layer thickness. In case of $c = 0$, the two-dimensional flow situation has been recovered. Fig. 3.15 depicts the effect of Biot number (γ) on the temperature distribution $\theta(\eta)$. An increment in the value of γ leads to a stronger convection which shows a higher temperature field and more thickness of the thermal layer. From Fig. 3.16 it has been noted that for higher values of Prandtl number Pr, the temperature $\theta(\eta)$ and its associated thermal boundary layer thickness decreases. Prandtl number has an inverse relationship with the thermal diffusivity. Higher Prandtl number Pr implies lower thermal diffusivity. Such lower thermal diffusivity is responsible for a decrease in the temperature distribution. Fig. 3.17 presents that an increasing behavior of Nt causes a stronger temperature distribution and more thickness of thermal layer. Higher values of thermophoresis parameter Nt yields a stronger thermophoretic force which is responsible for a deeper transfer of nanoparticles in the ambient fluid which corresponds to a stronger temperature field and more thickness of thermal layer. Fig. 3.18 elucidates that an increase in couple stress parameter K implies to an increment in the concentration field $\phi(\eta)$ and thicker thickness of concentration boundary layer. Fig. 3.19 is sketched to see that how concentration field $\phi(\eta)$ is effected by magnetic number M. Here we observed that the concentration and its related thickness of concentration boundary layer increases by increasing magnetic number M. Fig. 3.20 is sketched to examine that how concentration field $\phi(\eta)$ get effected by ratio parameter (c). From this Fig. it has been noticed that the concentration field is lower for the larger values of ratio parameter (c). Fig. 3.21 shows that the higher values of Biot number (γ) yields a stronger concentration profile $\phi(\eta)$. Fig. 3.22 shows the variation in $\phi(\eta)$ for distinct values of Lewis number Le. An inverse relation exists between Lewis number and Brownian diffusivity. By increasing Lewis number, Brownian diffusivity decreases and as a result concentration $\phi(\eta)$ and its related thickness of concentration boundary layer increases. Fig. 3.23 is sketched to analyze the behavior of Prandtl number (Pr) on concentration distribution $\phi(\eta)$. Here the concentration field $\phi(\eta)$ and associated thickness of boundary layer decreases by enhancing Pr. Fig. 3.24 depicts that the higher values of Brownian motion parameter Nb causes a weaker concentration profile $\phi(\eta)$. Fig. 3.25 shows how thermophoresis parameter Nt effects $\phi(\eta)$. By increasing thermophoresis parameter Nt, concentration $\phi(\eta)$ and thickness of concentration boundary layer also increases.

Table 3.1 is constructed to analyze the convergence of homotopic series solutions when $n = 1.5$, $K = 0.02,$, $M = 0.1 = Nt$, $c = 0.2 = Nb$, $\gamma = 0.3$, $Le = 1.0$ and $\Pr = 1.2$. It is clearly seen that the solutions of velocity, temperature and concentration distributions converge from 11th order of homotopic approximations. Hence 11th order of homotopic approximations is sufficient for convergence analysis of series solutions. Table 3.2 depicts skin friction coefficients $-C_{fx} \operatorname{Re}_x^{1/2}$ and $-C_{fy} \operatorname{Re}_y^{1/2}$ having the numerical values of couple stress parameter K, magnetic number M and ratio parameter c. It is clearly seen that the skin friction coefficients are enhanced for the increasing values of magnetic number M. Table 3.3 is prepared for numerical values of local Nusselt number $Nu_x \operatorname{Re}_x^{-1/2}$ corresponding to various values of K, M, c, γ, Nt, Nb, Le and $\Pr$. It is noted that the couple stress parameter K, magnetic number M and thermophoresis parameter Nt correspond to a lower Nusselt number while opposite behavior is observed for Biot number γ.
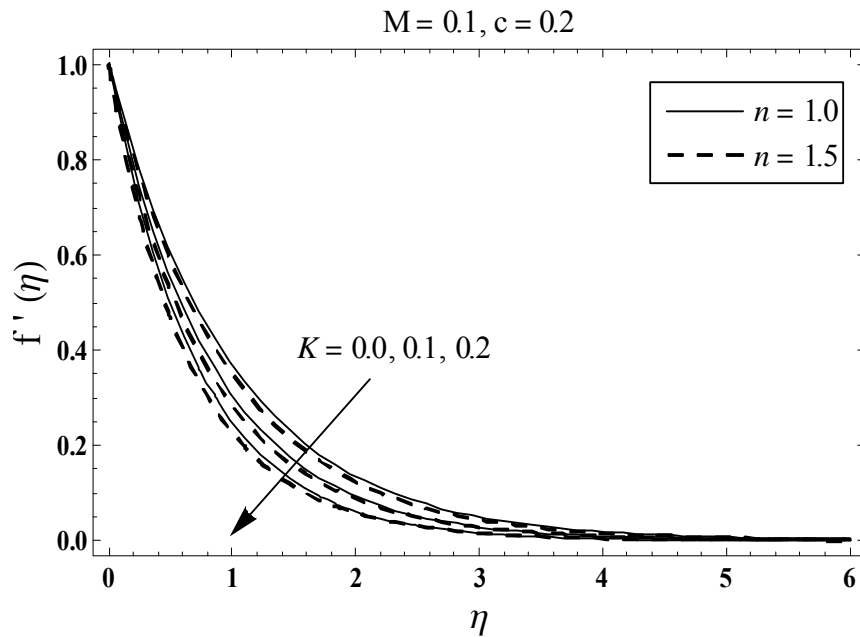
Fig. 3.6 : Behavior of K on $f'(\eta)$.
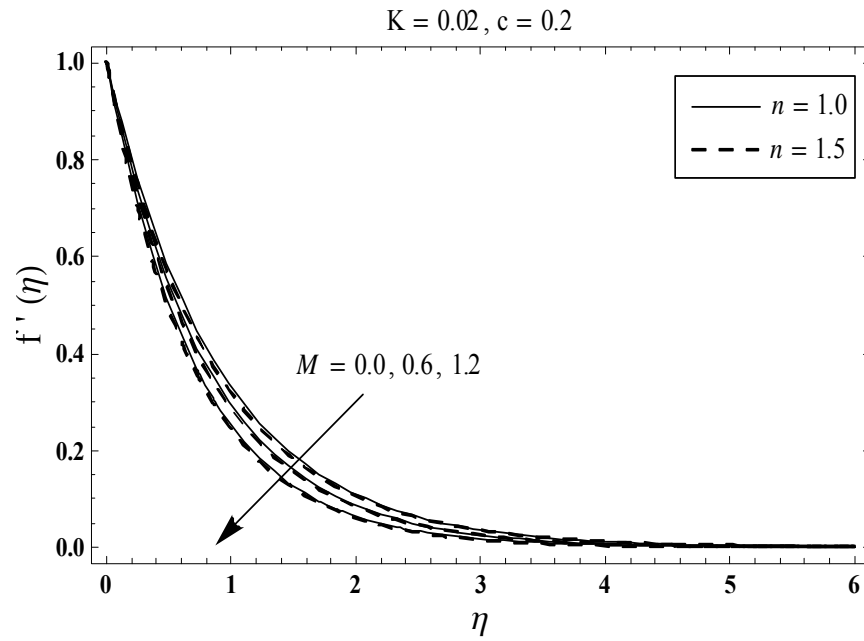
Fig. 3.7 : Behavior of M on $f'(\eta)$.
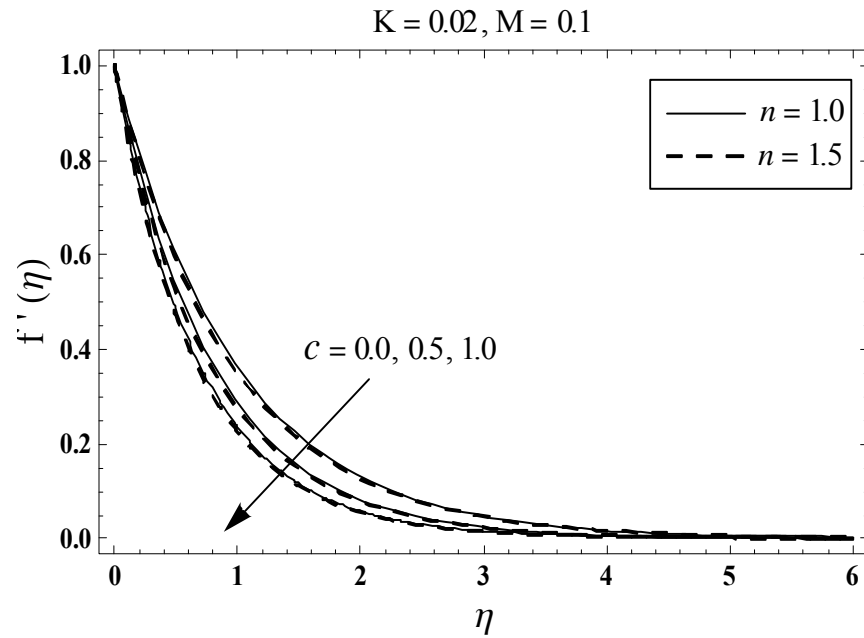
Fig. 3.8 : Behavior of c on $f'(\eta)$.

M = 0.1, c = 0.2
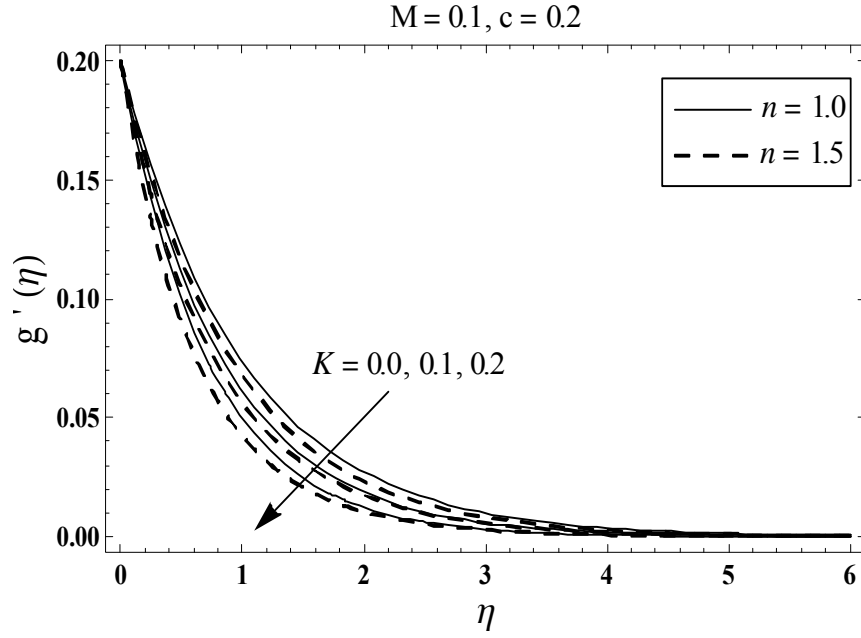
Fig. 3.9 : Behavior of K on $g'(\eta)$.

K = 0.02, c = 0.2
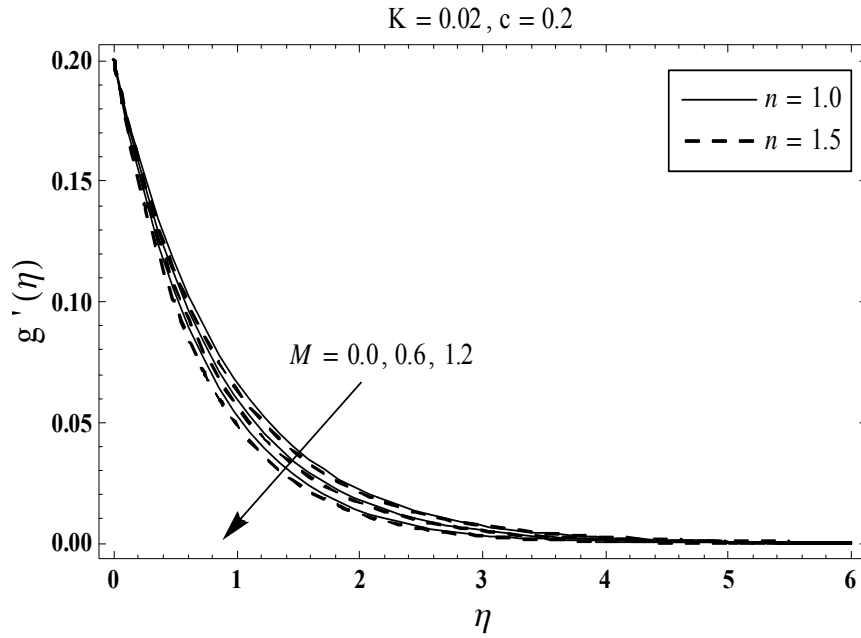
Fig. 3.10 : Behavior of M on $g'(\eta)$.
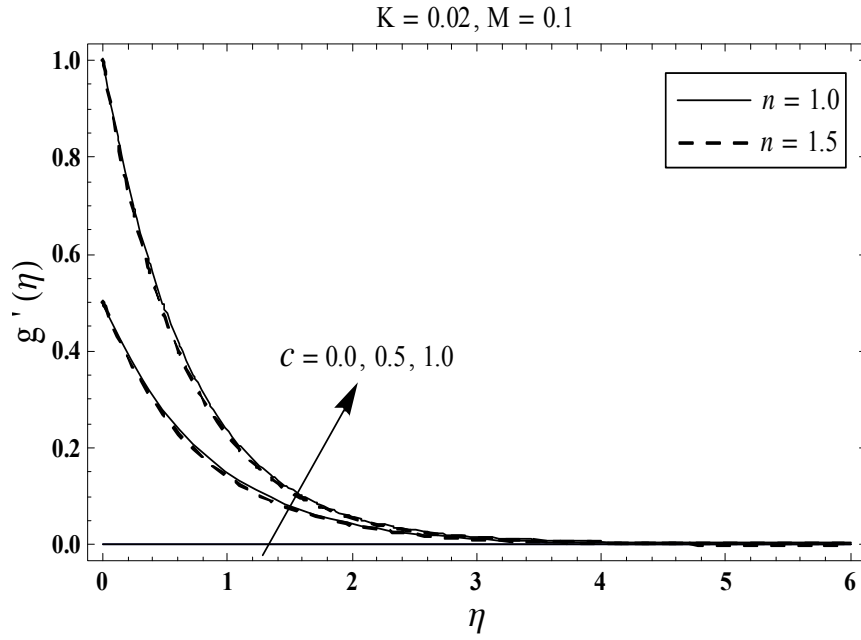
Fig. 3.11 : Behavior of c on $g'(\eta)$.

$\gamma = 0.3,\ c = 0.2 = Nb,\ M = 0.1 = Nt,\ Le = 1.0,\ Pr = 1.2$
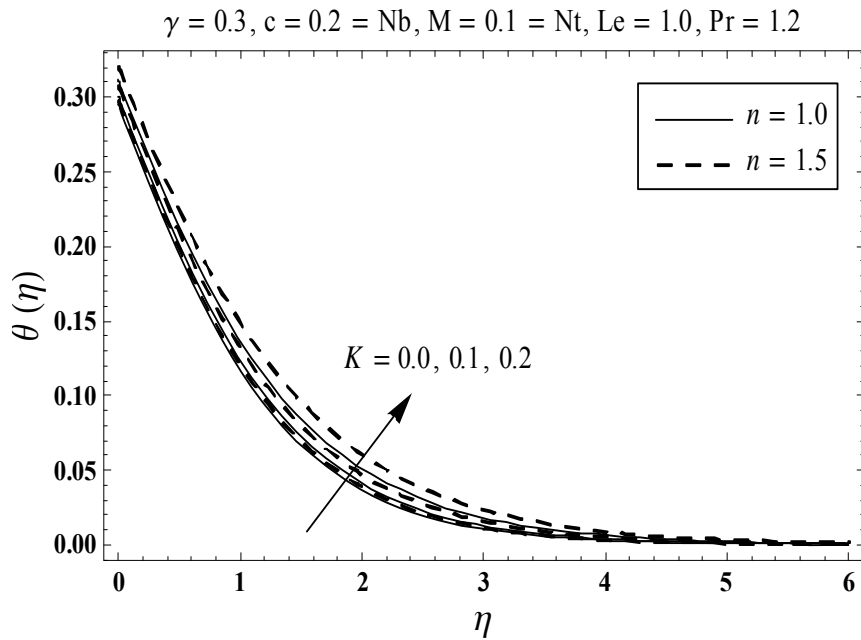
Fig. 3.12 : Behavior of K on $\theta(\eta)$.
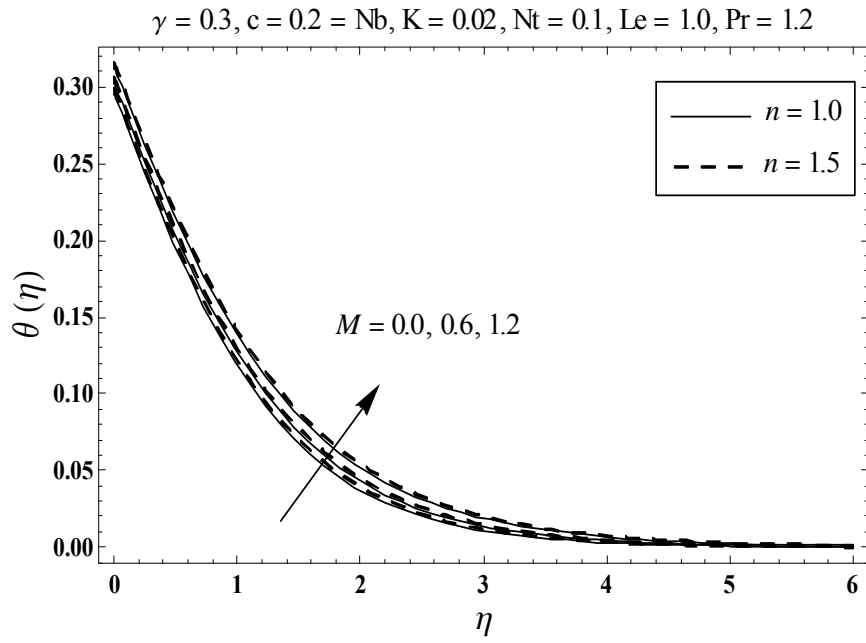
Fig. 3.13 : Behavior of M on $\theta(\eta)$.
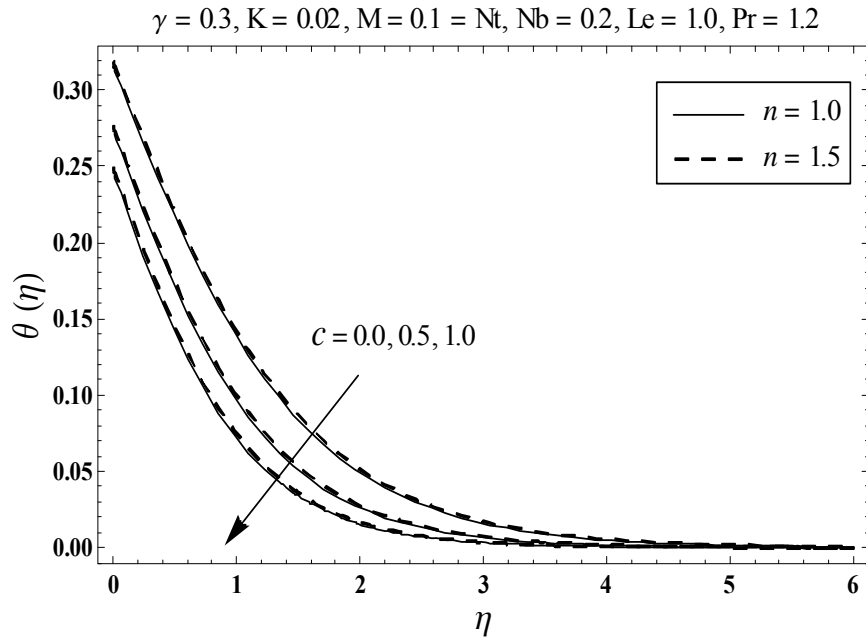
Fig. 3.14 : Behavior of c on $\theta(\eta)$.
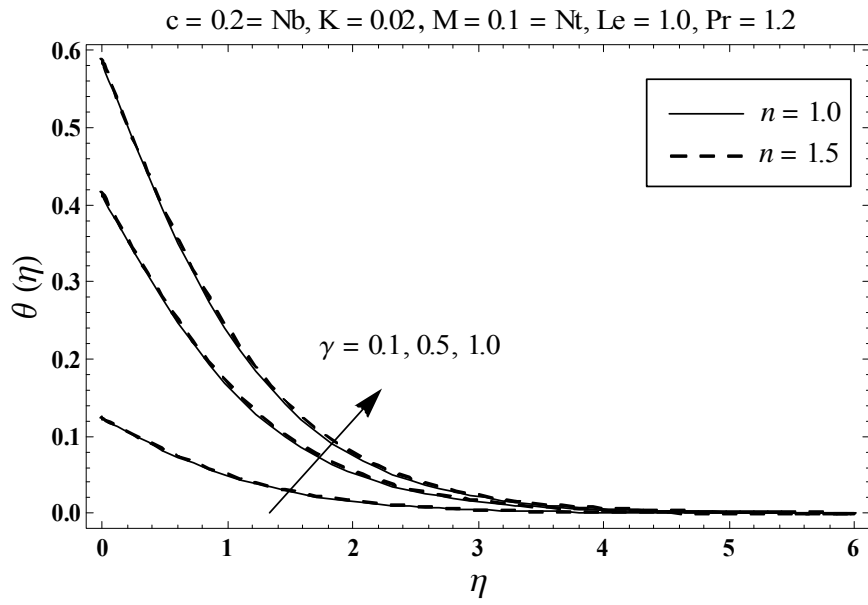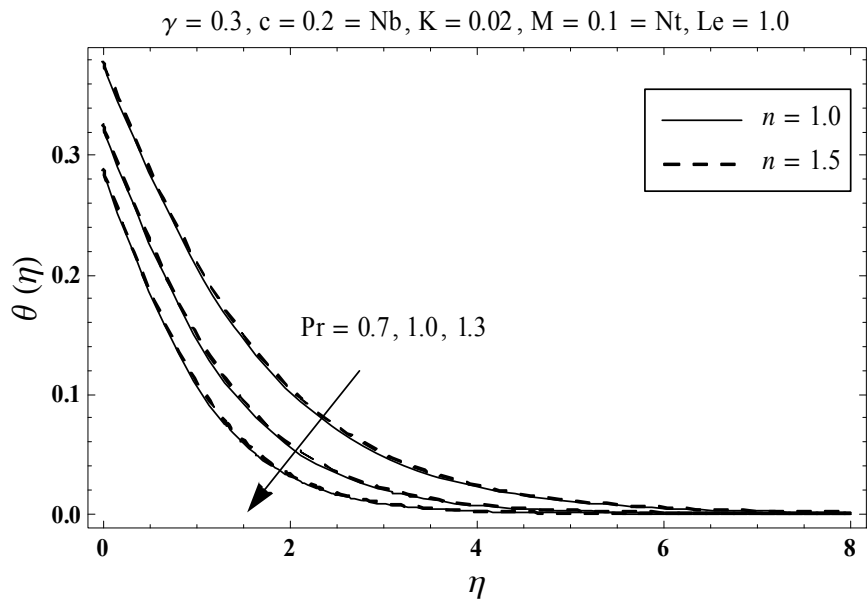
c = 0.2= Nb, K = 0.02, M = 0.1 = Nt, Le = 1.0, Pr = 1.2

Fig. 3.15 : Behavior of γ on $\theta(\eta)$.

$\gamma = 0.3$, c = 0.2 = Nb, K = 0.02, M = 0.1 = Nt, Le = 1.0

Fig. 3.16 : Behavior of Pr on $\theta(\eta)$.

γ = 0.3, c = 0.2 = Nb, K = 0.02, M = 0.1, Le = 1.0, Pr = 1.2

$n = 1.0$
$n = 1.5$

Nt = 0.1, 0.6, 1.2

Fig. 3.17 : Behavior of Nt on $\theta(\eta)$.

γ = 0.3, c = 0.2 = Nb, M = 0.1 = Nt, Le = 1.0, Pr = 1.2

$K = 0.0, 0.1, 0.2$

$n = 1.0$
$n = 1.5$

Fig. 3.18 : Behavior of K on $\phi(\eta)$.

$\gamma = 0.3$, c = 0.2 = Nb, K = 0.02, Nt = 0.1, Le = 1.0, Pr = 1.2

$M = 0.0, 0.5, 0.8$

$n = 1.0$
$n = 1.5$

Fig. 3.19 : Behavior of M on $\phi(\eta)$.

$\gamma = 0.3$, K = 0.02, M = 0.1 = Nt, Nb = 0.2, Le = 1.0, Pr = 1.2

$c = 0.0, 0.5, 1.0$

$n = 1.0$
$n = 1.5$
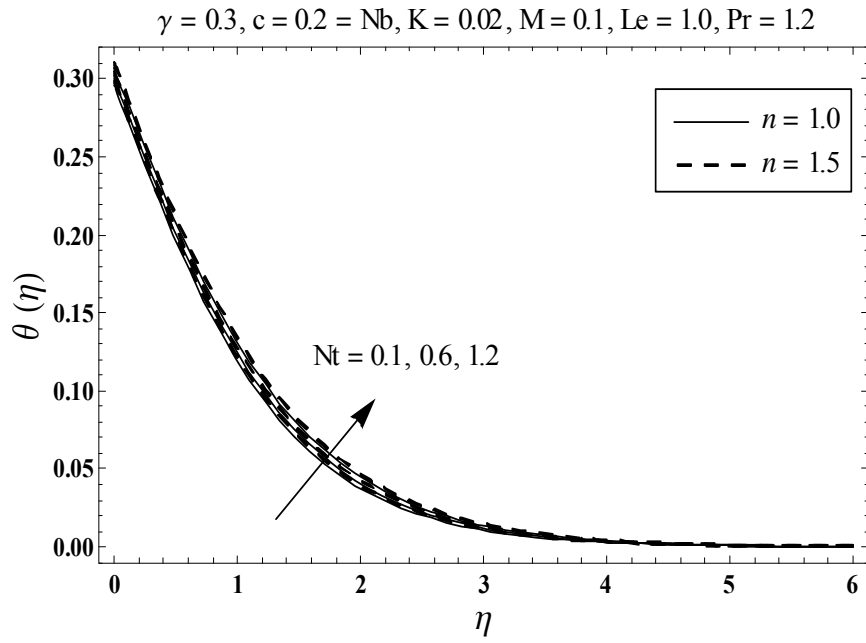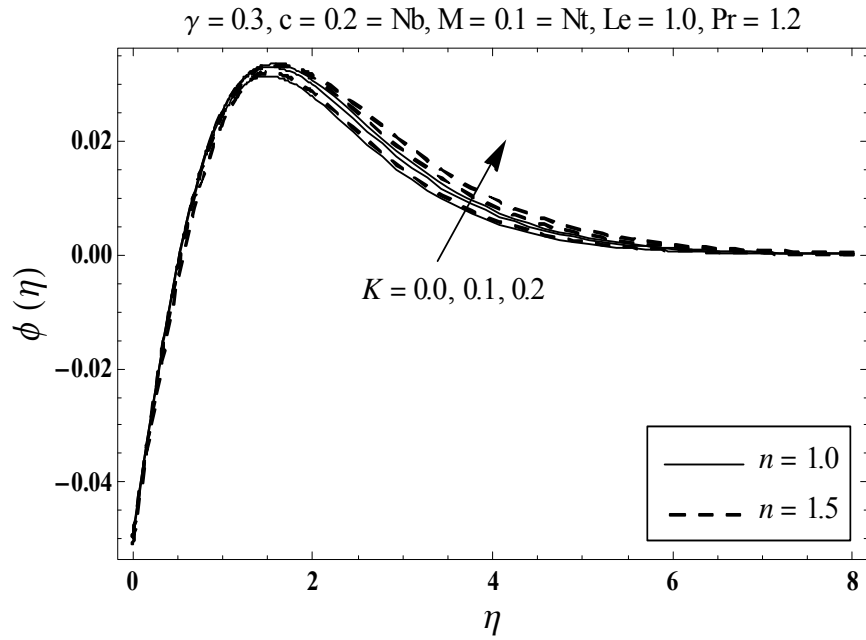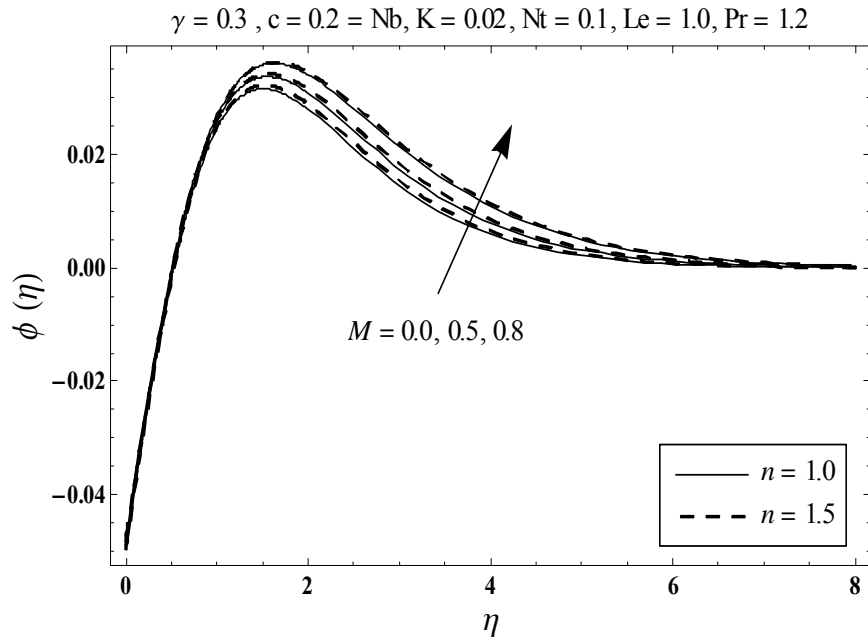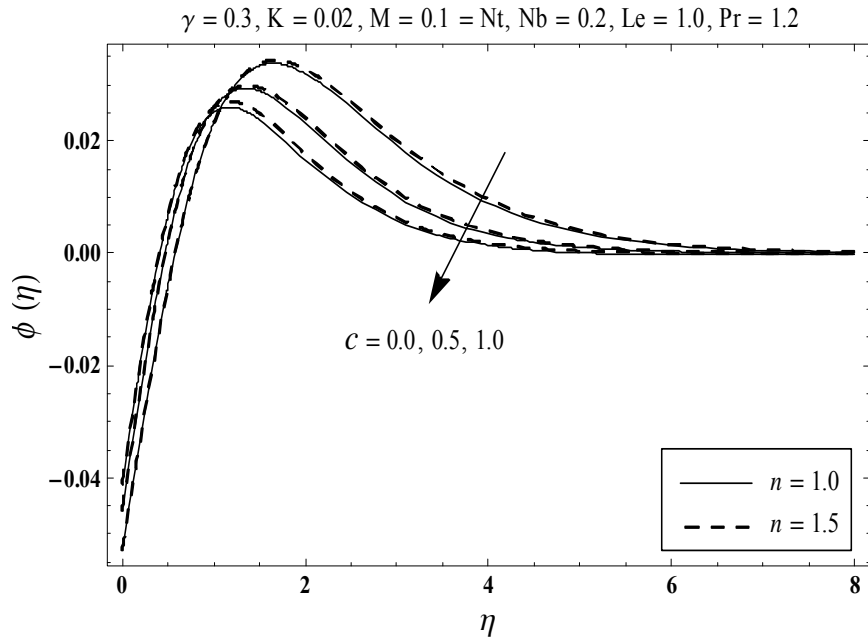
Fig. 3.20 : Behavior of c on $\phi(\eta)$.

53
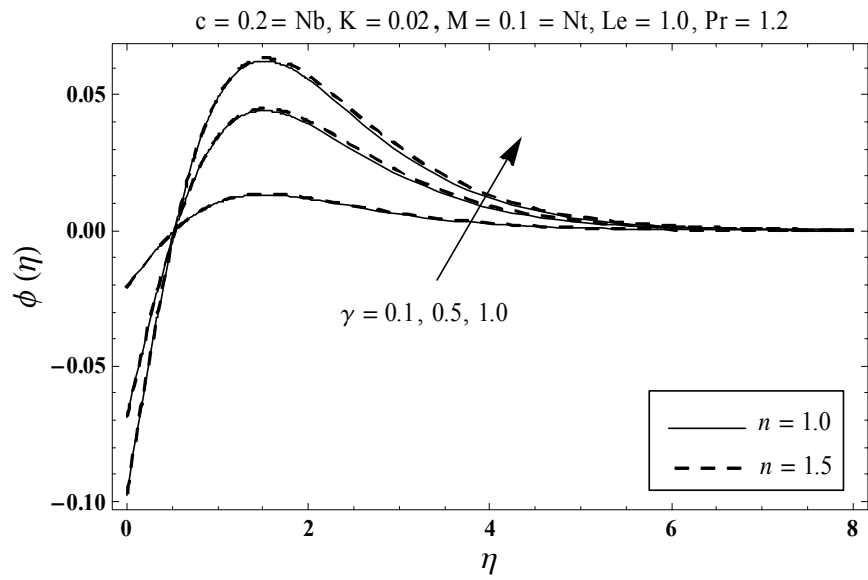
Fig. 3.21 : Behavior of γ on $\phi(\eta)$.
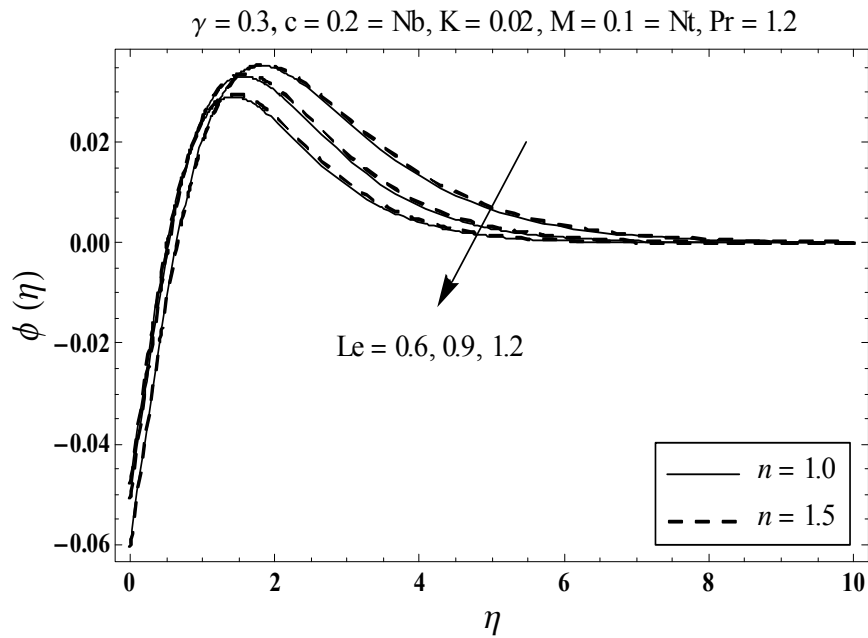
Fig. 3.22 : Behavior of Le on $\phi(\eta)$.

Fig. 3.23 : Behavior of Pr on $\phi(\eta)$.

$\gamma = 0.3$, c = 0.2, K = 0.02, M = 0.1 = Nt, Le = 1.0, Pr = 1.2
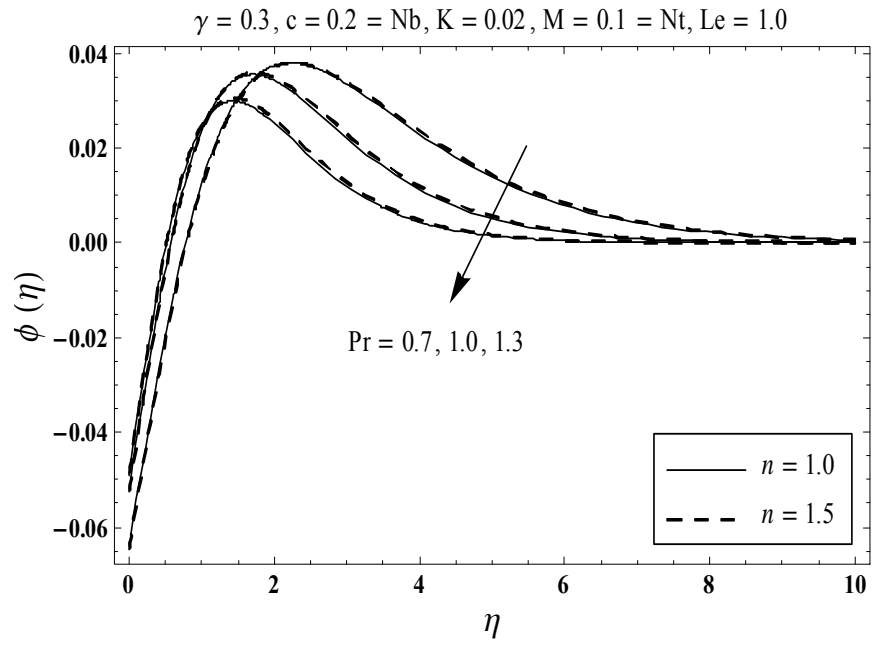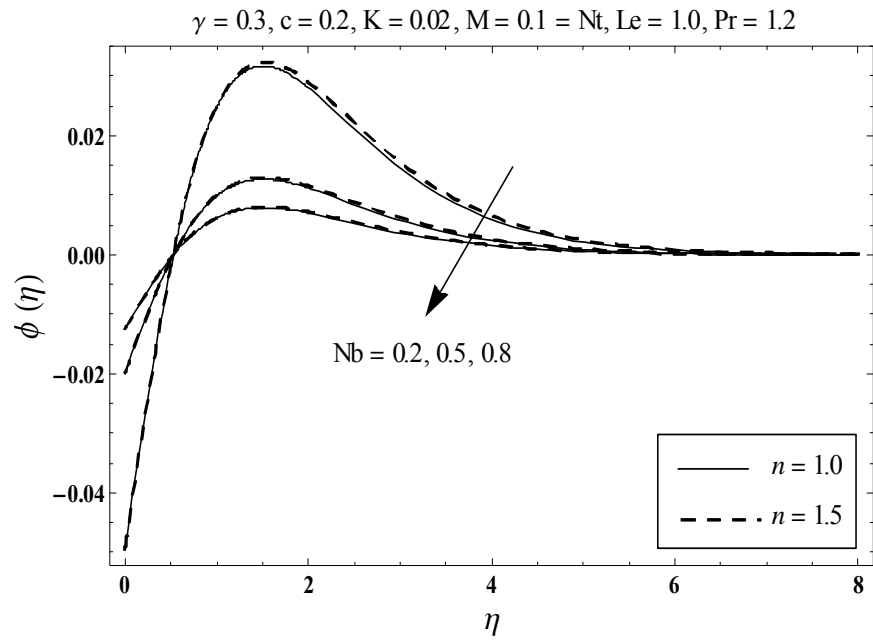
Fig. 3.24 : Behavior of Nb on $\phi(\eta)$.
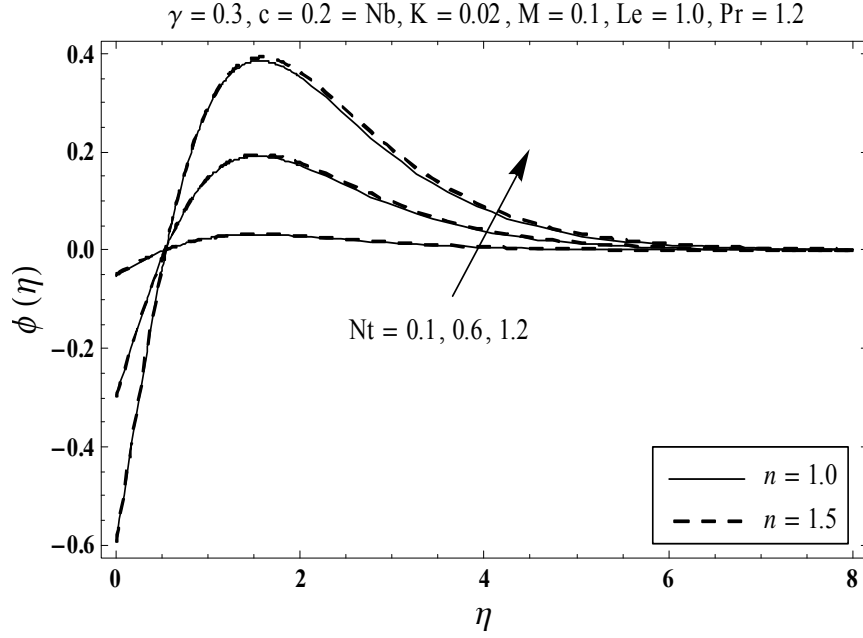
Fig. 3.25 : Behavior of Nt on $\phi(\eta)$.

Table 3.2: Numerical data for the coefficients of skin friction $-C_{fx}\,\mathrm{Re}_x^{1/2}$ and $-C_{fy}\,\mathrm{Re}_y^{1/2}$ for various values of K, M and c.

K	M	c	$-C_{fx}\,\mathrm{Re}_x^{1/2}$		$-C_{fy}\,\mathrm{Re}_y^{1/2}$	
			$n = 1.0$	$n = 1.5$	$n = 1.0$	$n = 1.5$
0.00	0.1	0.2	1.1000	1.3050	2.4597	2.9181
0.01			1.0932	1.2945	2.4446	2.8945
0.02			1.0863	1.2832	2.4290	2.8694
0.02	0.0	0.2	1.0819	1.2786	2.4192	2.8591
	0.2		1.0993	1.2970	2.4581	2.9001
	0.5		1.1860	1.3886	2.6520	3.1050
0.02	0.1	0.2	1.0863	1.2832	2.4290	2.8694
		0.3	1.1290	1.3332	2.0613	2.4341
		0.5	1.2095	1.4270	1.7105	2.0181

56

Table 3.3: Numerical data for the Nusselt number $Nu_x\,\mathrm{Re}_x^{-1/2}$ for various values of K, M, c, γ, Nt, Nb, Le, Pr.

K	M	c	γ	Nt	Nb	Le	Pr	$Nu_x\,\mathrm{Re}_x^{-1/2}$	
								$n=1.0$	$n=1.5$
0.00	0.1	0.2	0.3	0.1	0.2	1.0	1.2	0.2114	0.2356
0.02								0.2112	0.2352
0.05								0.2108	0.2344
0.02	0.0	0.2	0.3	0.1	0.2	1.0	1.2	0.2113	0.2353
	0.5							0.2091	0.2329
	0.8							0.2060	0.2295
0.02	0.1	0.0	0.3	0.1	0.2	1.0	1.2	0.2054	0.2287
		0.3						0.2136	0.2379
		0.5						0.2180	0.2427
0.02	0.1	0.2	0.1	0.1	0.2	1.0	1.2	0.0877	0.0979
			0.7					0.3527	0.3917
			1.2					0.4458	0.4943
0.02	0.1	0.2	0.3	0.0	0.2	1.0	1.2	0.2115	0.2355
				0.5				0.2100	0.2338
				1.0				0.2084	0.2321
0.02	0.1	0.2	0.3	0.1	0.5	1.0	1.2	0.2112	0.2352
					1.0			0.2112	0.2352
					1.5			0.2112	0.2352
0.02	0.1	0.2	0.3	0.1	0.2	0.5	1.2	0.2113	0.2353
						1.0		0.2112	0.2352
						1.5		0.2111	0.2351
0.02	0.1	0.2	0.3	0.1	0.2	1.0	0.5	0.1687	0.1874
							1.0	0.2034	0.2263
							1.5	0.2200	0.2451

3.5   Main findings

Magnetohydrodynamic (MHD) three-dimensional flow of couple stress nanofluid caused by non-linear stretching sheet having convective boundary condition has been analyzed. The main observations of this chapter are summarized below

- Larger values of couple stress parameter K present similar behavior for velocity distributions $f'(\eta)$ and $g'(\eta)$.

- An increment in the magnetic number M causes a reduction in the both components of velocity $f'(\eta)$ and $g'(\eta)$.

- An enhancement in the values of couple stress parameter K show increasing behavior for temperature and concentration distributions.

- Temperature distribution $\theta(\eta)$ enhances when the larger values of magnetic number M is taken into account.

- Both the temperature and concentration profiles are increased by enhancing Biot number γ.

- Temperature $\theta(\eta)$ and thickness of thermal layer are lower for the higher values of Prandtl number (Pr).

- Temperature and concentration profiles exhibit similar behavior for higher values of thermophoresis parameter Nt.

- An enhancement in Brownian motion parameter Nb yields a weaker concentration profile.

- Skin friction coefficient are increased for the higher values of magnetic number M.

- Heat transfer rate at the surface remains constant for Nb while it decreases for the larger values of Nt.

Bibliography

[1] K. Vajravelu, Viscous flow over a nonlinearly stretching sheet, Appl. Math. Comput., 124 (2001) 281-288.

[2] R. Cortell, Viscous flow and heat transfer over a nonlinearly stretching sheet, Appl. Math. Comput., 184 (2007) 864-873.

[3] R. Cortell, Effects of viscous dissipation and radiation on the thermal boundary layer over a nonlinearly stretching sheet, Phys. Lett. A., 372 (2008) 631-636.

[4] T. Hayat, Q. Hussain and T. Javed, The modified decomposition method and Padé approximants for the MHD flow over a non-linear stretching sheet, Nonlinear Anal.-Real World Appl., 10 (2009) 966-973.

[5] P. Rana and R. Bhargava, Flow and heat transfer of a nanofluid over a nonlinearly stretching sheet: A numerical study, Comm. Nonlinear Sci. Num. Simulat., 17 (2012) 212-226.

[6] S. Mukhopadhyay, Analysis of boundary layer flow over a porous nonlinearly stretching sheet with partial slip at the boundary, Alexandria Eng. J., 52 (2013) 563-569.

[7] F. Mabood, W.A. Khan and A.I.M. Ismail, MHD boundary layer flow and heat transfer of nanofluids over a nonlinear stretching sheet: A numerical study, J. Magn. Magn. Mater., 374 (2015) 569-576.

[8] M. Mustafa, J.A. Khan, T. Hayat and A. Alsaedi, Boundary layer flow of nanofluid over a nonlinearly stretching sheet with convective boundary condition, IEEE Trans. Nanotech., 14 (2015) 159-168.

[9] S.U.S. Choi, Enhancing thermal conductivity of fluids with nanoparticles, ASME, USA (1995) 99-105, FED 231/MD.

[10] J. Boungiorno, Convective transport in nanofluids, ASME J. Heat Transfer, 128 (2006) 240-250.

[11] W.A. Khan and I. Pop, Boundary-layer flow of a nanofluid past a stretching sheet, Int. J. Heat Mass Transfer, 53 (2010) 2477-2483.

[12] M. Turkyilmazoglu, Exact analytical solutions for heat and mass transfer of MHD slip flow in nanofluids, Chem. Eng. Sci., 84 (2012) 182-187.

[13] W. Ibrahim and O.D. Makinde, The effect of double stratification on boundary-layer flow and heat transfer of nanofluid over a vertical plate, Comput. Fluids, 86 (2013) 433-441.

[14] K.L. Hsiao, Nanofluid flow with multimedia physical features for conjugate mixed convection and radiation, Comp. Fluids, 104 (2014) 1-8.

[15] Y. Lin, L. Zheng and X. Zhang, Radiation effects on Marangoni convection flow and heat transfer in pseudo-plastic non-Newtonian nanofluids with variable thermal conductivity, Int. J. Heat Mass Transfer, 77 (2014) 708-716.

[16] A. Zeeshan, M. Baig, R. Ellahi and T. Hayat, Flow of viscous nanofluid between the concentric cylinders, J. Comp. Theoretical Nanoscience, 11 (2014) 646-654.

[17] M. Sheikholeslami, M.G. Bandpy, R. Ellahi, M. Hassan and S. Soleimani, Effects of MHD on Cu-water nanofluid flow and heat transfer by means of CVFEM, J. Magn. Magn. Mater., 349 (2014) 188-200.

[18] C. Zhang, L. Zheng, X. Zhang and G. Chen, MHD flow and radiation heat transfer of nanofluids in porous media with variable surface heat flux and chemical reaction, Appl. Math. Modell., 39 (2015) 165-181.

[19] M. Sheikholeslami, D.D. Ganji, M.Y. Javed and R. Ellahi, Effect of thermal radiation on magnetohydrodynamics nanofluid flow and heat transfer by means of two phase model, J. Magn. Magn. Mater., 374 (2015) 36-43.

[20] B.J. Gireesha, R.S.R. Gorla and B. Mahanthesh, Effect of suspended nanoparticles on three-dimensional MHD flow, heat and mass transfer of radiating Eyring-Powell fluid over a stretching sheet, J. Nanofluids, 4 (2015) 474-484.

[21] M. Mustafa, J.A. Khan, T. Hayat and A. Alsaedi, On Bödewadt flow and heat transfer of nanofluids over a stretching stationary disk, J. Mol. Liquids, 211 (2015) 119-125.

[22] T. Hayat, M. Imtiaz and A. Alsaedi, Impact of magnetohydrodynamics in bidirectional flow of nanofluid subject to second order slip velocity and homogeneous-heterogeneous reactions, J. Magn. Magn. Mater., 395 (2015) 294-302.

[23] V. K. Stokes, Couple stresses in fluids, Phys. Fluids, 9 (1966) 1709-1715.

[24] D. Srinivasacharya and K. Kaladhar, Mixed convection flow of couple stress fluid in a non-darcy porous medium with Soret and Dufour effects, J. Appl. Sci. Eng., 15 (2012) 415-422.

[25] M. Ramzan, M. Farooq, A. Alsaedi and T. Hayat, MHD three-dimensional flow of couple stress fluid with Newtonian heating, Eur. Phys. J. Plus, 128 (2013) 49.

[26] T. Hayat, M. Mustafa, Z. Iqbal and A. Alsaedi, Stagnation-point flow of couple stress fluid with melting heat transfer, Appl. Math. Mech. -Eng. Ed., 34 (2013) 167-176.

[27] M. Turkyilmazoglu, Exact solutions for two-dimensional laminar flow over a continuously stretching or shrinking sheet in an electrically conducting quiescent couple stress fluid, Int. J. Heat Mass Transfer, 72 (2014) 1-8.

[28] T. Hayat, T. Muhammad, A. Alsaedi and M.S. Alhuthali, Magnetohydrodynamic three-dimensional flow of viscoelastic nanofluid in the presence of nonlinear thermal radiation, J. Magn. Magn. Mater., 385 (2015) 222-229.

[29] O.D. Makinde and A. Aziz, Boundary layer flow of a nanofluid past a stretching sheet with a convective boundary condition, Int. J. Thermal Sci., 50 (2011) 1326-1332.

[30] T. Hayat, T. Muhammad, S.A. Shehzad, G.Q. Chen and I.A. Abbas, Interaction of magnetic field in flow of Maxwell nanofluid with convective effect, J. Magn. Magn. Mater., 389 (2015) 48-55.

[31] A.V. Kuznetsov and D.A. Nield, Natural convective boundary-layer flow of a nanofluid past a vertical plate: A revised model, Int. J. Thermal Sci., 77 (2014) 126-129.

[32] T. Hayat, T. Muhammad, S.A. Shehzad, M.S. Alhuthali and J. Lu, Impact of magnetic field in three-dimensional flow of an Oldroyd-B nanofluid, J. Mol. Liquids, 212 (2015) 272-282.

[33] S.J. Liao, Homotopy analysis method in nonlinear differential equations, Springer & Higher Education Press, Heidelberg, 2012.

[34] M. Turkyilmazoglu, Solution of the Thomas-Fermi equation with a convergent approach, Commun. Nonlinear. Sci. Numer Simulat., 17 (2012) 4097-4103.

[35] M. Sheikholeslami, M. Hatami and D.D. Ganji, Micropolar fluid flow and heat transfer in a permeable channel using analytic method, J. Mol. Liquids, 194 (2014) 30-36.

[36] S. Abbasbandy, T. Hayat, A. Alsaedi and M.M. Rashidi, Numerical and analytical solutions for Falkner-Skan flow of MHD Oldroyd-B fluid, Int. J. Numer. Methods Heat Fluid Flow, 24 (2014) 390-401.

[37] J. Sui, L. Zheng, X. Zhang and G. Chen, Mixed convection heat transfer in power law fluids over a moving conveyor along an inclined plate, Int. J. Heat Mass Transfer, 85 (2015) 1023-1033.

[38] R. Ellahi, M. Hassan and A. Zeeshan, Shape effects of nanosize particles in $Cu-H_2O$ nanofluid on entropy generation, Int. J. Heat Mass Transfer, 81 (2015) 449-456.

[39] T. Hayat, M. Imtiaz and A. Alsaedi, MHD 3D flow of nanofluid in presence of convective conditions, J. Mol. Liquids, 212 (2015) 203-208.

[40] T. Hayat, T. Muhammad, S.A. Shehzad and A. Alsaedi, A mathematical study for three-dimensional boundary layer flow of Jeffrey nanofluid, Z. Naturforsch. A, 70a (2015) 225-233.

Turnitin Originality Report

Thesis by Arsalan Aziz

From Thesis (Thesis)

- Processed on 07-Dec-2015 02:06 PKT
- ID: 610653742
- Word Count: 11031

Similarity Index
18%
Similarity by Source

Internet Sources:
    8%
Publications:
    9%
Student Papers:
    9%

sources:

1   2% match (student papers from 21-Sep-2015)

Submitted to Higher Education Commission Pakistan on 2015-09-21

2   1% match (student papers from 10-Jun-2013)

Submitted to Higher Education Commission Pakistan on 2013-06-10

3   1% match (publications)

Hayat, Tasawar, Taseer Muhammad, Sabir Ali Shehzad, and Ahmed Alsaedi. "Three-Dimensional Flow of Jeffrey Nanofluid with a New Mass Flux Condition", Journal of Aerospace Engineering, 2015.

4   1% match (student papers from 06-Nov-2013)

Submitted to Higher Education Commission Pakistan on 2013-11-06

5   < 1% match (Internet from 22-Feb-2014)

http://iisonline.org/files/uploads/2012/06/220_YAO-Kitty_and_Tony_for_ShinIIS_Yi_Kitty_Yao_v2.pptx

6 < 1% match (publications)

Hayat, T., Tariq Hussain, S. A. Shehzad, and A. Alsaedi. "Thermal and Concentration Stratifications Effects in Radiative Flow of Jeffrey Fluid over a Stretching Sheet", PLoS ONE, 2014.

7 < 1% match (student papers from 11-May-2012)

Submitted to Higher Education Commission Pakistan on 2012-05-11

8 < 1% match (Internet from 13-Sep-2014)

http://cinematography.net/Gothenburg/Alexa-plus-3_5-rec0021.dpx

9 < 1% match (publications)

Mustafa, M., T. Hayat, and A. Alsaedi. "Axisymmetric Flow of a Nanofluid Over a Radially Stretching Sheet with Convective Boundary Conditions", Current Nanoscience, 2012.

10 < 1% match (publications)

Shehzad, Sabir Ali, Tasawar Hayat, Ahmed Alsaedi, and Mustafa Ali Obid. "Nonlinear thermal radiation in three-dimensional flow of Jeffrey nanofluid: A model for solar energy", Applied Mathematics and Computation, 2014.

11 < 1% match (publications)

Hayat, Tasawar, Anum Shafiq, and Ahmed Alsaedi. "Effect of Joule Heating and Thermal Radiation in Flow of Third Grade Fluid over Radiative Surface", PLoS ONE, 2014.

12 < 1% match (student papers from 28-Dec-2014)

Submitted to Higher Education Commission Pakistan on 2014-12-28

13 < 1% match (publications)

Srinivasacharya, D.; Srinivasacharyulu, N. and Odelu, O.. "Flow of Couple Stress Fluid Between Two Parallel Porous Plates", International Journal of Applied Mathematics, 2011.

14 < 1% match ()

http://www.schaffner.uk.com/support/Binaries/c3drivers/_RSESPI7.edv

15   < 1% match (publications)

Hussain, Tariq, Sabir Ali Shehzad, Tasawar Hayat, Ahmed Alsaedi, Falleh Al-Solamy, and Muhammad Ramzan. "Radiative Hydromagnetic Flow of Jeffrey Nanofluid by an Exponentially Stretching Sheet", PLoS ONE, 2014.

16   < 1% match (Internet from 14-Feb-2015)

http://jafmonline.net/JournalArchive/download?file_ID=35753&issue_ID=221

17   < 1% match (publications)

Mustafa, M., M. Nawaz, T. Hayat, and A. Alsaedi. "MHD Boundary Layer Flow of Second-Grade Nanofluid over a Stretching Sheet with Convective Boundary Conditions", Journal of Aerospace Engineering, 2012.

18   < 1% match (Internet from 14-Jun-2011)

http://www.moris.ru/klients/godovoi_29042009.rtf

19   < 1% match (publications)

foresight, Volume 13, Issue 5 (2011-09-13)

20   < 1% match (publications)

Hayat, T., T. Muhammad, S. A. Shehzad, and A. Alsaedi. "Three-dimensional boundary layer flow of Maxwell nanofluid: mathematical model", Applied Mathematics and Mechanics, 2015.

21   < 1% match (Internet from 05-Nov-2015)

http://www.science.gov/topicpages/o/optimized+flow+sheet.html

22   < 1% match (publications)

Mustafa, M., Junaid A. Khan, T. Hayat, and A. Alsaedi. "Boundary Layer Flow of Nanofluid Over a Nonlinearly Stretching Sheet With Convective Boundary Condition", IEEE Transactions on Nanotechnology, 2015.

23   < 1% match (Internet from 29-Aug-2008)

http://hal.physast.uga.edu/~jss/1120L/data/CCJD/Lab%20%232/

Jupiter25sempty.fit

---

24 < 1% match (publications)

International Journal of Numerical Methods for Heat & Fluid Flow, Volume 25, Issue 3 (2015)

---

25 < 1% match (Internet from 01-Nov-2013)

http://permraion.ru/_res/fs/file11789.wmf

---

26 < 1% match (Internet from 07-Oct-2015)

http://article.sapub.org/10.5923.j.ajcam.20150504.04.html

---

27 < 1% match (student papers from 02-Jul-2015)

Submitted to Higher Education Commission Pakistan on 2015-07-02

---

28 < 1% match (Internet from 07-Jul-2015)

http://www.altronix.com/products/cad_drawings_enclosures/BC400SG.dwg

---

29 < 1% match (publications)

Rashidi, M.M. Momoniat, E. Ferdows, M. B. "Lie group solution for free convective flow of a nanofluid past a chemically reacting horizontal pla", Mathematical Problems in Engineering, Annual 2014 Issue

---

30 < 1% match (Internet from 03-Oct-2011)

http://db0sif.darc.de/cgi-bin/dpcmd?R%20SOFTWARE%204796

---

31 < 1% match (Internet from 21-May-2013)

http://thermalscience.vinca.rs/pdfs/papers-2011/TSCI110405119H.pdf

---

32 < 1% match (Internet from 06-Jan-2015)

http://manuscript.sciknow.org/uploads/hmmt/pub/HMMT-1585-page%20proof-final.pdf

---

33 < 1% match (publications)

Ibrahim, Wubshet, and O. D. Makinde. "Magnetohydrodynamic Stagnation Point Flow and Heat Transfer of Casson Nanofluid Past a Stretching Sheet with Slip and Convective Boundary Condition", Journal of Aerospace Engineering, 2015.

---

34   < 1% match (publications)

Khan, Junaid Ahmad, Meraj Mustafa, Tasawar Hayat, and Ahmed Alsaedi. "On Three-Dimensional Flow and Heat Transfer over a Non-Linearly Stretching Sheet: Analytical and Numerical Solutions", PLoS ONE, 2014.

---

35   < 1% match (publications)

Das, Kalidas. "Slip flow and convective heat transfer of nanofluids over a permeable stretching surface", Computers & Fluids, 2012.

---

36   < 1% match (student papers from 13-Jun-2012)

Submitted to Higher Education Commission Pakistan on 2012-06-13

---

37   < 1% match (Internet from 14-Jan-2015)

http://www.boundaryvalueproblems.com/content/2014/1/2

---

38   < 1% match (publications)

Mushtaq, Ammar, M. Mustafa, T. Hayat, and A. Alsaedi. "Nonlinear radiative heat transfer in the flow of nanofluid due to solar energy: A numerical study", Journal of the Taiwan Institute of Chemical Engineers, 2013.

---

39   < 1% match (Internet from 18-Mar-2012)

http://www.ngs-privod.ru/docs/ Ezhekvartalniy_otchet_emitenta_za_2_kvartal_2006_goda.rtf

---

40   < 1% match (Internet from 08-Oct-2010)

http://deneb.astro.warwick.ac.uk/phsaap/wdcharts/WD1247+575.fits

---

41   < 1% match (Internet from 26-Dec-2014)

http://www.rspublication.com/ijeted/2014/MAY14/23.pdf

---

42   < 1% match (publications)

International Journal of Numerical Methods for Heat & Fluid Flow, Volume 22, Issue 8 (2012-10-20)

---

43   < 1% match (student papers from 02-Jun-2015)

Submitted to Higher Education Commission Pakistan on 2015-06-02

---

44   < 1% match (student papers from 12-Nov-2013)

Submitted to Higher Education Commission Pakistan on 2013-11-12

---

45   < 1% match (Internet from 07-Jul-2013)

http://www.freewebs.com/books-nur-islam/mrekulli_ne_trupat_tane.rtf

---

46   < 1% match (Internet from 30-Jul-2015)

http://jafmonline.net/JournalArchive/download?file_ID=36940&issue_ID=222

---

47   < 1% match (Internet from 02-Feb-2012)

http://www.lana.lt/journal/32/Alam.pdf

---

48   < 1% match (student papers from 27-Mar-2014)

Submitted to Higher Education Commission Pakistan on 2014-03-27

---

49   < 1% match (publications)

Ul Haq, Rizwan, Sohail Nadeem, Z.H. Khan, and N.F.M. Noor. "Convective heat transfer in MHD slip flow over a stretching surface in the presence of carbon nanotubes", Physica B Condensed Matter, 2015.

---

50   < 1% match (publications)

International Journal of Numerical Methods for Heat & Fluid Flow, Volume 24, Issue 2 (2014-03-28)

---

51   < 1% match (student papers from 25-Oct-2013)

Submitted to Higher Education Commission Pakistan on 2013-10-25

---

52   < 1% match (Internet from 25-Feb-2014)

http://grb.mmto.arizona.edu/~ggwilli/research/wr/finder/regions/wr129_60min.
fits

53 < 1% match (Internet from 16-May-2015)

http://www.saaw.co.za/
documents/2014presentations/3_dr_johan_van_zyl_saaw_2014.pptx

54 < 1% match (Internet from 28-Mar-2010)

http://lambda.gsfc.nasa.gov/data/iras/skymaps_and_related/galactic-
plane_maps/data/GPL_14_H2B1.INTE

55 < 1% match (Internet from 03-Sep-2012)

http://www.aadet.com/article/heat_capacity

56 < 1% match (student papers from 14-Dec-2013)

Submitted to Higher Education Commission Pakistan on 2013-12-14

57 < 1% match (student papers from 20-Feb-2014)

Submitted to National Tsing Hua University on 2014-02-20

58 < 1% match (student papers from 19-Sep-2011)

Submitted to Higher Education Commission Pakistan on 2011-09-19

59 < 1% match (Internet from 22-Mar-2015)

http://www.daokedao.ru/blog/wp-content/pleco/MASS.pqb

60 < 1% match (Internet from 22-Feb-2015)

http://www.bun23.com/files/snes/Super%20Puyo%20Puyo%202%20(J).smc

61 < 1% match (Internet from 09-Sep-2015)

http://www.unitbv.ro/Portals/31/Abilitare/Teze/Standarde/03-Huminic-
_Standarde%20minimale%20pentru%20IM.pdf

62 < 1% match (publications)

International Journal of Numerical Methods for Heat & Fluid Flow, Volume 24,
Issue 2 (2014-03-28)

---

63   < 1% match (publications)

Nadeem, S., and Rizwan Ul Haq. "MHD Boundary Layer Flow of a Nano
Fluid past a Porous Shrinking Sheet with Thermal Radiation", Journal of
Aerospace Engineering, 2012.

---

64   < 1% match (Internet from 12-Feb-2013)

http://starbase.jpl.nasa.gov/mgs-m-mola-5-iegdr-l3-v2.0/mgsl_2013/data/pedr/
ap10966i.b

---

65   < 1% match (Internet from 07-Aug-2013)

http://journal-enertech.eu/papers-archive/doc_download/30-paper-25-2010-
118.html

---

66   < 1% match (student papers from 18-Apr-2012)

Submitted to Higher Education Commission Pakistan on 2012-04-18

---

67   < 1% match (Internet from 25-Jun-2015)

http://www.nanoscaleslett.com/content/7/1/229

---

68   < 1% match (Internet from 22-Dec-2009)

http://dahn.postech.ac.kr/class/273/New5.pdf

---

69   < 1% match (Internet from 10-Jan-2010)

http://deneb.astro.warwick.ac.uk/phsaap/wdcharts/WD0821+632.fits

---

70   < 1% match (Internet from 29-Jan-2015)

http://141.84.8.93/lehre/ss12/cg2/vorlesung/CG2-S12-05-DFT.pdf

---

71   < 1% match (Internet from 08-Feb-2014)

http://www.reflex.bestmail.ws/Games/Pokemon/Pokemon%20Blattgruen%20
(D).gba

---

72   < 1% match (Internet from 17-Aug-2015)

http://www.researchgate.net/publication/273958332_Three-dimensional_flow_of_nanofluid_over_a_non-linearly_stretching_sheet_An_application_to_solar_energy

73   < 1% match (Internet from 20-Oct-2014)

http://arquivoescolar.org/bitstream/arquivo-e/75/1/ALTP.pdf

74   < 1% match (Internet from 27-Mar-2015)

http://journals.plos.org/plosone/article?id=10.1371/journal.pone.0049499

75   < 1% match (Internet from 25-Feb-2012)

http://www.e-segments.com/?id=1517

76   < 1% match (publications)

Ali, Farhad Khan, Ilyas Haq, Sami Ul Sha. "Influence of thermal radiation on unsteady free convection MHD flow of brinkman type fluid in a poro", Mathematical Problems in Engineering, Annual 2014 Issue

77   < 1% match (publications)

Abbas, Z. Sheikh, Mariam Sajid, M.. "Hydromagnetic stagnation point flow of a micropolar viscoelastic fluid towards a stretching/shrinkin", Canadian Journal of Physics, Oct 2014 Issue

78   < 1% match (publications)

Ibrahim, Wubshet, and Bandari Shankar. "MHD boundary layer flow and heat transfer of a nanofluid past a permeable stretching sheet with velocity, thermal and solutal slip boundary conditions", Computers & Fluids, 2013.

paper text:

Contents 1 Some fundamental equations and laws 4 1.1

equations and laws The basic purpose of this chapter is to address the some primitive laws,

definitions and equations which are more essential to understand the analysis explained in chapters

two and three. 1.1 Fluid A substance which continuosly deforms under the implementation of applied

shear stress of any magnitude is called fluid. Liquids and gases are examples of fluid. 1.1.1 Liquid It

is type of fluid that has a definite volume but no definite shape. Blood, water and milk are examples

of liquids. 1.1.2 Gas It is type of fluid that has no definite volume and shape is known as gas. For

example oxygen, hydrogen and nitrogen etc. 1.2 Fluid mechanics Fluid mechanics is the class of

physical sciences which deals with the fluid's characteristics at rest or in motion. It can be classified

into two main branches which are defined as follows: 1.2.1 Fluid statics It describes the fluid

properties or features in state of rest. 1.2.2 Fluid dynamics Fluid dynamics deals with the

characteristics of fluids in state of motion. 1.3 Stress Stress is an applied force that acts on the

surface area of unit dimension within a deformable body. Mathematically it can be expressed as Stress (?) = Area Force = F ? ? (1.1) The unit and dimension of stress are ??−2 and ??−1?−2 respectively. Stress is mainly classified into two types. £ ¤ 1.3.1 Shear/tangential stress Stress is known as shear/tangential stress when an applied force acts parallel to the surface area of unit dimension within deformable body. 1.3.2 Normal/tension stress Stress is known as normal/tension stress when an applied force acts normal to the surface area of unit dimension within deformable body. 1.4 Strain Strain is utilized to measure the deformation of an object, when a force is acting on it. 1.5 Viscosity Viscosity is an inherent characteristic of fluid which measures the fluid resistance against any gradual deformation under the action of various forces. There are two ways to denote the viscosity. 1.5.1 Dynamic viscosity It is the fluid characteristic which measures the resistance of fluid against any gradual defor- mation when a force is acted on it. Mathematically, one can write it as dynamic viscosity (?) = gradient of velocity Shear stress ? (1.2) SI unit and dimension of dynamic viscosity are ???−1?−1and dimension ??−1?−1 respec- tively. £ ¤ 1.5.2

36**Kinematic viscosity (?) It is** stated **as ratio of** dynamic **viscosity (?) to the density of fluid (?). Mathematically it can be** expressed **as**

? = ? ? ? (1.3) Kinematic viscosity has the unit ?2?−1 and dimension ?2? −1 ? £ ¤ 1.6 Newton's viscosity law It is stated that the shear force which deforms the element of fluid is linearly and directly proportional to the shear rate (i.e rate of deformation). In mathematical form we can express it as follows ? ?? ∝ ?? ?? ? (1.4) or ?? ? ?? = ? ?? ? (1.5) µ ¶ In above relation ? ?? denotes the shear stress and ? represents proportionality constant. 1.6.1 Newtonian fluids Those fluids which satisfy the Newton's viscosity law are characterized as Newtonian fluids. In these types of fluids a direct and linear relation always exist between the shear force (???) and deformation rate ???? . Examples of Newtonian fluids are water, mercury and aqueous glycerine solution etc. ³ ´ 1.6.2 Non-Newtonian fluids The fluids for which Newton's viscosity law do not hold are the non-Newtonian fluids. In these types of fluids shear force has a direct and nonlinear relationship to the rate of deformation. In mathematical form we can express it as follows ?? ? τ ?? ∝ ?? ? ? =6 1? (1.6) µ ¶ or

τ ?? = ? ?? ?? ? ? (1.7) μ ¶ Here ? denotes the consistency index which is used to estimate the consistency of fluid and ? depicts the flow behavior's index which elucidates that the fluid differs from a Newtonian fluid. When ? = 1 and ? = ? then Eq. (1?7) transforms to the Newton's viscosity law. From Eq. (1?7) we have τ ?? = ?? ?? ? μ ?? ¶ with the following expression of apparent viscosity ?? is ?? = ? ?? ?−1 ? μ ?? ¶ (1.8) (1.9) In above expression ?? represents the apparent viscosity. Blood, ketchup and paints show the non-Newtonian fluid behavior. The fluid model which is considered in this dissertation is couple stress fluid model. The

13**force stress tensor ? and the couple stress tensor** ?

appears **in** couple stress fluids **theory**

which are defined in the following forms τ = −?+?div• ?+? grad• + grad• T˘ + ?×(div? +??)? 1 (1.10) ³ ´ μ ³ ´ ³ ´ ¶ 2 and ? = ?? + 2?∗ grad(curl •)+2?0(grad(curl •))T˘ ? (1.11) where the quantity ? represents the material constant, ?? denotes the body couple tensor, ? is the (1?3)rd trace of ? and ? 0 depicts

13**the constant associated with couple stresses.**

Material constant ? has dimension as

13**that of viscosity where as the dimensions of ?∗ and** ?0
are those of momentum. These material constants are
considered by **the** following **inequalities**

? ≥ 0? 3? + 2? ≥ 0? ?∗ ≥ 0? ?0 ≤ ?∗? (1.12) Using the Cartesian coordinates, we have ?? ?? grad• = • ???? ?? • ?? • ?? ?? ?? ?? ?? ?? ?? ?? ?? •? grad• T˘ ?? = • ???? ?? ?? ?? ?? ?? ?? ?? • ? (1.13) ?? ?? ?? ?? ?? • ³ ´ ?? • ?? ?? ?? ?? ?? • • • • By using the above expressions (1?10) − (1? 13)? the momentum equation for couple stress fluid takes the following form ? ?•= ∇? + ?∇2•−? ∗∇4•? (1.14) ?? By employing the operator ∇ on the velocity field, the quantities ∇2• and ∇4• can be

easily found which are ??2??2 + ??2??2 + ??2??2 ??4??4 + ??4??4 + ??4??4 ∇2• = • ??2??2 + ?? 2??2 + ?2? ??2 • ? ∇4• = • ??4??4 + ??4??4 + ??4??4 •? (1.15) • ??2??2 + ??2??2 + ??2??2 • • • • ??4??4 + ??4??4 + ??4??4 • • • By using Eqs. (1?14) and (1?15), we write ?? ?? ?? ?? ?? +??? +??? +??? ?2? ?2? ?2? = ? ??2 ??2 ??2 + + −?0 ?4? μ ¶ + ?4? ?4? ??4 ??4 + ? (1.16) μ ??4 ¶ ?? ?? ?? ?? ?2? ?2? ?2? ?? +??? +??? +??? =? ??2 ??2 ??2 + + −?0 ?4? μ + ?4? ?4? ¶ ??4 ??4 + ? (1.17) μ ??4 ¶ in which ?0 = ?∗?? is the couple stress viscosity. The governing boundary layer expressions for three dimensional flow of couple stress fluid are ???? + ? ???? + ? ???? + ? ???? = ? ??2??2 − ?0 ??4??4 ? μ ¶ μ ¶ ???? + ? ???? + ? ???? + ? ???? = ? ??2??2 − ?0 ??4??4 ? μ ¶ μ ¶ (1.18) (1.19) 1.7 Modes of heat transfer Heat transfer is a mechanism which deals with the transfer of heat within the system. Transport of

55**heat is the transfer of thermal energy from high to low temperature regions**

when two physical system or two objects are in contact. Three basic modes are utilized to develop heat transfer mechanism which are define as follows: 1.7.1 Conduction Conduction is the mode of heat transfer

2**in which heat is** shifted **from one place to another place**

due to the collisions of particles which are in contact but particles do not change their positions. Conduction is always occured in solid materials. In very rare cases conduction may be possible in liquids. 1.7.2 Convection Convection is the mode of heat transfer in which

35**heat is transferred from hot** places **to cold** places by **the**

transfer of particles or molecules. Convection plays major role in both liquid and gases. Forced convection Forced convection is a process of heat transfer in which some external source is utilized to produce motion in fluid. Examples of forced convection are pump, stretching, pressure and many

others. Natural convection This mechanism is always occured due to the differences of temperature without any external source. It is also known as free convection. Free convection is always occured due to gravity effects. Mixed convection Mixed convection is that type of convection in which transfer of heat takes place due to both natural and forced convections. 1.7.3 Radiation Radiation is that mechanism in which transfer of heat occurs directly by electromagnetic radi- ations. 1.8 Non-dimensional numbers 1.8.1 Prandtl number It describes the

38**ratio of momentum diffusivity (?) to the thermal diffusivity**

(?). In mathemat- ical form it can be written as momentum diffusivity (?) ??? Pr = thermal diffusivity (?) = ? ? (1.20) where ? stands for the dynamic viscosity, ?? represents the specific heat and ? designates the thermal conductivity. In heat transfer mechanism, Prandtl number controls the momentum and thermal boundary layers thicknesses. 1.8.2 Lewis number Lewis number is defined as the nondimensional quantity which explains the thermal diffusivity to Brownian diffusivity ratio. Mathematically thermal diffusivity ? ?? = Brownian diffusivity ?? = (1.21) Note that in above expression ? signifies the thermal diffusivity and ?? represents the Brownian diffusivity. 1.8.3 Magnetic number It is described as the ratio of electromagnetic to viscous forces. Mathematically it can be expressed as ?2 = ??02?? (1.22) ??? In which ? denotes the electrical conductivity, ?0 signifies the uniform magnetic field, ? shows the characteristic length, ? represents the fluid density and ?? depicts the velocity. 1.8.4 Reynolds number Inertial to viscous forces ratio is termed as Reynolds number. Mathematically one can write it as inertial force ?? ? ? ? Re = viscous force = ? = ? ? (1.23) Here ? denotes the fluid density, ? represents the mean velocity of fluid, ? stands for charac- teristic length and ? signifies the dynamic viscosity. Reynolds number is utilized to observe different flow behaviors like laminar or turbulent flows. Laminar flow is arised due to the low Reynolds number, where the viscous forces are dominant. At high Reynolds number turbulent flow arise, where the inertial forces are dominant. 1.8.5 Coefficient of skin friction It is the drag force between the fluid and solid's surface when fluid is passing through it which leads to slow down the motion of fluid. Mathematically it is stated as ?? = 12 ???2 ? ? ? (1.24) where ?? = ? ?? ??¶?=0 ?

(1.25) µ In above relation ? ? represents the shear stress at the surface, ?? stands for velocity and ? denotes the fluid density. 1.8.6 Nusselt number Convective to conductive heat transfer coefficients ratio is known as Nusselt number. In math- ematical form one can write ?? = ??? ?(?? − ?∞) ? (1.26) where ?? = −? ? (1.27) ?? µ ?? ¶?=0 where ?? denotes the wall heat flux, ?? represents the wall temperature, ?∞ stands for ambient fluid temperature and ? represents the thermal conductivity. 1.9 Fundamental laws 1.9.1 Mass conservation law It is stated that the total mass in any closed system will remain constant. Mathematically ?? ?? + ?∇?V = 0? (1.28) or ?? ?? + (V?∇) ? + ?∇?V = 0? (1.29) or ?? ?? + ∇? (?V) = 0? (1.30) The above expression represents the continuity equation. Here ? stands for fluid density and V depicts the velocity profile. Due to steady state flow Eq. (1?30) takes the following form ∇? (?V) = 0? (1.31) and if the fluid is incompressible then above equation takes the following form ∇?V = 0? (1.32) 1.9.2 Momentum conservation law This law states that the total momentum of a closed system is conserved. General form of this law is given below ? ?V ?? = ∇?τ +?b? (1.33) Here inertial, surface and body forces are indicated by the terms ? ??V? , ∇?τ and ? b respectively. Cauchy stress tensor is represented by τ = −?I + S, pressure is designated by ?, I shows the identity tensor, ??? shows the material time derivative, S stands for extra stress tensor and b denotes the body force. 1.9.3 Energy conservation law The energy equation for nanofluid can be written as ???? ???? = τ?L+?∇2? + ???? ??∇??∇? + ?? ∇??∇? ? ? (1.34) µ ∞ ¶ Where ?? stands for base fluid density, ?? represents the specific heat of base fluid, ? stands for temperature, τ represents the stress tensor, L stands for rate of strain tensor, ? denotes the thermal conductivity, ?? depicts the density of nanoparticles, ?? denotes Brownian diffusivity and ?? stands for thermophoretic diffusion coefficient. 1.9.4 Concentration conservation law The concentration equation for nanofluid can be written as ?? = ??∇2? + ?? ∇2? (1.35) ?? ?∞ where ? stands for nanoparticles concentration, ?? represents

74**the Brownian diffusion** co- efficient, ?? **stands for thermophoretic coefficient** and ? depicts **the**

temperature. 1.10 Homotopic analysis technique This technique is developed by Liao [33] to find the series solutions of nonlinear problems. This technique gives us convergent solutions for nonlinear

problems. In order to understand the basic concept of homotopy analysis technique (HAM), we assume a differential equation N [? (?)] = 0? (1.36) In above equation N represents the non-linear operator and ? (?) depicts the unknown function in which ? is the independent variable. Zeroth-order deformation equation is written in the following form (1 − Þ∗) L [?˘ (?; Þ∗) − ?0 (?)] = Þ∗~N [?˘ (?; Þ∗)] ? (1.37) where ?0 (?) depicts the initial approximation, L denotes the auxiliary linear operator, Þ∗ ∈ [0? 1] designates an embedding parameter, ~ represents the nonzero auxiliary parameter and ?˘ (?; Þ∗) stands for unknown function of ? and Þ∗. Setting Þ∗ = 0 and Þ∗ = 1, one has ?˘ (?; 0) = ?0 (?) and ?˘ (?; 1) = ? (?) ? (1.38) The solution ?˘ (?; Þ∗) shows the variation from initial approximation ?0 (?) to the final desired solution ? (?) when Þ∗ goes from 0 to 1. Taylor series expansion gives us the following relations By differentiating ?ˆ times the zeroth order deformation i. e., Eq. (1?37) with respect to Þ∗ then divided by ?ˆ! and by setting Þ∗ = 0 we have the following ?ˆth order equation ?˘ (?; Þ∗) = ?0 (?) + ?Xˆ=1 ??ˆ

40**(?)Þ∗?ˆ? ??ˆ(?)** = ?ˆ1! **??ˆ??˘ Þ(?∗??ˆÞ∗)‾Þ∗=** 0 ∞ ? ‾ ‾ For **Þ∗**

= 1 we get ‾ ∞ ? (?) = ?0 (?) + ??ˆ(?)? ?Xˆ=1 (1.39) (1.40) L

28**[??ˆ (?) − ??ˆ??ˆ−1** (?)] = ~R ˜?ˆ (?) ? **(1.** 41) where R ˜?ˆ (?) = (?ˆ **− 1)! 1**

??ˆN [?˘ (?; Þ∗)] ? Þ

28∗**?ˆ 0? ?ˆ ≤ 1? ??ˆ = •** ? **• 1? ?ˆ ? 1?** ? ‾ Þ∗=0 ‾ ‾ ‾ **(1.** 42) **(1.**

43) • Chapter 2 On

12**boundary layer flow of nanofluid** over **a** nonlinearly **stretching** surface **with convective** effect 2 **.1 Introduction** This **chapter** addresses **the** two dimensional flow **of**

incompressible Newtonian fluid

3**subject to the convective** surface **boundary condition.** The flow **is**

generated due to an impermeable sheet which is stretched nonlinearly.

15**Heat and mass transfer analysis is** studied through **the**

20**Brownian motion and thermophoresis effects. Newly** constructed **boundary** condition having **zero mass flux** of nanoparticles **at the boundary**

is incorporated. Mathematical formulation is made under boundary layer and small magnetic

Reynolds number assumptions. Suitable

24**transformations are employed to** convert **the** nonlinear **partial differential** system **into** the nonlinear **ordinary differential** system. Homotopic **series solutions of** resulting nonlinear system **are** constructed **and**

verified.

20**Graphs are** sketched **to** explore **the effects of** distinct emerging flow **parameters on the temperature and concentration**

profiles. Nusselt number is also computed and discussed. The contents of present chapter provides

review of research work examined by Mustafa et al. [8]. 2.2 Problem development We assume a

35**steady two dimensional** incompressible **flow of Newtonian fluid** past **over a surface**

which is stretched nonlinearly. Here we consider the Cartesian coordinate system

32**in such a** manner **that the ?–axis is** taken **in** that **direction along** which **the** sheet is stretched **and ?–axis is** orthogonal **to the** sheet. Stretching **of the**

sheet is assumed with velocity ??(?) = ??? along the ?–direction with ?? ? ? 0 as the constants.

21**Effects of Brownian motion and thermophoresis in the**

present flow problem are also taken into account. The surface temperature is regulated

3**by a convective heating** mechanism **which is** peculiarized **by the heat transfer coefficient ?? and temperature of hot fluid** ?? under **the** sheet. **The**

governing boundary layer expressions for present flow analysis are Fig. 2?1 : Physical sketch of the problem. ?? ?? ?? ?? = 0? + ? ?? ?? ?2? ?? + ? ?? = ? ??2 ? ? ?? ?? ?2? (??)? + ?? ?? + ?? ?? 2 ?? + ? ?? = ? ??2 (??)? Ã?? ?? ??

54**µ ¶ ? ? ∞ µ ?? ¶ ! (2.** 1) **(2.2) (2.** 3) ? ?? ?? ?? + ? ?? = ?? **??2 ? 2? + ? ? ?2? (2.** 4) **µ ¶ ?∞ ??2 ? µ**

¶ The subjected boundary conditions for the considered flow problem are ?=??(?)=???? ?=0?

−????? =??(??−?)? ?????? ??∞????? + = 0 at ? = 0? (2.5) ? → 0? ? → ?∞? ? → ?∞ as ? → ∞? (2.6)

Here ? and ? represent the flow velocities

> 41**in the** horizontal **and** vertical **directions respectively,** ? = ????
>
> stands for **kinematic viscosity,** ? denotes **the**

dynamic viscosity, ?? stands for density of¡base flu¢id, ? stands for temperature, ? (= ??(??)?)

denotes the thermal diffusivity, ? stands for thermal conductivity of fluid, (??)? stands for

> 67**heat capacity of fluid,** (??)? stands for **effective heat**
>
> **capacity of** nanoparticles, ?? denotes **the**

Brownian diffusivity, ? represents concentration, ?? stands for thermophoretic diffusion

coefficient, ?? = ?? ?−21 stands for non-uniform heat transfer coefficient. ?∞ denotes the ambient

fluid temperature and ?∞ represents the ambient fluid concentration. Using the following

transformations ? = ???? 0(?)? ? = − ??(?2+1) 1?2 (?) ?−21 {? + ??−+11 ?? 0}? ?(?) = ???−−??

∞∞ ? ?(?) =³ ?−??∞∞ ? ´? = ?(?2+?1) 1?2 (?) ?−21 ?? •• •

> 2**Eq. (2?1) is** now **identically satisfied and Eqs. (2?2) − (2?** 6)
>
> take **the** followin••g forms ³ ´ ? **000 + ? ? 00 − 2? ? 02**

= 0? ?+1 ?00 + Pr ??0 + ???0?0 + ???02 = 0? ?00 + ?? Pr ? ?0 + ? ? ?00 = 0? ³ ´ ?? ?(0)=0? ?0(0)

=1? ?0(0)=−?(1−?(0))? ???0(0)+???0(0)=0? ?0(∞)→0? ?(∞)→0? ?(∞)→0? (2.7) (2.8) (2.9) (2.10)

(2.11) (2.12) In above expressions Pr stands for

> 26**Prandtl number,** ? ? depicts **the Brownian motion**
>
> **parameter,** ? ? represents **the thermophoresis parameter,** ?
>
> stands for Biot **number and** ?? denotes the Lewis **number.**

3**These parameters can be** specified **by the following definitions**

Pr = ?? ? ? ? = (??()????)????∞ ? ? ? = (??)?(????)?(????∞–?∞) ? ? = ??? ?? ? ?? = ??? ? •••

(2.13) The nondimensional forms of coefficient of skin-friction and Nusselt nu•mber are given below

p • ??? Re1??2 = ? + 1 1?2 ?00(0)? μ 2 ??? Re–?1?2 = – ? + 1 1?2 ?0(0)? ¶ (2.14) μ 2 ¶ where

Re? = ????? represent the local Reynold number. From the above it can be analyzed that the

nondimensional

3**mass flux represented by a Sherwood number ??? is zero.**

2.3 Series solutions The approximate series solutions through the homotopy analysis technique

(HAM) requires the appropriate initial approximations and auxiliary linear operators for the governing

problems which are given below

70**?0(?) = 1 − exp(–?)? ?0(?) = 1 + ? exp(–?)? ?0(?) = –1 + ? ?? exp(–?)?**

? ? ?? (2.15)

73**L? = ??3 − ?? L? = ??2 − ?? L? = ??2 − ?? ?3?** ?? ? ?2? **?2?**

(2.16) The above linear operators have the following

4**properties L? [?1 + ?2 exp(?) + ?3 exp(–?)] = 0? L? [?4 exp (?) + ?5 exp(–?)] = 0?•** (2.17) **L? [?6 exp(?) + ?7 exp(–?)] = 0?**

• • in which ?? (? = 1 − 7) stands for

2**arbitrary constants. •• 2.3.1 Zeroth-order** deformation

equations **(1**− Þ ∗**)L?** ?˘ (?? Þ∗) − ?0(?) = Þ∗~? **N?**

[?˘ (?? Þ∗)]? (2.18) (1 − Þ∗)L? ˘ ?(??

19**Þ∗) − ?0(?) = Þ∗~?** N?[?˘ (?? **Þ∗)? ˘ ?(?? Þ∗)? ?˘ (?? Þ∗)]?** h i

(2. 19) (1 − **Þ∗)** L?[˘ ?(?? **Þ∗)− ?0(?)] = Þ∗~?**

N?[?˘ (?? Þ∗)? ˘ ?(?? Þ∗)? ?˘ (?? Þ∗)]? h i (2.20) ?˘ (0?

30**Þ∗) = 0? ?˘ 0(0? Þ∗) = 1? ?˘ 0(∞? Þ∗) = 0? ˘ ?0(** 0? Þ∗) = −? 1

− ˘ **?(0? Þ∗) ? ?˘ (∞? Þ∗) = 0? ??˘ ?0(** 0? Þ∗) + **???˘ 0(0?**Þ∗) =

0? ?˘ (∞?³Þ∗) = **0?**

´ • (2.21) • N? ?˘ (?; Þ∗) = ??3??3˘ + ?˘ ??2??2˘ − 2? ??˘ 2 • ? (2.22) h i ?+1 ?? Ã ! N? ?˘ (?;

Þ∗)? ?˘ (?? Þ∗)? ?˘ (?? Þ∗) = ??2??˘ 2 + Pr ?˘ ??˘ ?? ?˘ ???˘ ?˘ ? 2 +Pr?????? +Pr?? ??!

Ã ? (2.23) h i

69**N? ?˘ (?;Þ∗)??˘ (??Þ∗)??˘ (??**Þ∗) = **??2??˘ 2** +??Pr?˘ ???

˘ ? **???????2˘ ?2 + ? (2.** 24) h **i**

Here Þ∗ ∈ [0? 1] denotes the embedding parameter, ~? ? ~? and ~? stands for nonzero auxiliary

parameters and N? ?

56**N? and N?** represent **the nonlinear operators. 2.3.2 ?ˆth-**

order deformation problems

L?

23**[??ˆ(?) − ??ˆ??ˆ− 1(?)]** = ~?R ˜**??ˆ(?)? (2.** 25) L? **[??ˆ(?) − ??ˆ??ˆ−1**

(?)] = ~?R ˜**??ˆ(?)?** (2.26) L? **??ˆ(?) − ??ˆ??ˆ−** 1(?) = ~?R ˜**??ˆ(?)?**

(2.27) **??ˆ(**

5**0) = ??0ˆ(0) = ??0ˆ(∞) = 0? ?0?¤ˆ (0)** + ???ˆ **(0) = 0? £ ???0?ˆ**

(0) + ???0?ˆ (0) = 0? ??ˆ(∞) = ??ˆ(∞) = 0? • **(2.** 28) • ?ˆ **−1** ?ˆ **−1** R˜??ˆ

(?) = ??0ˆ00 **−1 (??0ˆ−1−???0)?**• + (? ?ˆ **−1−???** 00) − **2? (2.** 29) X **?**

=0μ ? + **1¶** X?=0 ?ˆ **−1** ?ˆ **−1** ?ˆ **−1** R˜??ˆ(?) = ??0ˆ0 **−1** + Pr (? ?ˆ **−1−??**

0?) + Pr ?? (?0?ˆ−1−???0) + Pr ?? (?0?ˆ−1−??0?)? (2.30)

45**X?=0 X?=0 X?=0** R ˜**??ˆ(?)=?0?0ˆ−** 1(?)+??Pr **?ˆ−** 1 **(??ˆ−** 1 **−???**

0)+ ??????0ˆ0−1? X **?=0 0? ?ˆ**

≤ 1? χ?ˆ= • • 1? ?ˆ ? 1? Putting Þ∗ = 0 and Þ∗ = 1 we have • ?˘ (?;0) = ?0(?)? ?˘ (?;1) = ?(?)? ?˘ (??0) = ?0(?)? ˘ ?(??1) = ?(?)? ?˘ (??0) = ?0(?)? ?˘ (??1) = ?(?)? (2.31) (2.32) (2.33) (2.34) (2.35) When Þ∗ varies from 0 to 1 then ?˘ (?;Þ∗)? ˘ ?(??Þ∗) and ?˘ (??Þ∗) display variation

43**from the initial** approximations **?0(?)?** ?0(?) **and ?0(?) to the** desired **final solutions ?(?)? ?(?) and ?(?) respectively.** By using **Taylor's series** expansion we get **the**

following expressions ∞ ?˘ (?; Þ∗) = ?0(?) + ??ˆ(?)Þ∗?ˆ? ??ˆ(?) = ?ˆ1! ??ˆ??˘ Þ(?∗??ˆÞ∗) ¯¯ Þ∗=0 ? (2.36) ?Xˆ=1 ¯ ∞ ??ˆ

40**(?)Þ**∗**?ˆ? ??ˆ(?)** = ?ˆ1! **??ˆ?˘ ?Þ(?∗??ˆÞ∗)**¯¯¯**Þ**∗= 0 ¯ ?˘ (?? **Þ∗)**

= ?0(?) + ? (2.37) ?Xˆ=1 ∞ ??ˆ(?)Þ∗?ˊ? ??ˆ(?) = ?ˆ1! ??ˆ?˘ ?Þ(?∗??ˆÞ∗)¯¯¯ ∗ ¯ ?˘ (?? Þ∗) = ?0(?)

+ ? (2.38) ?Xˆ=1 ¯Þ =0 The convergence of Eqs. (2?36) – (2?38) highly depends upon the ~?? ~?

¯¯ and ~?. Considering ¯ that the values of non-zero auxiliary parameters ~? ? ~? and ~? are

selected in such a way that Eqs. (2?36) – (2?38) converge at Þ∗ = 1, then ∞ ?(?) = ?0(?) + ??ˆ(?)? ?

Xˆ=1 ∞ ?(?) = ?0(?) + ??ˆ(?)? ?Xˆ=1 (2.39) (2.40) ∞ ?(?) = ?0(?) + ??ˆ(?)? (2.41) ?Xˆ=1 The general

solutions (??ˆ? ??ˆ? ??ˆ) of the Eqs. (2?25) – (2?27) in terms of special solutions (??∗ˆ? ??∗ˆ? ?∗?ˆ)

are presented by the following expressions ??ˆ(?) = ??∗ˆ(?) + ?1 + ?2 exp(?) + ?3 exp(−?)? (2.42) ??

ˆ(?) = ?∗?ˆ(?) + ?4 exp(?) + ?5 exp(−?)? (2.43) ??ˆ(?) = ?∗?ˆ(?) + ?6 exp(?) + ?7 exp(−?)? (2.44) in

which the constants ?? (? = 1 − 7) through the boundary conditions (2?28) are given by ?2 = ?4 = ?6

= 0? ?3 = ????∗ˆ?(?) ?=0 ? ?1 = −?3 −

<div style="color:red">
60**??∗ˆ(0)?** ¯ **??∗?ˆ(?)**¯ ?5 = **1** + ? 1 Ã ?? − **??∗?ˆ(0)** ? ?=0 ! **??∗?ˆ(?)**¯ ?

7 = ?? **?=0** ?? + ?? ¯ Ã −?5 + **???∗?ˆ?(?) ?=0!** ? 2.
</div>

3.3 Convergence analysis ¯ ¯ ¯ ¯ (2.45) (2.46) (2.47) Here the series solutions (2?39) – (2?41)

involve the auxiliary parameters ~? ? ~? and ~?? No doubt the auxiliary parameters ~? ? ~? and ~?

in series solutions accelerate the convergence. The ~−curves at 15th order of approximations are

sketched to see the appropriate range of ~? ? ~? and ~?. It is apparent from Figs. (2?2) – (2?4) that

the admissible ranges of ~? ? ~? and ~? are −1?70 ≤ ~? ≤ −0?15? −1?90 ≤ ~? ≤ −0?28 and −2?20 ≤

~? ≤ −0?20. Moreover the series solutions are convergent in the entire zone of ? when ~? = −1?0 =

~? = ~?. g = 0.2, Nt = 0.1, Nb = 0.2, Le = 1.0 = Pr, n = 1.5 0.0 -0.5

<div style="color:red">
27**f '' ?0? -1.0 -1.** 5 -2.0 **-2.0 -1.5 -1.0 -0.5 0.0**Ñ f Fig. **2?** 2 : ~

−**curve for the function**
</div>
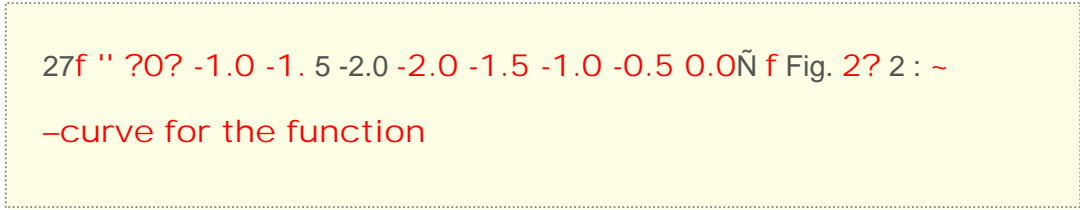
?(?)? n = 1.5, g = 0.2,

<div style="color:red">
66**Nt = 0.1, Nb = 0.** 2, **Le = 1.0** = Pr **-0.** 10 q ' **?0?**
</div>

-0.15 -0.20 -2.5 -2.0 -1.5 -1.0 -0.5 0.0 Ñq Fig. 2?3 : ~–curve for the function ?(?)? g = 0.2, Nt = 0.1, Nb = 0.2, Le = 1.0 = Pr, n = 1.5 0.3 0.2 f ' ?0? 0.1 0.0 -0.1 -0.2 -2.5 -2.0 -1.5 -1.0 -0.5 0.0 0.5 Ñf Fig. 2

4**?4 : ~–curve for** the **function ?(?)? Table** 2 **.1: Convergence of** homotopic **solutions**

when ? = 1?5? ? = 0?2? ?? = 0?2? ?? = 0?1? ?? = 1?0 and Pr = 1?0? Order of Approximation −? 00 (0) −?0(0) ?0 (0) 1 1?06667 0?15741 0?07870 5 1?06162 0?14918 0?07459 11 1?06160 0?14829 0?07414 16 1?06160 0?14824 0?07412 25 1?06160 0?14824 0?07412 35 1?06160 0?14824 0?07412 50 1?06160 0?14824 0?07412 2.4 Results and discussion Figs. (2?5) − (2?12)

17**are sketched to** investigate **the** behaviors **of** some physical **parameters on the** nondimensional **temperature ? (?) and**

concentration ?(?). The

22**results are** achieved **at two** distinct **values of ? just to compare the** corresponding **profiles in** cases **of** linear **and**

nonlinear stretching surfaces. Fig. 2?5 elucidates the influence of Prandtl number (? ?) on the temper- ature profile ?(?). From fig. 2?5 it is observed that when we enhance the value of Prandtl number ?? reduction is occured in the temperature distribution and its related thickness of thermal layer. Physically larger and smaller Prandtl fluids correspond to weaker and stronger thermal diffusivities respectively. An enhancement in Prandtl number causes a

16**weaker thermal diffusivity.** Such **weaker thermal**

diffusivity causes a **lower temperature**

distribution ?(?) and less thickness of the thermal layer. Fig. 2?6 is plotted to see the impact

17**of Biot number ? on the temperature** distribution ?(?). **An** increment **in**

? causes a stronger convection which depicts higher temperature distribution and thicker thickness

of the thermal layer. Fig. 2?7 is drawn to see the

37**influence of thermophoresis parameter ?? on the temperature distribution**

?(?). Larger values of thermophoresis parameter ?? causes a stronger temperature distribu- tion. An

enhancement in ?? leads to a stronger thermophoretic force which is responsible for a deeper

transfer of nanoparticles in the ambient fluid which corresponds to a stronger temper- ature

distribution and more thickness of thermal layer. From Fig. 2?8 we have seen that the concentration

field ?(?) and

33**thickness of concentration boundary layer** are depreciated **with an** increment **in Lewis number**

??. Lewis number is based on Brownian diffusivity.

3**The higher Lewis number corresponds to lower Brownian**

diffusivity. This lower Brownian diffusivity yields weaker concentration field ?(?). Fig. 2?9

9**depicts the behavior of** Prandtl **number** (Pr) **on the concentration**

distribution ?(?). Due to higher Prandtl number ?? decreasing behavior is noted in the concentration field ?(?). From Fig. 2?10? it is clearly analyzed that the concentration field ?(?) enhances

3**for the** higher **values of Biot number**

?. Fig. 2?11 displays the behavior

3**of Brownian motion parameter ?? on concentration**

field ?(?). From this Fig. it is clearly ana- lyzed that both concentration ?(?) and associated thickness of

3**boundary layer are reduced with** an increment **in**

??. Fig. 2?12 shows concentration field ?(?) corresponding to various values of thermophoresis parameter ??. Here we examined that by increasing thermophoresis parame- ter ??, an enhancement is occured

6**in the concentration** field ?(?) **and its related** thickness of **boundary layer.**

Table 2?1 is developed to analyze the numerical values of −?00(0)? −?0(0) and ?0(0) at distinct order of homotopic deformations when ? = 1?5? ? = 0?2? ?? = 0?2? ?? = 0?1? ?? = 1?0? Pr = 1?0. It is clearly shown that the solution of velocity converges from 11th order of deformations while solutions of temperature and concentration

10**converge from** 16th **order of** homotopic **approximations. Hence** 16th **order of**

deformation is essential for convergent solu- tions of velocity, temperature and concentration profiles. Table 2?2 is computed to investigate the

11**numerical values of Nusselt number ? ?? Re−?1?2 for** several **values of physical parameters.**

From this table we noticed that

50**the values of Nusselt number are** decreased **with an** increment **in** Lewis **number** ??. However **the** Nusselt number **is a** constant function **of**

Brownian motion parameter ? ?. g = 0.2 = Nb,

29**Nt = 0.1, Le = 1.0** 0.30 n = **1.0** 0.25 **n = 1.**

5 0.20 q ?h? 0.15 Pr = 0.7, 1.0, 1.3 0.10 0.05 0.00 0 2 4 6 8 h Fig. 2?5 : Behavior of

9**Pr on ?(?)? Nb** = 0.2, **Nt = 0.1, Le = 1.0** = Pr **0.** 6 n = **1.0**

0.5 n = 1.5 0.4 q ?h? 0.3 g = 0.1, 0.5, 1.0 0.2 0.1 0.0 0 1 2 3 4 5 6 h Fig. 2?6 : Behavior of ? on ?(?)? g = 0.2 = Nb, Le = 1.0 = Pr 0.25 0.20 q ?h? 0.15 0.10 0.05 0.00 n = 1.0 n = 1.5 Nt = 0.1, 1.0, 1.9 0 2 4 6 8 h Fig. 2?7 : Behavior of ?? on ?(?)? g = 0.2 = Nb, Nt = 0.1, Pr =1.0 0.02 0.01 0.00 f ?h? -0.01 -0.02 -0.03 -0.04 Le = 1.0, 1.25, 1.5 n = 1.0 n = 1.5 0 2 4 6 8 10 h Fig. 2?8 : Behavior of ?? on ?(?)? g = 0.2 = Nb, Nt = 0.1,

1**Le = 1.0 0.** 02 **0.** 00 f **?h ? -0.** 02 **Pr = 0.** 7, **1.0, 1.**

3 -0.04 n = 1.0 n = 1.5 0 2 4 6 8 10 12 h Fig. 2?9 : Behavior of

9**Pr on ?(?)? Nb** = 0.2, **Nt = 0.1, Le = 1.0** = Pr **0.**

05 0.00 f ?h? -0.05 g = 0.1, 0.5, 1.0 n = 1.0 n = 1.5 -0.10 0 2 4 6 8 10 h Fig. 2?10 : Behavior of ? on ?

(?)? g = 0.2, Nt = 0.1, Le = 1.0 = Pr 0.02 0.01 f ?h ? 0.00 -0.01 -0.02 -0.03 -0.04 Nb = 0.2, 0.5, 0.8 n

= 1.0 n = 1.5 0 2 4 6 8 10 h Fig. 2?11 : Behavior of ?? on ?(?)? 0.10 0.05 0.00 f ?h? -0.05 -0.10 -

0.15 -0.20 g = 0.2 = Nb, Le = 1.0 = Pr Nt = 0.1, 0.3, 0.5 n = 1.0 n = 1.5 0 2 4 6 8 10

7**h Fig. 2?12** : Behavior **of ? ? on ?(?)? Table 2.**

2: Numerical

58**values of Nusselt number ? ?? Re–?1?2 for** several **values**

of ?? ? ?? ? ?? ?? and **Pr** ? ? ?? ?? ?? Pr ? ?? Re –**?1?**

2 ? = 1?0 ? = 1?5 0?1 0?7 1?2 0?2 0?1 0?0 0?5 1?0 0?2 0?2 1?0 1?0 1?0 1?0 0?0853 0?3166 0?

3896 0?1488 0?1482 0?1476 0?0953 0?3515 0?4319 0?1659 0?1652 0?1644 0?2 0?1 0?5 1?0 1?5

1?0 1?0 0?1487 0?1487 0?1487 0?1658 0?1658 0?1658 0?2 0?1 0?2 0?5 1?0 1?5 1?0 0?1488 0?

1487 0?1486 0?1658 0?1657 0?1656 0?2 0?1 0?2 1?0 0?7 1?0 1?3 0?1388 0?1487 0?1551 0?

1545 0?1658 0?1729 2.5 Main findings Two-dimensional

49**flow of** viscous **nanofluid over a** nonlinearly **stretching sheet**

subject to the convective surface **boundary condition is**

addressed. The key points of the present chapter are given below: • An enhancement in the Biot

number ? shows stronger temperature and concentration profiles. •

72**Influence of Prandtl number Pr on the temperature**

and concentration fields are qualita- tively similar. • Temperature profile ?(?) enhances by increasing

thermophoresis parameter ??? • concentration profile ?(?) is decreased by an increment in ?? while

it is enhanced for higher values of ??? • Nusselt number reduces by increasing ?? but it remains

constant in case of ??.

12**Chapter 3 MHD three dimensional flow of** couple stress **nanofluid** over **a** nonlinearly **stretching** surface **with convective** effect **3.1 Introduction** This **chapter** explores **the** magnetohydrodynamic (MHD) steady **three dimensional flow of**

cou- ple stress

3**nanofluid in the presence of convective**

surface boundary condition. The sheet is stretched nonlinearly in two lateral directions in order to

generate the flow. Temperature and concentration distributions are studied

34**in the presence of Brownian motion and thermophoresis effects.**

Couple stress fluid is considered electrically conducting through non-uniform applied magnetic field.

Mathematical formulation is developed via boundary layer approach. Nonlin- ear ordinary differential

systems are constructed by employing suitable transformations.

38The resulting system has been solved for the convergent homotopic series **solutions**

of velocities, tem- perature and concentration.

57Effects of various **pertinent parameters on the temperature and concentration** distributions **are** sketched **and discussed. Numerical**

computations are performed to analyze the

34values of skin friction coefficients and local Nusselt number.

3.2 Problem development We assume the

21steady three-dimensional flow of an incompressible couple stress **nanofluid**

due to a bidirectional nonlinear stretching sheet. The fluid is assumed an electrically conducting through non

37-uniform magnetic field applied in the ?−direction. Here **the** electric field **and**

Hall effects are not considered. Due to the low magnetic Reynolds number, induced magnetic field effects are neglected.

9Brownian motion and thermophoresis effects are also

taken into the consideration. We adopt the

46Cartesian coordinate system in such a manner that ?– and ?–axis are taken along the stretched surface and ?–axis is perpendicular to the

surface (see Fig. 3?1). The sheet at ? = 0 is stretched in the ?– and ?–directions with velocities ?? (?? ?) = ?(? + ?)? and ??(?? ?) = ?(?+?)? respectively with ?? ?? ? ? 0 as the constants. The surface temperature is managed through

1a convective heating mechanism which is characterized by a coefficient of heat transfer ?? and temperature of the hot fluid ?? under the sheet.

Boundary layer expressions governing the flow of couple stress nanofluid are given by Fig. 3?1 : Physical sketch of the problem. ?? ?? ?? ?? ?? + + = 0? (3.1) ?? ? ???? + ? ???? + ? ???? = ? ?? 2???2 – ?0 ?4? ??2(?? ?) ??4 – ?? ?? ? ???? + ? ???? + ? ???? = ? ??2??2 – ?0 ?4? ??2(?? ?) ??4 – ?? ?? ? ???? + ? ???? + ? ???? = ? ??2??2 ((????))?? Ã?? + ?? ?? + ? ? ?? 2 ? μ ?? ?? ¶ ?∞ μ ?? ¶ ! ? ?? ?? ?? ?2? ?? + ? ?? + ? ?? = ??

1??2 + ? ? ?2? ¶ ?∞ ??2 ? μ μ ¶ The subjected boundary conditions are ?=??? ?=??? ?=0? –????? =??(?? –?)? ?????? ??∞????? =0at?=0?

+ (3.2) (3.3) (3.4) (3.5) (3.6) ? → 0? ? → 0? ? → ?∞? ? → ?∞ as ? → ∞? (3.7) Note that ?? ? and ? are the fluid velocities

41in the ?–? ?– and ?–directions respectively, ? = ???? denotes

the kinematic viscosity,

? stands for dynamic viscosity, ?? represents the de¡nsity of¢base liquid, ?0(= ?∗???) stands for couple stress viscosity, ?∗ denotes the couple stress viscosity parameter, ? stands for electrical conductivity, ?(?? ?) = ?0(? + ?)?–21 denotes the non-uniform magnetic field, ? stands for temperature, ? = ??(??)? represents the thermal diffusivity, ? stands for thermal conductivity of fluid, (??)? stands for

42**heat capacity of fluid,** (??)? stands for **effective heat capacity of nanoparticles,**

?? represents Brownian diffusivity, ? stands for concentration and ?? represents thermophoretic diffusion coefficient, ?? = ?(? + ?)?–21 stands for non-uniform heat transfer coefficient. ?∞ denotes the ambient fluid temperature and ?∞ represents the ambient fluid concentration.

1**We now introduce the following** transformations ? = ?(? + **?)??0 (?)? ? = ?(? + ?)??0(?)? ? = − ??(?2+1) 1?2** (? + ?)?–21 {((? + ?) + **??−+11?(?0** + ?0)}? • ?(?) = ??³?—??∞∞ ? ?(´?) = ?–??∞∞ ? ? = ?(?2 **+?1) 1?2** (? + ?)?–21 ?? • • **Eq.** (3?1) **is now** automatically **satisfied and Eqs.**

(3?2) − (3?7) have the follow•ing forms ³ ´ • ?000 + (? + ?)?00 − 2? (?0 + ?0)?0 − ??(?) − ?2?0 = 0? ? + 1 (3.8) (3.9) ?000 + (? + ?)?00 − 2? (?0 + ?0)?0 − ??(?) − ?2?0 = 0? ? + 1 (3.10) ?00 + Pr (? + ?)?0 + ???0?0 + ???02 = 0? (3.11) ?00 + ?? Pr(? + ?)?0 + ?? ?00 = 0? ³ ´ (3.12) ? ? ? (0) = ?(0) = 0? ? 0(0) = 1? ?0(0) = ?? ?0(0) = −? (1 − ? (0)) ? ? ??0(0) + ? ??0(0) = 0? (3.13) ?0(∞) → 0? ?0(∞) → 0? ?(∞) → 0? ?(∞) → 0? (3.14) In above expressions ? denotes couple stress parameter, ? represents the magnetic number, ? stands for ratio parameter, Pr stands for

26**Prandtl number,** ?? depicts **Brownian motion parameter,** ??

stands for **thermophoresis parameter,** ? stands for Biot **number and**

?? stands for Lewis number. These parameters are defined by ? = (?+2?1)2?0? (? + ?)?–1? ? 2 = ?? 2??(??+201) ? ? = ?? ? Pr = ?? ? ? ? = (??)(????)????∞ ? ? ? = (??)?(????)?(????∞–?∞) ? ? = ?? ?? ? ?? = ?? ? (3.15) ? ? • • p Dimensionless forms of skin friction coefficients and Nusselt number can be written as follows • ??? Re?1?2 = (?+21)1?2(?00(0) – ????(0))? ??? Re?1?2 = ?–3? 2(?+21)1?2(?00(0) – ????(0))? • (3.16) ??? Re–?1?2 = –(?+21)1?2?0(0)? •• where

1**Re? = ??(? + ?)?? and Re? = ??(? + ?)?? depict the local Reynolds numbers.**

It is also •• noted that

3**the dimensionless mass flux** showed **by a Sherwood number ??? is now identically zero**

3.3 Series solutions Our purpose now is to compute the series solutions via homotopy analysis technique (HAM). In homotopic solutions, the suitable initial approximations (?0?

1**?0? ?0? ?0) and the** corresponding auxiliary **linear operators (L??L??L?? L?) for** the above problem **are**

?0(?) = 1–exp(–?)?

44**?0(?) = ?(1–exp(–?))? ?0(?) = 1 + ? exp(–?)? ?0(?)** = – ? ? ?? 1 + ? ?? **exp(–?)? (3.** 17) **?3? ?? ?3? ?? ?2?** ?2? **L? = ??3 – ?? ? L?** = ??3 – ?? ? **L?**

= ??2 − ?? L? = ??2 − ?? (3.18) The above operators have the properties given below

4**L? [?1 + ?2 exp(?) + ?3 exp(−?)] = 0? L? [?4 + ?5 exp(?) + ? 6 exp(−?)] = 0? •** (3. 19) **L? [?7 exp(?) + ?8 exp(−?)] = 0?**

L? [?9 exp(?) + ?10 exp(−?)] = 0? • in which ?? (? = 1 − 10) denote the

4**arbitrary constants.•** 3 **.3.1 Zeroth-order** deformation equations **(1− Þ∗)L?**

?˘ (??

64**Þ∗) − ?0(?) = Þ∗~?** N? [?˘ (?? **Þ∗)? ?˘ (?? Þ∗)]?** (3.20) (1 − **Þ∗)** L? [?˘ (?? **Þ∗)− ?0(?)] = Þ∗~?** N?[?˘ (?? **Þ∗)? ?˘ (?? Þ∗)]?**

h i (3.21) (1 − Þ∗)L? ˘ ?(??

19**Þ∗) − ?0(?) = Þ∗~?** N?[?˘ (?? **Þ∗)? ?˘ (?? Þ∗)? ˘ ?(?? Þ∗)? ˘ ? (?? Þ∗)]?** (3.22) (1 − **Þ∗)** L? ?˘ (?? **Þ∗) − ?0(?) = Þ∗~?** N?[?˘ (?? **Þ∗)? ?˘ (?? Þ∗)? ?˘ (?? Þ∗)? ?˘ (?? Þ∗)]?**

h i (3.23) h i

18**?˘ (0? Þ∗) = 0? ?˘ 0(0? Þ∗)** = 1? ?˘ **0(∞? Þ∗) = 0?** ?˘ **(0? Þ∗) = 0?** ?˘ 0(0 **?Þ∗)=?? ?˘ 0(∞?Þ∗)=0?˘** ?0(0 **?Þ∗)=−?** 1−?˘ (0 **?Þ∗)** ? • (3.24) **?˘ (∞?Þ∗)=0?** ???˘ 0(0 **?Þ∗)+???˘ 0(0 ?Þ∗)=0?³?˘ (∞?Þ∗)= ´0?••** N? **?˘ (?;Þ∗)??˘ (?;Þ∗)**

= ??3??3˘ + ?˘ +?˘ ??2??2˘ ?2+?1Ã????˘ ???˘ ?!????˘ −??••?(?5()5?˘)−?2 − + ? ?˘ ? h i

³´? ? (3.25) N? ?˘ (?;Þ∗)??˘ (?;Þ∗) = ?3˘ ?+ ?˘ +?˘ ?2?˘ 2? ??˘ ??˘ ??˘ −??(5)?˘ −?2 −

+ ??˘ ? (3.26) h i ??3 ³´??2 ?+1Ã?? ??!?? ??(5) ?? N? ?˘ (?; Þ∗)? ?˘ (?; Þ∗)? ?˘ (?? Þ∗)? ?˘

(?? Þ∗) = ?2˘ ? + Pr ?˘ + ?˘ ?˘ ? h i ??2 ³´?? +Pr???? ?? + Pr?? ??! ??˘ ??˘ ?˘ ? 2 Ã ?

(3.27) N? ?˘ (?;Þ∗)??˘ (?;Þ∗)??˘ (??Þ∗)??˘ (??Þ∗) = ??2?˘ ?2 +??Pr ?˘ +?˘ ????˘ + ?? ?

2˘ ? i ³´?? ??2 ? (3.28) h Here Þ∗ ∈ [0?1] denotes the

<div style="border:1px solid #ccc; background:#ffffe0; padding:1em;">

10embedding parameter, the non-zero auxiliary parameters are de- picted **by ~?? ~?? ~? and**

</div>

~? and N?? N?? N? and N? represent the non-linear operators. 3.3.2 ?ˆth-order deformation equations L?

<div style="border:1px solid #ccc; background:#ffffe0; padding:1em;">

8**[??ˆ(?) − ??ˆ??ˆ− 1(?)] = ~?R ˜??ˆ(?)? L? [??ˆ(?) − ??ˆ??ˆ− 1(?)] = ~?R ˜??ˆ(?)? L? [??ˆ(?) − ??ˆ??ˆ− 1(?)] = ~?R ˜??ˆ(?)? L? ??ˆ(?) − ??ˆ??ˆ− 1(?) = ~?R ˜??ˆ(?)? £ ¤ ??ˆ(** 0) = **??0ˆ(0) = ??0ˆ(∞) = 0? ??ˆ(0) = ?0?ˆ(0) = ??0ˆ(∞) = 0? ??0ˆ(0) + ???ˆ(0) = 0? ???0?ˆ(0) + ???0?ˆ(0) = 0? ??ˆ(∞) = ??ˆ(∞)**

</div>

= 0? (3.29) (3.30) (3.31) (3.32) (3.33) R˜??ˆ(?) = ??0ˆ00−1

<div style="border:1px solid #ccc; background:#ffffe0; padding:1em;">

5**?2+?1 ?ˆ −1(??0ˆ−1−???0 + ??0ˆ−1−???0)**− µ ?ˆ −1¶ ?X=0 + (??ˆ **−1−??? 00 + ??ˆ −1−??? 00) − ???(ˆ ?−)1− ?2 ??0ˆ−1?**

</div>

(3.34) X?=0 R

<div style="border:1px solid #ccc; background:#ffffe0; padding:1em;">

71**˜??ˆ(?) = ?0?ˆ00−1 ?2 +?1¶!?? X ˆ=−01 (??0ˆ−1−??? 0 +??0ˆ−**

</div>

59**1–???0)**– μ **?ˆ–1 + (??ˆ–1–???** 00 + **??ˆ–1–???** 00) – **???(ˆ?)–1**– ?

2??0ˆ –**1?**

(3.35) X?=0 ?ˆ–1 R

25˜**??ˆ(?) = ?0?ˆ0**– 1 + Pr **(??ˆ– 1 –???0 + ??ˆ– 1 –??0?) ?ˆ–** 1 X **?**

=0 ?ˆ– 1 + Pr ?? **(?0?ˆ– 1 –??0?)** + Pr ?? **(?0?ˆ– 1 –??0?)?** (3.36) X **?**

=0 X **?=0** ?ˆ– 1 R ˜**??ˆ(?) = ?0?ˆ0**–

1(?) + ?? Pr (? (3.37) ?X

53**=0 ?ˆ–1–??0? + ??ˆ–1–??0?)** + ?????0?ˆ0 –**1?**χ **?ˆ=** 0? **?ˆ ≤ 1?•**

(3.38) • 1? **?ˆ ? 1?**

Putting Þ∗ = 0 and Þ∗ = 1 we have • ?˘ (?;0) = ?0(?)? ?˘ (?;1) = ?(?)? (3.39) ?˘ (?;0) = ?0(?)? ?˘ (?;1) = ?(?)? (3.40) ?˘ (??0) = ?0(?)? ˘ ?(??1) = ?(?)? (3.41) ?˘ (??0) = ?0(?)? ?˘ (??1) = ?(?)? (3.42) When Þ∗ varies from 0 to 1 then ?˘ (?;Þ∗)? ?˘ (?;Þ∗)? ˘ ?(??Þ∗) and ˘ ?(??Þ∗)

51**vary from the initial** approximations **?0(?)? ?0(?)?** ?0(?) **and ?0**

(?) to the desired **final solutions ?(?)? ?(?)? ?(?) and ?(?)**

respectively.

The following expressions are obtained via Taylor's series expansion ?˘ (?; Þ∗) =

23**?0(?) + ??ˆ(?)**Þ ∗**?ˆ? ??ˆ(?) =** ∞ 1 **??ˆ?˘ (??**Þ∗) ?Xˆ **=1 ?ˆ!** ?Þ ∗**?ˆ**

¯¯Þ∗=0 ? ¯ ?˘ (?; Þ∗) =

5**?0(?) + ??ˆ(?)**Þ ∗**?ˆ? ??ˆ(?) = ∞ 1 ??ˆ?˘ (??**Þ∗) ¯ ¯ ?Xˆ=1 **?ˆ!** ?Þ ∗**?ˆ**

¯Þ∗=0 ? ¯ ∞ ¯ ?˘ (?? Þ∗) = ?0(?) + ? ?Xˆ=1 ??ˆ

52**(?)Þ∗?ˆ? ??ˆ(?)** = ?ˆ1! **??ˆ?˘ ?Þ(?∗??ˆÞ∗)¯¯¯Þ∗=** 0 ?˘ (?? Þ∗) = ?0

(?) + **??ˆ(?)**Þ ∗?ˆ? ??ˆ(?) = 1 **??ˆ?˘ (??**Þ∗)¯¯ ∞ ¯ ?Xˆ=1 **?ˆ!** ?Þ ∗?ˆ

¯ ∗ ? ¯ ¯Þ =0 ¯ ¯ (3.43) (3.44) (3.45) (3.46) The convergence of Eqs. (3?43) – (3?46) strongly depends upon the ~?? ~?? ~? and ~?. Consid- ering that ~?? ~?? ~? and ~? are selected in such a way that Eqs. (3?43) – (3?46) converge at Þ∗ = 1, Then ∞ ?(?) = ?0(?) + ??ˆ(?)? (3.47) ?Xˆ=1 ∞ ?(?) = ?0(?) + ??ˆ(?)? (3.48) ?Xˆ=1 ∞ ?(?) = ?0(?) + ??ˆ(?)? (3.49) ?Xˆ=1 ∞ ?(?) = ?0(?) + ??ˆ(?)? (3.50) ? Xˆ=1 The general solutions (??ˆ? ??ˆ? ??ˆ? ??ˆ) of the Eqs. (3?29) – (3?32) in terms of special solutions (??∗ˆ? ??∗ˆ? ?∗?ˆ? ?∗?ˆ) are presented by the following expressions ??ˆ(?) = ??∗ˆ(?) + ?1 + ?2 exp(?) + ?3 exp(−?)? (3.51) ??ˆ(?) = ??∗ˆ(?) + ?4 + ?5 exp(?) + ?6 exp(−?)? (3.52) ??ˆ(?) = ?∗?ˆ (?) + ?7 exp(?) + ?8 exp(−?)? (3.53) ??ˆ(?) = ?∗?ˆ(?) + ?9 exp(?) + ?10 exp(−?)? (3.54) in which ?? (? = 1 − 10) by means of the boundary conditions (3?33) have the following values ?2 = ?5 = ?7 = ?9 = 0? ?3 = ????∗ˆ?(?) ?=0 ? ?1 = −?3 −

39**??∗ˆ(0)?¯** ?6 = **????∗ˆ?(?) ?=0** ? ?4 = −?6 − **?∗?ˆ(0)?** ?8 = 1

+ ? **????∗ˆ?(?) ?=0** − **??∗?ˆ(0)** ? 1 ¯ **Ã** ! ¯ ¯ ¯ ?10 = **??∗?ˆ(?) ? ? ?? ?**

=0 ? ? + Ã−?8 + **???∗?ˆ?(?) ?=¯0!**

? ¯ ¯ ¯ ¯ (3.55) (3.56) (3.57) 3.3.3 Convergence analysis No doubt the auxiliary parameters ~?? ~?? ~? and ~? in the series solutions (3?47) – (3?50) have key role regarding convergence. In order to develop the convergent approximate

3**series solutions, the** suitable **values of these parameters play a** key **role.** To select **the**

appropriate values of ~?? ~?? ~? and ~?,

3~–**curves are** sketched **at 15th order of** deformations. **Figs.**

(3?2) – (3?5) clearly denote that the region of convergence lies within the ranges −1?35 ≤ ~? ≤ −0?

35? −1?40 ≤ ~? ≤ −0?25? −1?40 ≤ ~? ≤ −0?25 and −1?50 ≤ ~? ≤ −0?25. Moreover the series

solutions are convergent in the entire zone of ? when ~? = ~? = −1?0 = ~? = ~?. Table 3?1 presents

that the 11th deformations is enough

1**for the convergent series solutions of** velocities,

temperature and concentration profiles. K = **0.** 02, **M = 0.**

1 = Nt, Nb = 0.2 = c,

1**g = 0.3, Le = 1.0, Pr = 1.2,**

n = 1.5 -0.8 -1.0 f '' ?0? -1.2 -1.4 -1.6 -1.5 -1.0 -0.5 0.0 Ñ f Fig. 3?2 : ~–curve for the function ? (?)? K

= 0.02, M = 0.1 = Nt, Nb = 0.2 = c, g = 0.3, Le = 1.0, Pr = 1.2, n = 1.5 0.2 0.0 g '' ?0? -0.2 -0.4 -0.6 -

1.5 -1.0 -0.5 0.0 Ñg Fig. 3?3 : ~–curve for the function ?(?)? -0.10 K = 0.02, M = 0.1 = Nt, Nb = 0.2 =

c, g = 0.3, Le = 1.0, Pr = 1.2, n = 1.5 -0.15 q ' ?0? -0.20 -0.25 -0.30 -1.5 -1.0 -0.5 0.0 Ñq Fig. 3?4 : ~

–curve for the function ?(?)? 0.25 0.20 0.15 f ' ?0? 0.10 0.05 0.00 K = 0.02, M = 0.1 = Nt, Nb = 0.2 =

c, g = 0.3, Le = 1.0, Pr = 1.2, n = 1.5 -0.05 -2.0 -1.5 -1.0 -0.5 0.0 Ñf Fig. 3?5 : ~–curve for the

function ?(?)? Table 3.1: Convergence of homotopic solutions when ? = 1?5? ? = 0?02?? ? = 0?1

= ??? ? = 0?2 = ??? ? = 0?3? ?? = 1?0 and Pr = 1?2. Order of Approximation −? 00(0) −?00(0) −?0

(0) ?0 (0) 1 1?19500 0?23900 0?21692 0?10846 5 1?19041 0?23808 0?21043 0?10521 11 1?

19035 0?23807 0?21033 0?10516 15 1?19035 0?23807 0?21033 0?10516 25 1?19035 0?23807 0?

21033 0?10516 35 1?19035 0?23807 0?21033 0?10516 50 1?19035 0?23807 0?21033 0?10516

3.4

31Results and discussion In **this section the** impact **of various** emerging flow **parameters**

like couple stress parameter ?? magnetic number ?? ratio parameter ?? Biot number ??

42Brownian motion parameter ??? thermophoresis parameter ??? Lewis number

??

31and Prandtl number ?? on the velocity com- ponents ?0(?) **and** ?0(?), **temperature** ?(?) and concentration ?(?) **are**

sketched in the Figs. (3?6) – (3?25). The results are achieved for two distinct

22values of ? just to compare the corre- sponding **profiles in** cases **of** linear **and**

nonlinear stretching surfaces. The influence of couple stress parameter ? on the component of

velocity ?0(?) has been shown in Fig. 3?5. It has been observed that component of velocity reduces

by increasing couple stress parameter ?. The couple stress parameter involves couple stress

viscosity ? which makes the fluid more viscous and hence the velocity is retarted. Fig. 3?6 depicts

the impact of magnetic number ? on the velocity component ?0(?). An enhancement in magnetic

number causes reduction in velocity field and its associated boundary layer thickness. Physically

Lorentz force enhances by increas- ing magnetic number ? which shows retarding effect. Hence

Lorentz force opposes the fluid motion and the

33velocity of the fluid decreases. Fig. 3? 7 illustrates

that how ratio parameter ef- fects the component of velocity ?0(?). Here the

> 6**velocity and its** associated momentum **boundary layer**
>
> **thickness** show **decreasing** behavior by increasing **ratio**

parameter ?. The reason behind this phenomena is that with an increment in the ratio parameter,

the ?–component of velocity decreases which yields reduction in

> 16**the velocity and** its **associated boundary layer thickness.**
>
> Influence **of** couple stress **parameter ? on the** component of **velocity**

?0(?) is sketched in Fig. 3?8. In this Fig. we observe

> 6**that the velocity** ?0(?) **and its** associated **boundary layer**
>
> **thickness**

decreases by enhancing couple stress parameter ?. Fig. 3?9 shows that how velocity compo- nent

get effected by magnetic number ?.

> 6**This Fig** presents **that velocity** ?0(?) **and its related boundary**
>
> **layer thickness**

decreases by enhancing magnetic number ?.

> 11**The influence of** ratio **parameter ? on the** component of
>
> **velocity**

?0(?) has been sketched in Fig. 3?10, which represents

6**that the velocity** ?0(?) **and its** associated **boundary layer thickness are** enhancing **functions of ratio** parameter ?. Variation **of**

couple stress

2**parameter ? on temperature** field ?(?) **is displayed in Fig. 3? 11.**

15**Larger values of** couple stress **parameter** ? gives **rise the**

temperature field and their related thickness of

16**thermal boundary layer. Fig.** 3?12 **is** interpreted **to** examine **the** effect **of**

magnetic number ? on temperature field ? (?). Here ? =6 0 yields hydromagnetic flow situation and ? = 0 represents hydrodynamic flow case. We examined that the

77**temperature distribution and** thickness of **the thermal boundary layer are**

higher for hydromagnetic flow as compared to the hydrodynamic flow situation. An increment in the values of magnetic number ? corresponds stronger temperature distribution and more

47**thickness of** the **thermal boundary layer.** Impact **of** ratio **parameter ? on the** temperature **field ? (?) is** drawn **in Fig.** 3?13.

Fig. it is observed that greater

tem- perature field ? (?) alongwith its related

two-dimensional flow situation has been recovered. Fig. 3?15 depicts

the value of ? leads to a stronger convection which shows a higher temperature field and more

thickness of the thermal layer. From Fig. 3?16 it has been noted that for higher

Prandtl number has an inverse relationship with the thermal diffusivity. Higher Prandtl number ? ?

implies lower ther- mal diffusivity. Such lower thermal diffusivity is responsible for

Fig. 3?17 presents that an increasing behavior of ? ? causes a stronger temperature distribution and

more thickness of thermal layer. Higher values of thermophoresis parameter ? ? yields a stronger

thermophoretic force which is responsible for a deeper transfer of nanopar- ticles in the ambient fluid

which corresponds to a stronger

1**temperature field and** more **thickness of thermal layer. Fig.**

3?18 elucidates

1**that an increase in** couple stress **parameter** ? implies to **an**

increment **in the concentration field** ?(?) and thicker thickness **of**

concentration boundary layer. Fig. 3?19 is sketched to see that how concentration field ?(?) is

effected by magnetic number ? . Here we observed

15**that the concentration and its related** thickness of

concentration **boundary layer** increases **by increasing**

magnetic number ? . Fig. 3?20 is sketched to examine that how concentration field ?(?) get effected

by ratio parameter (?). From this Fig. it has been noticed

10**that the concentration** field **is** lower **for the larger values of**

ratio **parameter**

(?). Fig. 3?21 shows

3**that the** higher **values of Biot number** (?) yields **a**

stronger concentration pro- file ?(?). Fig. 3?22 shows the variation in ?(?) for distinct values of Lewis

number ??. An inverse relation exists between Lewis number and Brownian diffusivity. By increasing

Lewis number, Brownian diffusivity decreases and as a result concentration ?(?) and its related

thick- ness of concentration boundary layer increases. Fig. 3?23

76**is sketched to** analyze **the** behavior **of Prandtl number (? ?)**

on

concentration distribution ?(?). Here

15**the concentration** field ?(?) **and associated** thickness of

boundary layer

decreases by enhancing ? ?. Fig. 3?24 depicts that the higher values of Brownian motion

parameter ? ? causes a weaker concentration profile ?(?). Fig. 3?25 shows how thermophoresis

parameter ? ? effects ?(?). By increasing thermophoresis parameter ? ?, concentration ?(?) and

thickness of concentration boundary layer also increases. Table 3?1 is constructed to analyze the

convergence of homotopic series solutions when ? = 1?5? ? = 0?02? ? ? = 0?1 = ? ?? ? = 0?2

= ? ?? ? = 0?3? ?? = 1?0 and Pr = 1?2. It is clearly seen that the solutions of velocity, temperature

and concentration distributions

10**converge from** 11th **order of** homotopic **approximations.**

Hence 11th **order of homotopic**

approximations is sufficient for convergence analysis of series solutions. Table 3?2 depicts skin

friction coefficients −?? ? Re?1?2 and −?? ? Re1??2 having the numerical values of couple stress

parameter ?, magnetic number ? and ratio parameter ?. It is clearly

65**seen that the skin friction coefficients are** enhanced **for**

the increasing values **of**

magnetic number ? . Table 3?3 is prepared for

11**numerical values of** local **Nusselt number ? ?? Re**−**?1?2**

corresponding to various values of ?? ?? ?? ?? ? ?? ? ?? ?? and Pr. It is noted that the couple stress

parameter ?, magnetic number ? and thermophoresis parameter ? ? correspond to a lower Nusselt

number while opposite behavior is observed for Biot number ?. M = 0.1, c = 0.2

14**1.0 n = 1.0** 0.8 **n** = 1.5 f ' **?h? 0.**

6 0.4 K = 0.0, 0.1, 0.2 0.2 0.0 0 1 2 3 4 5 6 h Fig. 3?6 : Behavior of ? on ?0(?)? K = 0.02 , c = 0.2

14**1.0 n = 1.0** 0.8 **n** = 1.5 f ' **?h? 0.**

7**6 0.4 M = 0.0, 0.** 6, **1.** 2 0 **.2 0.** 0 **0 1 2 3 4 5 6 h Fig.**

3?7:Behaviorof? on?0(?)? K=0.02

68,**M=0.1 1.0 n = 1.0** 0.8 **n**

= 1.5 f ' ?h? 0.6 0.4 c = 0.0, 0.5, 1.0 0.2 0.0 0 1 2 3 4 5 6 h Fig. 3?8 : Behavior of ? on ?0(?)? M =

0.1, c = 0.2 0.20 n = 1.0 0.15 n = 1.5 g ' ?h? 0.10 K = 0.0, 0.1, 0.2 0.05 0.00 0 1 2 3 4 5 6 h Fig. 3?

9 : Behavior of ? on ?0(?)? K = 0.02 , c = 0.2 0.20 n = 1.0 n = 1.5 0.15 g ' ?h? 0.10

7**M = 0.0, 0.** 6, **1.** 2 0.05 **0.** 00 **0 1 2 3 4 5 6 h Fig.** 3?10 : Behavior

of ? on ?0(?)? K = **0.** 02, **M = 0.**

1

14**1.0 n = 1.0** 0.8 **n** = 1.5 g ' **?h? 0.**

6 0.4 c = 0.0, 0.5, 1.0 0.2 0.0 0 1 2 3 4 5 6 h Fig. 3?11 : Behavior of ? on ?0(?)? g = 0.3, c = 0.2 = Nb, M = 0.1 = Nt, Le = 1.0, Pr = 1.2 0.30 n = 1.0 0.25 n = 1.5 0

1.**20 q ?h? 0.15** K = **0.0, 0.** 1, **0.** 2 0.10 **0.05 0.00 0 1 2 3 4 5 6 h**

Fig. 3?12 : Behavior **of ? on** ?(?)? g = **0.** 3, c = **0.2**

= Nb, K = 0.02,

29**Nt = 0.1, Le = 1.0,** Pr = **1.** 2 0.30 **n = 1.0**

0.25 n = 1.5 0.20

1**q ?h? 0.15 M = 0.0, 0.6, 1.2** 0.10 **0.**

05 0.00 0 1 2 3 4 5 6 h Fig. 3?13 : Behavior of ? on ?(?)? g = 0.3, K = 0.02, M = 0.1 = Nt, Nb = 0.2, Le = 1.0, Pr = 1.2 0.30 n = 1.0 0.25 n = 1.5 0.20 q ?h? 0.15 c = 0.0, 0.5, 1.0 0.10 0.05 0.00 0 1 2 3 4 5 6 h Fig. 3?14 : Behavior of ? on ?(?)? c = 0.2= Nb, K = 0.02 , M = 0.1 = Nt, Le = 1.0, Pr = 1.2 0.6 0.5 n = 1.0 n = 1.5 0.4 q ?h? 0.3 0.2 g = 0.1, 0.5, 1.0 0.1 0.0 0 1 2 3 4 5 6 h Fig. 3?15 : Behavior of ? on ?(?)? g = 0.3 , c = 0.2 = Nb , K = 0.02 , M = 0.1 = Nt, Le =

14**1.0 n = 1.0** 0.3 **n** = 1.5 q **?h? 0.**

2 Pr = 0.7, 1.0, 1.3 0.1 0.0 0 2 4 6 8 h Fig. 3?16 : Behavior of Pr on ?(?)? 0.30 n = 1.0 0.25 n = 1.5 0

1.**20 q ?h? 0.15 Nt = 0.** 1, **0.6, 1.2** 0.10 **0.** 05 **0.** 00 **0**

1 2 3 4 5 6 h Fig. 3‑17 : Behavior of ? ? on ?(?)? g = 0.3, c = 0.2 = Nb, M = 0.1 = Nt, Le = 1.0, Pr = 1.2 0.02 f ?h? 0.00 K = 0.0, 0.1, 0.2 -0.02 -0.04 n = 1.0 n = 1.5 0 2 4 6 8 h Fig. 3‑18 : Behavior of ? on ?(?)? 0.02 f ?h? 0.00 M = 0.0, 0.5, 0.8 -0.02 -0.04 n = 1.0 n = 1.5 0 2 4 6 8 h Fig. 3‑19 : Behavior of ? on ?(?)? g = 0.3 , K = 0.02 , M = 0.1 = Nt,

1Nb = 0. 2 , **Le = 1.0 , Pr = 1.2 0.** 02 **0.** 00 **f ?h?** -0.02 c = **0.0, 0.5, 1.0**

-0.04 n = 1.0 n = 1.5 0 2 4 6 8 h Fig. 3‑20 : Behavior of ? on ?(?)? c = 0.2= Nb, K = 0.02, M = 0.1 = Nt,

1Le = 1.0, Pr = 1.2 0. 05 **0.** 00 **f ?h?** g = **0.** 1, **0.5, 1.0**

-0.05 n = 1.0 n = 1.5 -0.10 0 2 4 6 8 h Fig. 3‑21 : Behavior of ? on ?(?)? g = 0.3, c = 0.2 = Nb, K = 0.02, M = 0.1 = Nt, Pr = 1.2 0.02 0.00 f ?h? -0.02 Le = 0.6, 0.9, 1.2 -0.04 n = 1.0 -0.06 n = 1.5 0 2 4 6 8 10 h Fig. 3‑22 : Behavior of ?? on ?(?)? 0.04 0.02 0.00 f ?h? -0.02 Pr = 0.7, 1.0, 1.3 -0.04 -0.06 n = 1.0 n = 1.5 0 2 4 6 8 10 h Fig. 3‑23 : Behavior of Pr on ?(?)? g = 0.3, c = 0.2, K = 0.02, M = 0.1 = Nt,

1Le = 1.0, Pr = 1.2 0. 02 **0.** 00 **f ?h? -0.** 02 **Nb = 0.** 2, **0.**

5, 0.8 n = 1.0 -0.04 n = 1.5 0 2 4 6 8 h Fig. 3‑24 : Behavior of ?? on ?(?)? 0.4 0.2 0.0 f ?h? -0.2 Nt = 0.1, 0.6, 1.2 -0.4 n = 1.0 -0.6 n = 1.5 0 2 4 6 8 h Fig. 3‑25 : Behavior of ?? on ?(?)? Table 3.2: Numerical data for the coefficients of skin friction $-???$ Re1??2 and $-???$ Re1??2 for various values of ?? ? and ?? ? ? ? $-???$ Re1??2 $-???$ Re1??2 ? = 1?0 ? = 1?5 ? = 1?0 ? = 1?5 0?00 0?01 0?02 0?02 0?1 0?0 0?2 0?5 0?2 0?2 1?1000 1?0932 1?0863 1?0819 1?0993 1?1860 1?3050 1?2945 1?2832 1?2786 1?2970 1?3886 2?4597 2?4446 2?4290 2?4192 2?4581 2?6520 2?9181 2?8945 2?8694 2?8591 2?9001 3?1050 0?02 0?1 0?2 0?3 0?5 1?0863 1?1290 1?2095 1?2832 1?3332 1?

4270 2?4290 2?0613 1?7105 2?8694 2?4341 2?0181 Table 3.3: Numerical data for the

11**Nusselt number ???Re–?1?2 for** various **values**

of ?? ?? ?? ?? ??? ??? ??? Pr? ? ? ? ? ?? ?? ?? Pr ? ?? Re −**?1?**

2 ? = 1?0 ? = 1?5 0?00 0?02 0?05 0?02 0?1 0?0 0?5 0?8 0?2 0?2 0?3 0?3 0?1 0?1 0?2 0?2 1?0 1?0 1?2 1?2 0?2114 0?2112 0?2108 0?2113 0?2091 0?2060 0?2356 0?2352 0?2344 0?2353 0?2329 0?2295 0?02 0?1 0?0 0?3 0?5 0?3 0?1 0?2 1?0 1?2 0?2054 0?2136 0?2180 0?2287 0?2379 0?2427 0?02 0?1 0?2 0?1 0?7 1?2 0?1 0?2 1?0 1?2 0?0877 0?3527 0?4458 0?0979 0?3917 0?4943 0?02 0?1 0?2 0?3 0?0 0?5 1?0 0?2 1?0 1?2 0?2115 0?2100 0?2084 0?2355 0?2338 0?2321 0?02 0?1 0?2 0?3 0?1 0?5 1?0 1?5 1?0 1?2 0?2112 0?2112 0?2112 0?2352 0?2352 0?2352 0?02 0?1 0?2 0?3 0?1 0?2 0?5 1?0 1?5 1?2 0?2113 0?2112 0?2111 0?2353 0?2352 0?2351 0?02 0?1 0?2 0?3 0?1 0?2 1?0 0?5 1?0 1?5 0?1687 0?2034 0?2200 0?1874 0?2263 0?2451 3.5 Main findings Magnetohydrodynamic (MHD)

21**three-dimensional flow of** couple stress **nanofluid** caused **by** non- linear **stretching sheet**

having convective boundary condition has been analyzed. The main observations of this chapter are summarized below • Larger values of couple stress parameter ? present similar behavior for velocity distrib- utions ?0(?) and ?0(?)? • An increment in the magnetic number ? causes a reduction in the both components of velocity ?0(?) and ?0(?). • An enhancement in the values of couple stress parameter ? show increasing behavior for temperature and concentration distributions. • Temperature distribution ?(?) enhances when the larger values of magnetic number ? is taken into account. • Both the temperature and concentration profiles are increased by enhancing Biot number ?. • Temperature ?(?) and thickness of thermal layer are lower for the

24**higher values of Prandtl number (Pr).**• Temperature **and concentration**

profiles exhibit similar behavior for higher

1values of ther- mophoresis parameter ??. • An enhancement in Brownian motion parameter ?? yields a weaker

concentration profile. •

1Skin friction coefficient are increased for the higher values of magnetic

number ?. •

1Heat transfer rate at the surface remains constant for ?? while it decreases for

the larger values of ??. Bibliography [1] K. Vajravelu, Viscous flow over a nonlinearly stretching sheet, Appl. Math. Comput., 124 (2001) 281-288. [2] R. Cortell, Viscous flow and heat transfer over a nonlinearly stretching sheet, Appl. Math. Comput., 184 (2007) 864-873. [3] R. Cortell, Effects of viscous dissipation and radiation on the thermal boundary layer over a nonlinearly stretching sheet, Phys. Lett. A., 372 (2008) 631-636. [4] T. Hayat, Q. Hussain and T. Javed, The modified decomposition method and Padé approx- imants for the MHD flow over a non-linear stretching sheet, Nonlinear Anal.-Real World Appl., 10 (2009) 966-973. [5] P. Rana and R. Bhargava, Flow and heat transfer of a nanofluid over a nonlinearly stretch- ing sheet: A numerical study, Comm. Nonlinear Sci. Num. Simulat., 17 (2012) 212-226. [6] S. Mukhopadhyay, Analysis of boundary layer flow over a porous nonlinearly stretching sheet with partial slip at the boundary, Alexandria Eng. J., 52 (2013) 563-569. [7] F. Mabood, W.A. Khan and A.I.M. Ismail, MHD boundary layer flow and heat transfer of nanofluids over a nonlinear stretching sheet: A numerical study, J. Magn. Magn. Mater., 374 (2015) 569-576. [8] M. Mustafa, J.A. Khan, T. Hayat and A. Alsaedi, Boundary layer flow of

nanofluid over a nonlinearly stretching sheet with convective boundary condition, IEEE Trans. Nanotech., 14 (2015) 159-168. [9] S.U.S. Choi, Enhancing thermal conductivity of fluids with nanoparticles, ASME, USA (1995) 99-105, FED 231/MD. [10] J. Boungiorno, Convective transport in nanofluids, ASME J. Heat Transfer, 128 (2006) 240-250. [11] W.A. Khan and I. Pop, Boundary-layer flow of a nanofluid past a stretching sheet, Int. J. Heat Mass Transfer, 53 (2010) 2477-2483. [12] M. Turkyilmazoglu, Exact analytical solutions for heat and mass transfer of MHD slip flow in nanofluids, Chem. Eng. Sci., 84 (2012) 182-187. [13] W. Ibrahim and O.D. Makinde, The effect of double stratification on boundary-layer flow and heat transfer of nanofluid over a vertical plate, Comput. Fluids, 86 (2013) 433-441. [14] K.L. Hsiao, Nanofluid flow with multimedia physical features for conjugate mixed convec- tion and radiation, Comp. Fluids, 104 (2014) 1-8. [15] Y. Lin, L. Zheng and X. Zhang, Radiation effects on Marangoni convection flow and heat transfer in pseudo-plastic non-Newtonian nanofluids with variable thermal conductivity, Int. J. Heat Mass Transfer, 77 (2014) 708-716. [16] A. Zeeshan, M. Baig, R. Ellahi and T. Hayat, Flow of viscous nanofluid between the concentric cylinders, J. Comp. Theoretical Nanoscience, 11 (2014) 646-654. [17] M. Sheikholeslami, M.G. Bandpy, R. Ellahi, M. Hassan and S. Soleimani, Effects of MHD on Cu-water nanofluid flow and heat transfer by means of CVFEM, J. Magn. Magn. Mater., 349 (2014) 188-200. [18] C. Zhang, L. Zheng, X. Zhang and G. Chen, MHD flow and radiation heat transfer of nanofluids in porous media with variable surface heat flux and chemical reaction, Appl. Math. Modell., 39 (2015) 165-181. [19] M. Sheikholeslami, D.D. Ganji, M.Y. Javed and R. Ellahi, Effect of thermal radiation on magnetohydrodynamics nanofluid flow and heat transfer by means of two phase model, J. Magn. Magn. Mater., 374 (2015) 36-43. 60 [20] B.J. Gireesha, R.S.R. Gorla and B. Mahanthesh, Effect of suspended nanoparticles on three-dimensional MHD flow, heat and mass transfer of radiating Eyring-Powell fluid over a stretching sheet, J. Nanofluids, 4 (2015) 474-484. [21] M. Mustafa, J.A. Khan, T. Hayat and A. Alsaedi, On Bödewadt flow and heat transfer of nanofluids over a stretching stationary disk, J. Mol. Liquids, 211 (2015) 119-125. [22] T. Hayat, M. Imtiaz and A. Alsaedi, Impact of magnetohydrodynamics in bidirectional flow of nanofluid subject to second order slip velocity and homogeneous-heterogeneous reactions, J. Magn. Magn. Mater., 395 (2015) 294-302. [23] V. K. Stokes, Couple stresses in fluids, Phys. Fluids, 9 (1966) 1709-1715. [24] D. Srinivasacharya and K. Kaladhar, Mixed convection flow of couple stress fluid in a non-darcy porous medium with Soret and

Dufour effects, J. Appl. Sci. Eng., 15 (2012) 415-422. [25] M. Ramzan, M. Farooq, A. Alsaedi and T. Hayat, MHD three-dimensional flow of couple stress fluid with Newtonian heating, Eur. Phys. J. Plus, 128 (2013) 49. [26] T. Hayat, M. Mustafa, Z. Iqbal and A. Alsaedi, Stagnation-point flow of couple stress fluid with melting heat transfer, Appl. Math. Mech. -Eng. Ed., 34 (2013) 167-176. [27] M. Turkyilmazoglu, Exact solutions for two-dimensional laminar flow over a continuously stretching or shrinking sheet in an electrically conducting quiescent couple stress fluid, Int. J. Heat Mass Transfer, 72 (2014) 1-8. [28] T. Hayat, T. Muhammad, A. Alsaedi and M.S. Alhuthali, Magnetohydrodynamic three- dimensional flow of viscoelastic nanofluid in the presence of nonlinear thermal radiation, J. Magn. Magn. Mater., 385 (2015) 222-229. [29] O.D. Makinde and A. Aziz, Boundary layer flow of a nanofluid past a stretching sheet with a convective boundary condition, Int. J. Thermal Sci., 50 (2011) 1326-1332. [30] T. Hayat, T. Muhammad, S.A. Shehzad, G.Q. Chen and I.A. Abbas, Interaction of mag- netic field in flow of Maxwell nanofluid with convective effect, J. Magn. Magn. Mater., 389 (2015) 48-55. 61 [31] A.V. Kuznetsov and D.A. Nield, Natural convective boundary-layer flow of a nanofluid past a vertical plate: A revised model, Int. J. Thermal Sci., 77 (2014) 126-129. [32] T. Hayat, T. Muhammad, S.A. Shehzad, M.S. Alhuthali and J. Lu, Impact of magnetic field in three-dimensional flow of an Oldroyd-B nanofluid, J. Mol. Liquids, 212 (2015) 272-282. [33] S.J. Liao, Homotopy analysis method in nonlinear differential equations, Springer & Higher Education Press, Heidelberg, 2012. [34] M. Turkyilmazoglu, Solution of the Thomas-Fermi equation with a convergent approach, Commun. Nonlinear. Sci. Numer Simulat., 17 (2012) 4097-4103. [35] M. Sheikholeslami, M. Hatami and D.D. Ganji, Micropolar fluid flow and heat transfer in a permeable channel using analytic method, J. Mol. Liquids, 194 (2014) 30-36. [36] S. Abbasbandy, T. Hayat, A. Alsaedi and M.M. Rashidi, Numerical and analytical solutions for Falkner-Skan flow of MHD Oldroyd-B fluid, Int. J. Numer. Methods Heat Fluid Flow, 24 (2014) 390-401. [37] J. Sui, L. Zheng, X. Zhang and G. Chen, Mixed convection heat transfer in power law fluids over a moving conveyor along an inclined plate, Int. J. Heat Mass Transfer, 85 (2015) 1023-1033. [38] R. Ellahi, M. Hassan and A. Zeeshan, Shape effects of nanosize particles in Cu-H2O nanofluid on entropy generation, Int. J. Heat Mass Transfer, 81 (2015) 449-456. [39] T. Hayat, M. Imtiaz and A. Alsaedi, MHD 3D flow of nanofluid in presence of convective conditions, J. Mol. Liquids, 212 (2015) 203-208. [40] T. Hayat, T. Muhammad, S.A. Shehzad and A. Alsaedi, A mathematical study for three- dimensional boundary

layer flow of Jeffrey nanofluid, Z. Naturforsch. A, 70a (2015) 225-233. g = 0.3, c = 0.2 = Nb, K =

0.02 , M = 0.1, Le = 1.0, Pr = 1.2 g = 0.3 , c = 0.2 = Nb, K = 0.02, Nt = 0.1, Le = 1.0, Pr = 1.2 g =

0.3 , c = 0.2 = Nb , K = 0.02 , M = 0.1 = Nt, Le = 1.0 g = 0.3 , c = 0.2 = Nb, K = 0.02 , M = 0.1 , Le =

1.0 , Pr = 1.2 1 2 3 4 5 6 7 8 9 10 11 12 13 14 15 16 17 18 19 20 21 22 23 24 25 26 27 28 29 30 31

32 33 34 35 36 37 38 39 40 41 42 43 44 45 46 47 48 49 50 51 52 53 54 55 56 57 58 59 62